SUPPLEMENTAL INVESTIGATION

SERVICE WATER POND WEST EMBANKMENT

REPORT NO. 2

VIRGIL C. SUMMER NUCLEAR STATION

Prepared for:

SOUTH CAROLINA ELECTRIC & GAS CO.

COLUMBIA, SOUTH CAROLINA

Prepared by:

WOODWARD-CLYDE CONSULTANTS
PLYMOUTH MEETING, PENNSYLVANIA
and
GILBERT ASSOCIATES, INC.
READING, PENNSYLVANIA

SUPPLEMENTAL INVESTIGATION
SERVICE WATER POND WEST EMBANKMENT
REPORT NO. 2
VIRGIL C. SUMMER NUCLEAR STATION

TABLE OF CONTENTS

ATTACHMENTS

LIST OF TABLES

LIST OF FIGURES

1.0 INTRODUCTION

Presented herein is Report No. 2 of the Supplemental Investigation of the as-built condition of the West Embankment at the Virgil C. Summer Nuclear Station. The original report was submitted on March 6, 1981. The purpose of Report No. 2 is to present the results of long-term laboratory tests (with associated engineering analysis) which were incomplete at the time of the initial submittal. This report also includes the results of other tests which were requested to be performed by NRC Staff and addresses various specific concerns expressed by NRC Staff since the initial submittal.

2.0 UNDRAINED CREEP TESTS

A total of four series of undrained creep tests, consisting of three tests per series, were conduced on relatively undisturbed select fill and saprolite samples obtained by means of a 3-inch O.D. thin-walled Shelby tube sampler. A Pitcher sampler was also used to obtain some of the saprolite samples. The selection of specimens, testing loads and data obtained are discussed below.

2.1 SPECIMEN SELECTION AND PREPARATION

The test specimens were selected on the basis of the results of Standard Penetration Resistance (SPR) tests performed in the borings above or below each undisturbed sample. The specimens used for testing had SPR values representative of the range of values measured in the borings. The SPR values of the test specimens from the select fill ranged from 13 to 28 blows per foot and those for the saprolite from 31 to 53 blows per foot.

The test specimens were cut to a length equal to twice the diameter and were not trimmed from the original diameter of 2.87 inches. The specimen ends were carefully trimmed square. As the saprolite specimens were considered likely to contain slickensided fissures, care was taken to prevent separation of the specimens during preparation for testing.

2.2 CREEP DEVIATOR STRESS

The specimens tested were consolidated to the estimated in-situ effective vertical pressure. The specimens were consolidated at least for four days prior to being loaded so that the volumetric deformations due to consolidation pressure would be essentially complete and would not unduly affect the pore pressures during the undrained creep phase of the test.

The specimens were loaded with a deviatoric stress of 30, 50 and 70 percent of their estimated undrained strengths at the appropriate consolidation pressure. To estimate the strength of the specimens for this purpose, the strength data from consolidated undrained ($\overline{CIU}$) triaxial compression tests was utilized. The results of these tests have been presented in Section 4.3 of the original report. To obtain the undrained strength, the $\overline{CIU}$ test data was analyzed in terms of total stress. Linear regression analyses were conducted to determine the average strength of the select fill and saprolite. The results obtained from the regression analyses are as below:

For select fill:

$$(\sigma_1 - \sigma_3)_f = 1.50 + 2\,\sigma_c \tan 26.2^\circ \qquad \text{Eq. (1)}$$

For saprolite:

$$(\sigma_1 - \sigma_3)_f = 1.78 + 2\ \sigma_c \tan 18.4° \qquad \text{Eq. (2)}$$

where: $(\sigma_1 - \sigma_3)_f$ = maximum deviator stress at failure (tsf)
σ_c = consolidation pressure (tsf).

The deviatoric loads were applied to the specimens pneumatically to mitigate any impact load effects. It should be noted that none of the samples failed during the creep tests.

2.3 CREEP TEST DATA

After the deviatoric loads were applied to the specimens, deformations were monitored with time. The duration of all the tests was 28 days or longer (approximately 40,000 minutes). The test results, in the form of plots of deformation vs. time are included in Appendix A. After 28 days of creep loading, the specimens were failed to determine the actual undrained strength of each specimen and, thus, the actual percentage of the failure load that the creep load represented. In some cases the creep stress ratio was much lower than planned because the samples were much stronger than estimated. The strength tests were controlled stress tests with the deviator loads being imposed in small steps. Stress-strain curves from these tests are also presented in Appendix A.

At the end of the test, each specimen was analyzed for grain size distribution, unit weight, Atterberg limits and specific gravity. This data is presented in Appendix A.

2.4 ANALYSIS OF CREEP TEST DATA

The creep test data was analyzed following procedures

described by Singh and Mitchell[1]. The stress-strain-time functions proposed by Singh and Mitchell are:

$$\varepsilon = a + \frac{A}{1-m} e^{\alpha D} t^{(1-m)} \quad (m \neq 1) \qquad \text{Eq. (3)}$$

$$\varepsilon = \varepsilon_1 + A \cdot e^{\alpha D} \ln(t) \quad (m = 1, t > 1) \qquad \text{Eq. (4)}$$

where:
ε = strain at any time t
D = ratio of deviatoric stress to failure stress
m, α, A = constants depending upon material properties
a, ε_1 = integration constants
e = base of natural logarithms

In the above relationship the three parameters m, α and A are evaluated from the laboratory experimental data. The procedure which was followed to determine the values of these parameters is outlined briefly as follows:

Step 1. Deformations were plotted against time and a smooth curve passed through the data points. Any abrupt changes in deformations which are believed to be due to disturbance, temperature change or fluctuations in pneumatic pressure were ignored. This data is shown in Appendix A.

Step 2. The strain rates ($\dot{\varepsilon}$) at various values of time were computed mathematically:

$$\dot{\varepsilon} = \frac{\varepsilon_2 - \varepsilon_1}{t_2 - t_1} \text{ at } t = (t_2 + t_1)/2$$

and the strain rates were then plotted against time on log-log graphs. These plots are shown on Figures 1 through 12. Straight lines were fitted to the data using linear regression analyses. The slopes of these straight lines give the values of "m" for each test.

---

(1) Singh, A. and Mitchell, J.K. (1968) "General Stress-Strain-Time Function for Soils", Journal of the Soil Mechanics and Foundations Division, ASCE, Vol. 94, No. 1, January, pp. 21-46.

Step 3: Values of strain rates at a known time (i.e. t = 1 minute) were determined for each test from the regression analyses in Step 2. This value has been denoted as ε_o. The values of ε_o versus the value of corresponding D were then plotted, as shown in Figures 13 and 14. A best fit line was drawn through these points, again using linear regression analysis. The slope of this line is the value of α and its intercept at D = 0 is the value of A. The value of D was calculated using the failure stress obtained at the end of the creep test for each specimen.

2.5 CREEP TEST PARAMETERS

Using the method described in the previous section, the following creep test parameters were obtained:

Select fill:
$A = 2.13 \times 10^{-3}$ %/min
$\alpha = 1.695$
$m = 0.819$ (average)

Saprolite:
$A = 3.66 \times 10^{-3}$ %/min
$\alpha = 1.415$
$m = 0.847$ (average)

3.0 SUPPLEMENTAL LABORATORY TESTING

In addition to the creep tests, isotropically consolidated-undrained ($\overline{CIU}$) triaxial compression tests (with pore pressure measurements) were conducted on samples of select fill from Borings WE-14 and WE-15. These borings were located adjacent to the Service Water Intake Structure. The samples selected for

testing were those within the backfill zone of the structure, where Standard Penetration Resistance (SPR) values were found in the borings to range from 4 to 9 blows per foot.

The test results are included in Appendix A. On Figure 15 the test results are summarized and compared with the design shear strength of the West Embankment as well as the results of other tests conducted on samples with higher SPR values. It was found that the effective stress shear strength of the lower SPR soil was similar to that of the previously tested samples and exceeded the strength used for design in all cases.

An unconfined compression test was also conducted on a sample from Boring WE-14 which yielded a compressive strength of 1.2 tons per square foot. While there is no specific design requirement for unconfined compressive strength for this project, this value is representative of a stiff[(2)] material. The design value for unconsolidated-undrained (UU) compressive strength without confinement is 1.6 tons per square foot, but this was for unsaturated samples at the end-of-construction condition. The unconfined compressive strength would be expected to be lower after saturation.

Physical property tests were also conducted on samples of the select fill from Borings WE-14 and WE-15, at depths which are above the base of the Service Water Intake Structure. The test results, shown in Appendix A and summarized in Table 1, indicate that the average moisture content of the select fill in the backfill zone of the structure is about 3.5 percentage points higher than the average moisture content in the deep fill under the crest of the West Embankment. However, this backfill area is completely submerged and has relatively little vertical confinement. This area would, therefore, be expected to exhibit more

---

(2) Terzaghi, K. and Peck, R.B. (1967) Soil Mechanics in Engineering Practice, John Wiley & Sons, New York, p. 30.

swelling, and hence a higher moisture content, than the deep fill area. Also, some of the samples indicated a plasticity index in the range of 13 to 28 percent, whereas all of the samples obtained from the mass fill were non-plastic.

4.0 ANALYSIS OF CREEP SETTLEMENT

4.1 CREEP DEFORMATION CALCULATIONS

Creep settlements expected under the Service Water Pumphouse and Intake Structure during the 40-year projected life of the nuclear plant were estimated using the creep characteristics of the select fill and saprolite obtained from the creep tests described in detail in Section 2.0. The Pumphouse weight is approximately equal to the weight of soil displaced, and thus, for stress calculations the presence of the Pumphouse does not need to be considered. The stresses within the West Embankment were estimated using vertical and horizontal stress contours for embankments by Poulos, Brooker and Ring[3] for a 1.7:1 slope. The value of deviatoric stress was obtained as the difference in the vertical and horizontal stresses, $(\sigma_1 - \sigma_3)$, at a particular level. The value of the failure stress, $(\sigma_1 - \sigma_3)_f$, was estimated based on the design shear strength and the horizontal stress at each level. The embankment and underlying saprolite were divided into seven layers below the Pumphouse for this purpose. This method of analysis does not take into account the effect of rotation of principal planes in the embankment slope, but this assumption is believed to be reasonable. Since the slope inclination of the West Embankment is 3:1 as compared to a 1.7:1 slope, the deviatoric stresses computed are conservative.

The value of D, the stress ratio, was obtained at each level for the seven layers as $(\sigma_1 - \sigma_3)/(\sigma_1 - \sigma_3)_f$ and the expected creep strains were calculated for each layer using Equation (3). The constant of integration, which represents instantaneous strain

---

(3) Poulous, H.G., Booker, J.R. and Ring G.J. (1972), "Simplified Calculations of Embankment Deformation," Soils and Foundations, Vol. 12, No. 4, pp. 1-17.

at time zero, was eliminated by considering a finite time period beginning at a time other than time zero. Equation (3) then becomes:

$$\varepsilon_2 - \varepsilon_1 = \frac{A}{1-m} e^{\alpha D}(t_2^{1-m} - t_1^{1-m}) \qquad \text{Eq. (5)}$$

The time period selected was from t_1 = 4 years to t_2 = 44 years. (In the actual calculations the base of natural logarithms, e, was replaced with the base of common logarithms, 10, since all data reduction was performed using common logarithm graph paper.) The strains were then converted to settlements by multiplying by the height of each layer. The creep settlements for the Pumphouse and the Intake Structure were then estimated by summing the deformation of soil layers under each structure.

The magnitude of undrained creep computed for the Pumphouse, assuming a 1.7:1 slope angle, is about 4.0 inches. However, using the same method, the magnitude of creep for level ground is computed to be about 3.0 inches. Since undrained creep does not occur in the level ground situation because of lateral restraint, it is believed that the actual undrained creep in the field, if any, would more likely be the difference between these values, or about 1.0 inch. The creep settlement of the Pumphouse end of the Intake Structure was calculated to be about 2/3 of that of the Pumphouse.

If 4.0 inches of creep settlement were to occur during the next 40 years, which may be considered to be a conservative upper bound estimate, the theory indicates that the present rate of creep settlement for the Pumphouse would be about 0.3 inches per year, decreasing gradually to about 0.2 inches per year during the next 6 years. This amount of settlement would be readily detected by the existing monitoring system. The actual recorded movement of the Pumphouse and the west end of the Intake Structure for the 12 months from March 1980 through March 1981 has been 0.09 inches and 0.04 inches, respectively, upwards (rebound). Thus, there is no

evidence of creep occurring beneath the Pumphouse almost four years after the completion of construction in the area.

4.2 DISCUSSION OF RESULTS

The creep deformations calculated in Section 4.1 are believed to be very conservative estimates. The reasons for this are discussed below.

4.2.1 Creep Parameters: The creep parameters used in the analysis were obtained from undrained tests. During the undrained tests the pore pressure continues to increase and the stress path moves toward the Mohr-Coulomb yield criterion. The actual field conditions, however, allow the dissipation of all construction pore pressures after a certain time has elapsed. The use of undrained creep parameters will therefore yield conservative estimates of future creep deformation.

4.2.2 Effect of Groundwater: The groundwater level in the embankment has been raised to about elevation 420 due to filling of the Service Water Pond. This has resulted in the reduction of effective stresses, constituting unloading. The unloading is resulting in rebound of the Pumphouse and Intake Structure. This stress history was not simulated in the laboratory creep tests, which would probably significantly reduce any creep deformations.

4.2.3 Lack of Similitude: The creep tests were conducted under triaxial test conditions, wherein the test samples were permitted to strain laterally. In the field, the soils beneath the Pumphouse and the heavily loaded portion of the Intake Structure are confined laterally and significant creep deformations can occur only as a result of secondary compression. Based on one-dimensional oedometer tests conducted previously it is estimated that future secondary compression will not exceed about 0.7 to 1.2

inch.

4.2.4 Lack of Verification: The theory of creep settlements is based on laboratory testing and the literature is not known to contain any field verification data for conditions similar to the West Embankment. Therefore, the level of confidence in the upper bound estimate is low, and it is believed that any actual creep settlement which occurs would be much smaller. It is expected that the creep settlement will not exceed about one inch during the project life of the structure, if it occurs at all.

5.0 SELECT FILL INTRUSION POTENTIAL

Cracks which occurred in the Service Water Intake Structure due to excessive settlement were grouted during December, 1977 and January, 1978. All cracks having widths greater than 0.012 inches were grouted. Although it is considered unlikely that any future significant cracking will occur, the intrusion potential of the compacted select fill through open cracks has been evaluated. This evaluation is described in the following subsections.

5.1 ASSUMPTIONS

For the purpose of this analysis, it was assumed that unfilled open cracks could exist above the base anywhere along the 167-feet length of the Intake Structure. It was also very conservatively postulated that the width of any crack could be as large as 1/2 inch. The flow velocity of water through the Intake Structure under emergency operating conditions will be less than 0.5 feet per second and, therefore, no turbulent flow is expected within the cracks.

5.2 PUBLISHED DATA

In 1967, Broms and Bennermark[4] conducted laboratory extrusion tests by applying various vertical pressures to undisturbed samples contained within a brass liner with a circular hole of 0.4 to 0.8 inches in diameter at mid-height. Other tests were conducted by applying various vertical pressures to remolded, large diameter samples containing a central, hollow brass cylinder with a circular hole of 0.4 to 1.6 inches in diameter on its side. The results of these tests, summarized in Figure 16, indicate that when the ratio of the applied effective vertical stress, $(\sigma_o - p_o)_f$, to the undrained shear strength, S_u (also referred to as c_u), is equal to 6 or greater clay extrusion occurred.

The results of field observations on clay extrusion problems in sheeted retaining walls and tunnel walls and liners were also reported in the same paper by Broms and Bennermark, as shown by Figure 17, and in 1969 by Peck[5], as shown in Figure 18. These observations indicate that when the ratio of the effective overburden pressure to the undrained shear strength was between 5 and 6 slight squeezing of the clay was observed, but the system was stable. However, when the ratio was greater than 6, the system was unstable and excessive squeeze of the clay was encountered. In addition, Broms and Bjerke[6] reached the same conclusion based on the extrusion of soft clay through a retaining wall with an opening of 1.5 meters by 2 meters.

5.3 UNDRAINED SHEAR STRENGTH OF EMBANKMENT MATERIALS

The undrained shear strengths of the West Embankment materials obtained from the isotropically consolidated undrained

---

(4) Broms, B.B. and Bennermark, H. (1967), "Stability of Clay at Vertical Openings", Proc. Am. Soc. Civ. Eng., Journal of the Soil Mech. and Found. Div., Vol. 93, No. SM1, pp. 71-94.

(5) Peck, R.B. (1969), "Deep Excavations and Tunneling in Soft Ground", Proc. 7th Int. Conf., Soil Mech. and Found. Eng., Mexico, State-of-the-Art Volume, pp. 225-290.

(6) Broms, B.B. and Bjerke, H. (1973), "Extrusion of Soft Clay through a Retaining Wall", Canadian Geotechnical Journal Vol. 10, pp. 103-109.

triaxial compression tests ($\overline{CIU}$) are summarized in Figure 19 as a function of the effective confining pressure ($\bar{\sigma}_{fc}$). Also shown on that figure is the shear strength from an unconfined compression test ($\bar{\sigma}_{fc} = 0$). From the $\overline{CIU}$ results, the lower bound undrained shear strength is conservatively estimated as:

$$S_u = \frac{(\sigma_1 - \sigma_3)_f}{2} = 0.5 + \bar{\sigma}_{fc} \tan 26.2° \qquad \text{Eq. (6)}$$

where: S_u = undrained shear strength, tsf

$(\sigma_1 - \sigma_3)_f$ = principal stress difference at failure, tsf

$\bar{\sigma}_{fc}$ = effective confining pressure, tsf

In Eq. (6), $\bar{\sigma}_{fc} = 0$ represents the case of unconfined compression.

5.4 INTRUSION POTENTIAL

The intrusion potential of the embankment material above the base or the top of the Intake Structure is summarized in Figure 20 in terms of the effective overburden pressure ($\bar{\sigma}_{vo}$) and 6 times the undrained shear strength ($6S_u$) for various fill thicknesses. It is shown that $6S_u$ is considerably greater than $\bar{\sigma}_{vo}$ for all fill thicknesses for both the $\overline{CIU}$ strength, which includes the confinement effect, and the unconfined strength, which conservatively neglects the confinement effect. Therefore, it is concluded that there will not be any soil extrusion through any postulated crack in the Service Water Intake Structure.

5.5 ADDITIONAL CONSIDERATIONS

Aside from the squeezing of soil into a crack because of overburden stress, additional modes of soil infiltration could be postulated, consisting of dispersion and erosion. However, dispersion tests conducted on the select fill during construction

determined that the soil is non-dispersive and resistant to erosion, as described in FSAR Section 2.5.6.4.6.5. The water pressure in the Intake Structure and the pore water pressure in the soil are essentially the same. Both are essentially equivalent to the hydraulic head in the Service Water Pond, except for the slight differential due to the flow of water through the Intake Structure at a rate of less than 0.5 feet per second. Thus, there would be no significant gradient or water flow into a crack from the outside of the structure and no potential for erosion.

6.0 STABILITY ANALYSIS

At the request of NRC Staff, a static stability analysis and parametric study was conducted for the West Embankment. The purpose of the study was to determine the influence on the stability of the embankment if the shear strength of the soil in the backfill zone of the Intake Structure was reduced to a value below the design strength.

The results of this analysis, conducted using the simplified Bishop method of slices, are shown on Figure 21. For all cases, the minimum factor of safety was found at the maximum permissible depth of the trial failure arcs, i.e., elevation 367, the base of the Intake Structure slab. A typical failure arc is shown on Figure 21. For the design shear strength of $\bar{c}$ = 300 psf and $\bar{\emptyset}$ = 28 degrees, the static factor of safety was found to be 2.41. For assumed values of 60 percent and 40 percent of the design shear strength the factors of safety were found to be 1.46 and 0.96, respectively. (It should be noted that for these parametric studies, the shear strength was very conservatively reduced along the entire failure arc, not just in the backfill zone adjacent to the Intake Structure.) From these results, an actual shear strength of 52 percent of the design shear strength would provide a static factor of safety of 1.3, which is the design criteria for the West Embankment slope. However, laboratory testing of samples from

Borings WE-14 and WE-15, adjacent to the Intake Structure, indicate that the shear strength in this area actually exceeds the design shear strength, as described in Section 3.0. It is concluded, therefore, that a slope failure will not occur adjacent to the Service Water Intake Structure.

7.0 CONCLUSIONS

Based on the data presented in the previous sections of this report, the following conclusions have been determined:

A. The future settlement of the Service Water Pumphouse and Intake Structure due to soil creep during the life of the nuclear plant is estimated to be not more than about 1 inch. This amount is about equal to the rebound which has occurred since filling of the Service Water Pond and would not be detrimental to the structures. It is believed, however, that undrained creep deformations would be negligible due to the lateral constraint of the soil beneath the structures and that any settlement which occurs would actually be due to secondary compression.

B. The shear strength of the select fill in the backfill zone of the Service Water Pumphouse exceeds design requirements. The shear strength could be considerably reduced and still provide an adequate factor of safety, however.

C. Soil intrusion through a postulated 0.5-inch crack in the Service Water Intake Structure will not occur.

TABLES

TABLE 1

SUMMARY OF PHYSICAL PROPERTY TESTS OF SELECT FILL

Property	No. of Tests	Maximum	Minimum	Average
Borings WE-18 and WE-19[a]:				
Water Content (%)	17	35.7	20.8	27.0
Liquid Limit (%)	17	NP	NP	NP
Plasticity Index (%)	17	NP	NP	NP
Specific Gravity	17	2.76	2.58	2.69
Unit Dry Weight (pcf)	17	105.5	83.5	95.6
Degree of Saturation (%)	17	100.0	89.1	95.6
Borings WE-14 and WE-15[b]:				
Water Content (%)	22	37.6	24.7	30.5
Liquid Limit (%)	9	70	NP	----
Plasticity Index (%)	9	28	NP	----
Specific Gravity	5	2.73	2.65	2.69
Unit Dry Weight (pcf)	5	98.9	85.7	91.1
Degree of Saturation (%)	5	100.0	95.3	97.9

Notes: (a) Borings WE-18 and WE-19 are located on the crest of the West Embankment.

(b) Borings WE-14 and WE-15 are located in the backfill zone of the Service Water Intake Structure.

FIGURES

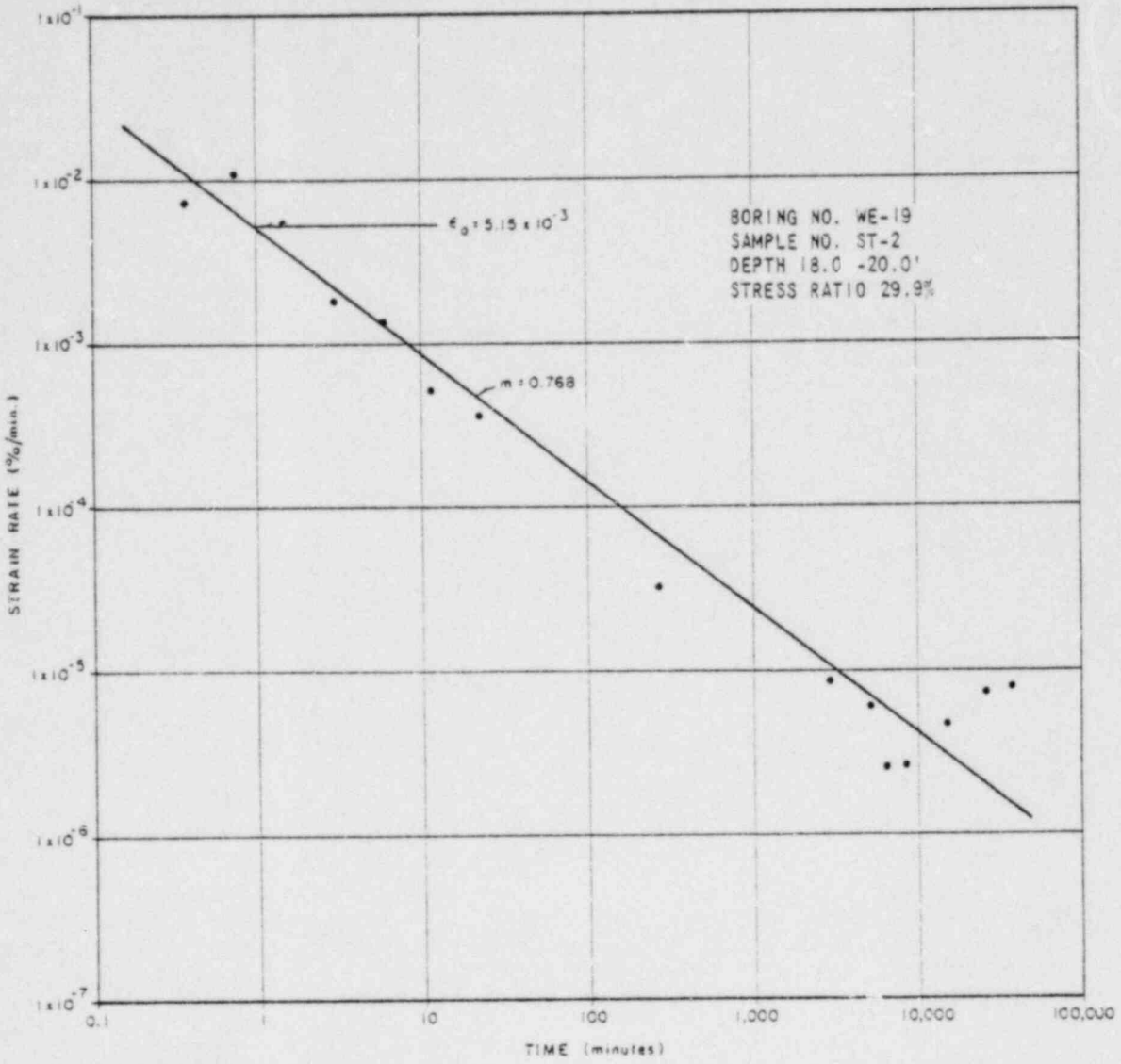

UNDRAINED CREEP TEST
SELECT FILL
VIRGIL C. SUMMER NUCLEAR STATION

FIGURE 1

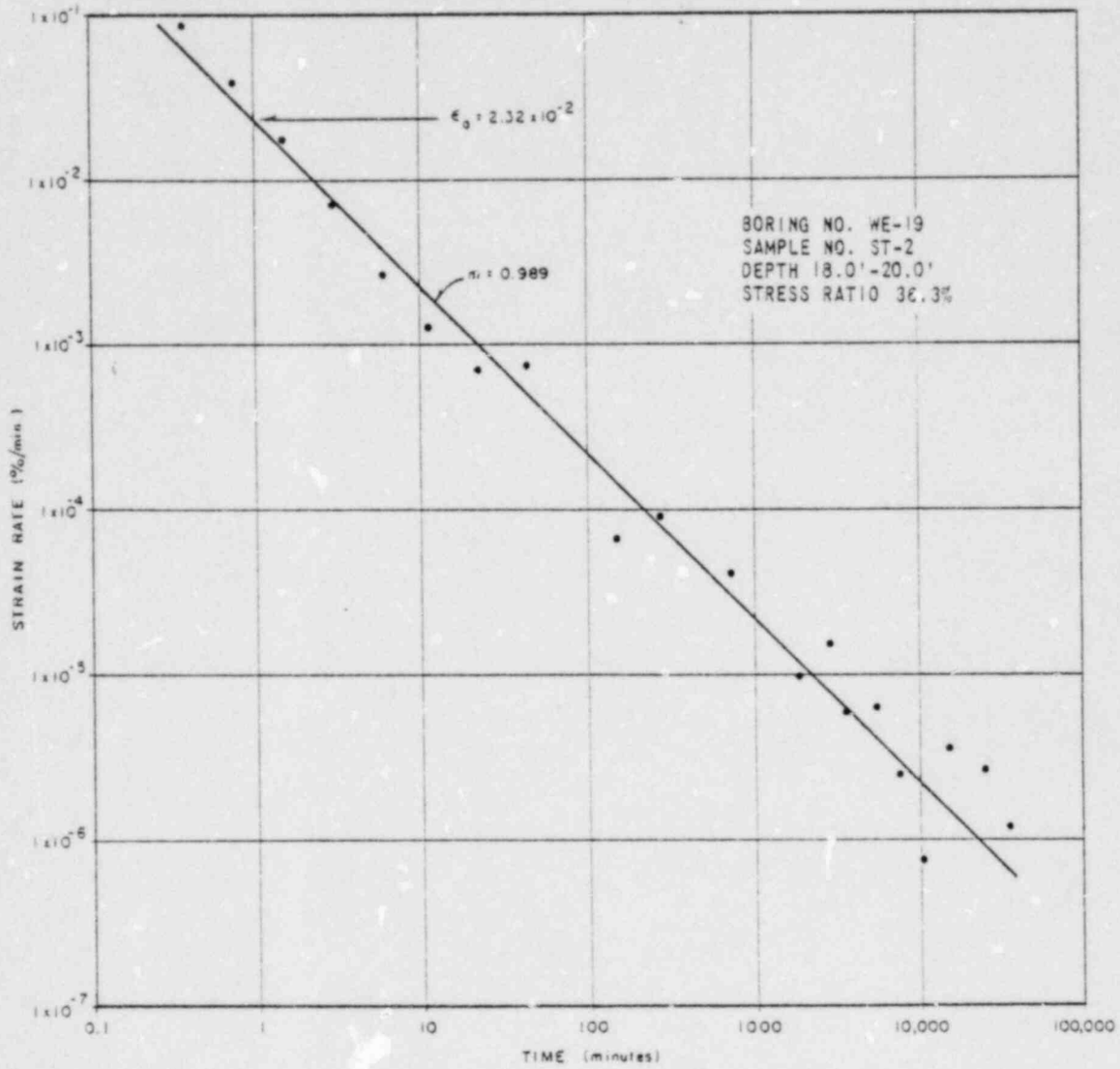

UNDRAINED CREEP TEST
SELECT FILL
VIRGIL C. SUMMER NUCLEAR STATION

FIGURE 2

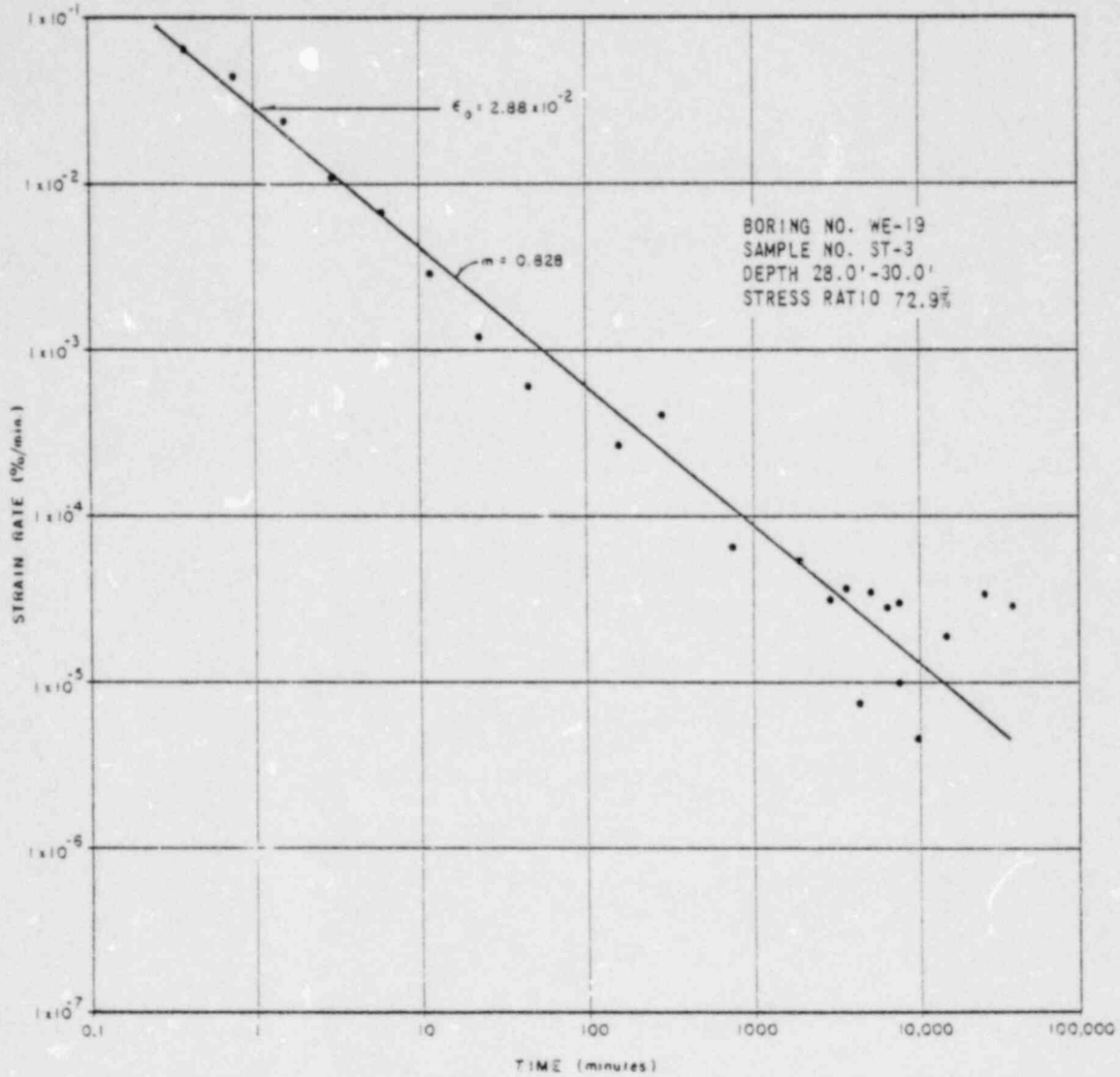

UNDRAINED CREEP TEST
SELECT FILL
VIRGIL C. SUMMER NUCLEAR STATION

FIGURE 3

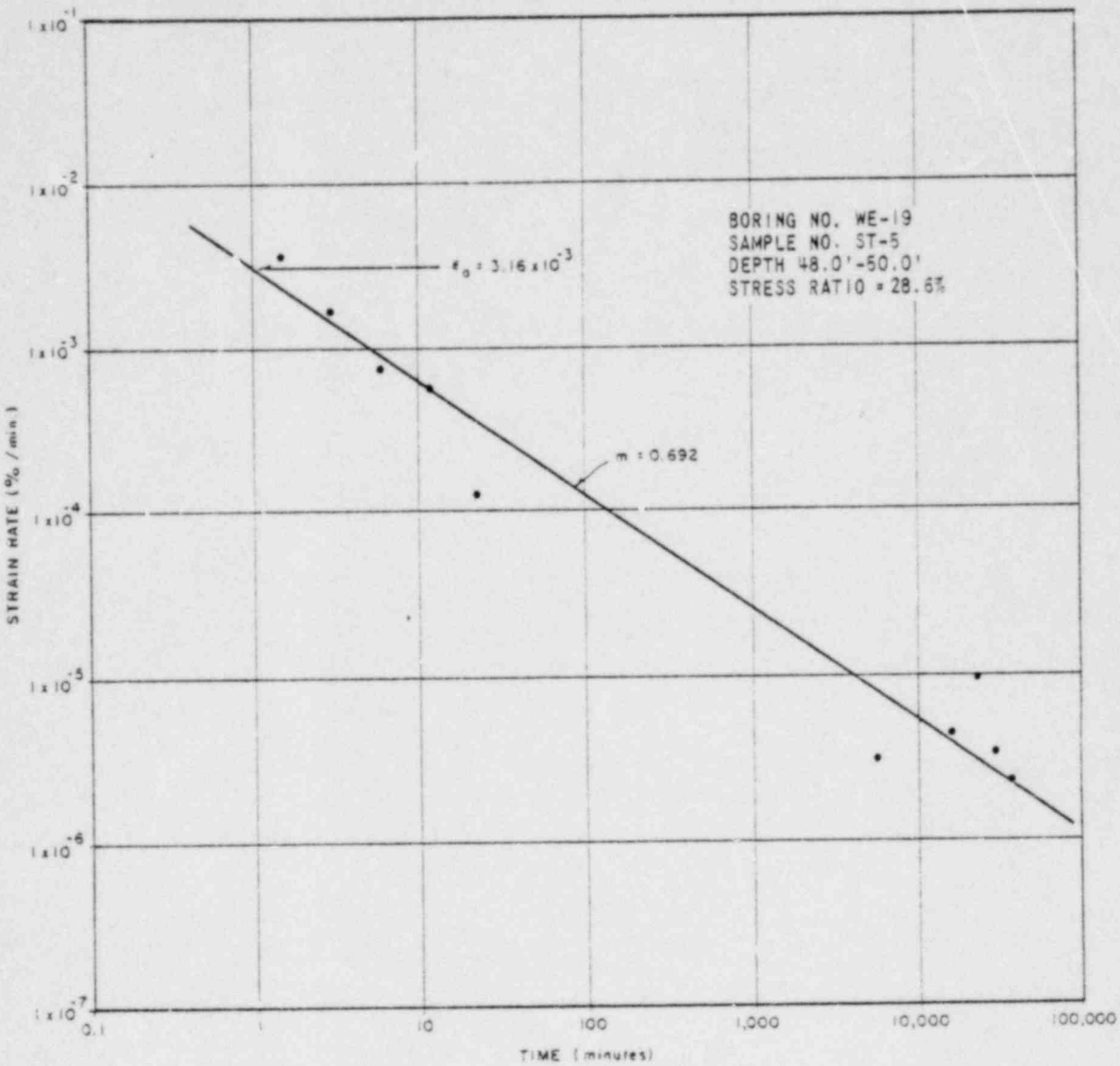

UNDRAINED CREEP TEST
SELECT FILL
VIRGIL C. SUMMER NUCLEAR STATION

FIGURE 4

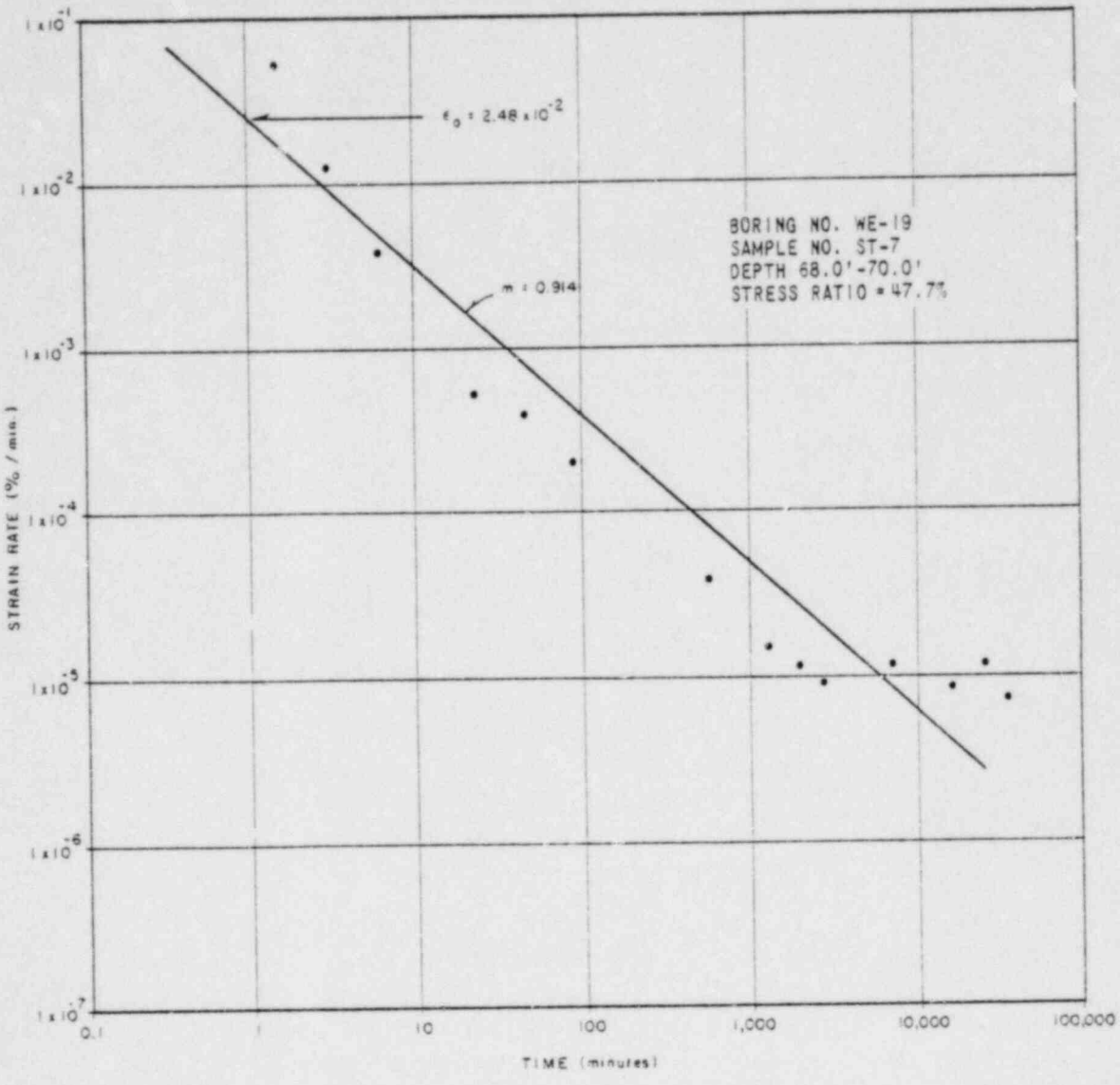

UNDRAINED CREEP TEST
SELECT FILL
VIRGIL C. SUMMER NUCLEAR STATION

FIGURE 5

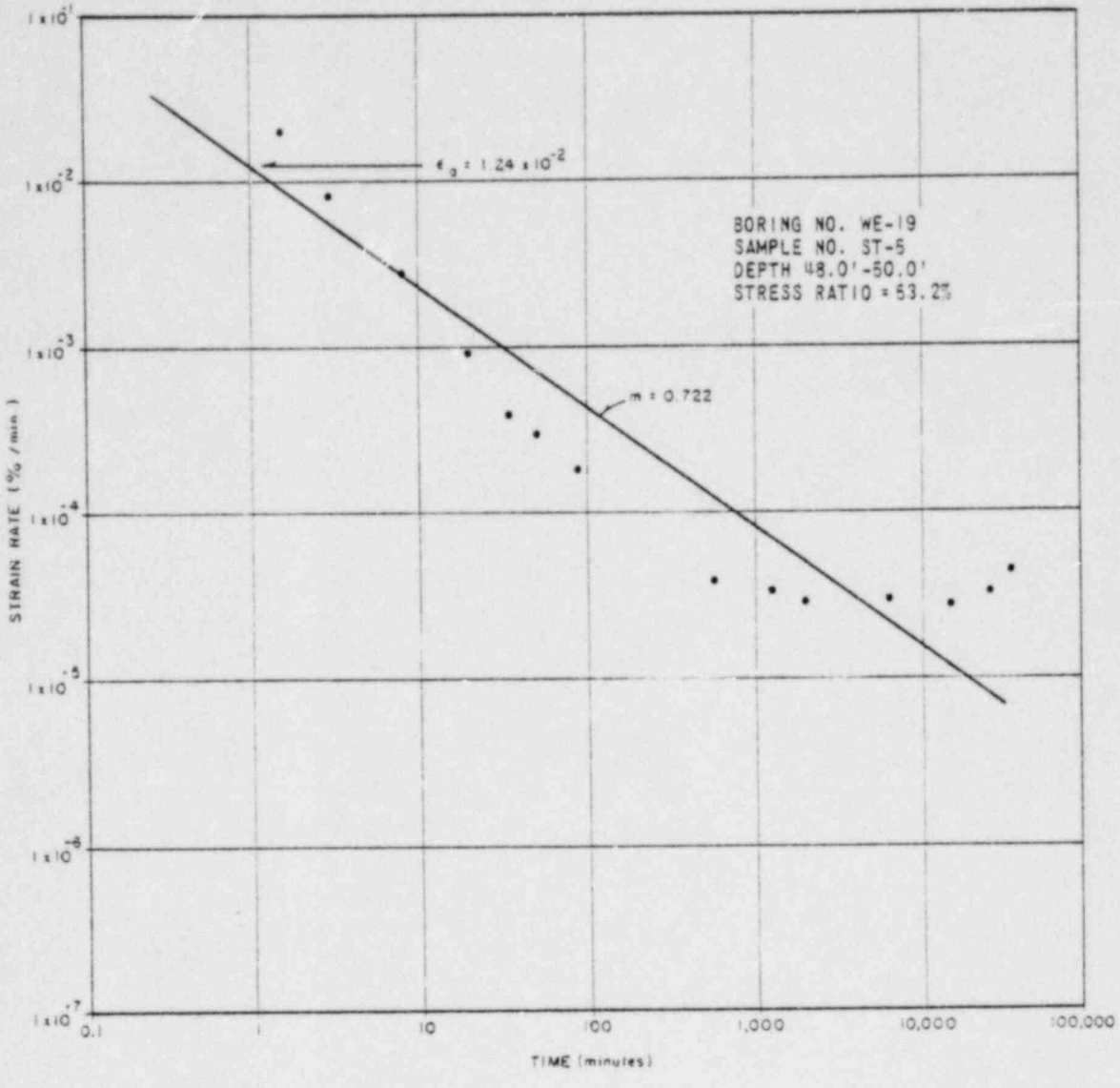

UNDRAINED CREEP TEST
SELECT FILL
VIRGIL C. SUMMER NUCLEAR STATION

FIGURE 6

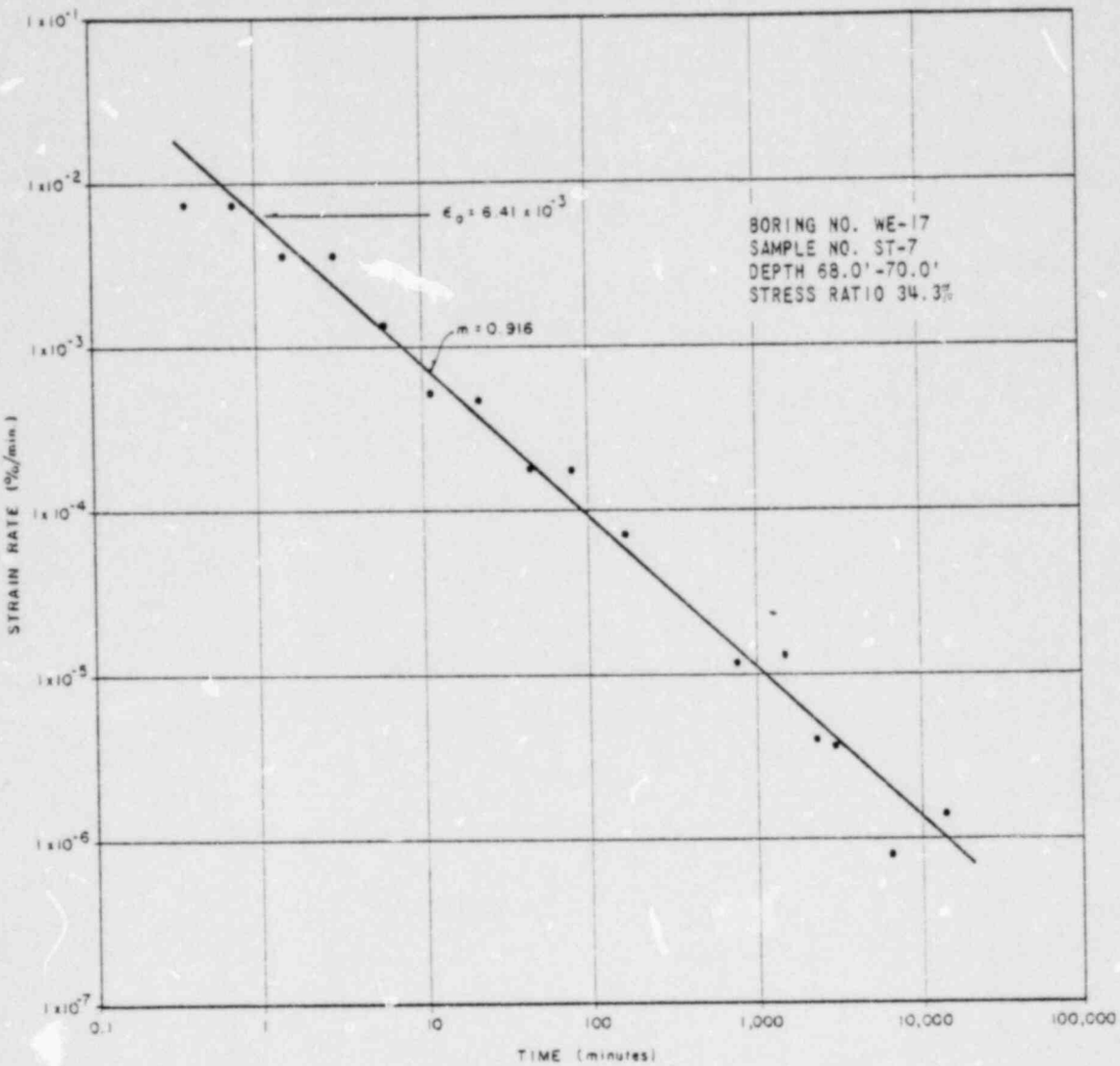

UNDRAINED CREEP TEST
SAPROLITE
VIRGIL C. SUMMER NUCLEAR STATION

FIGURE 7

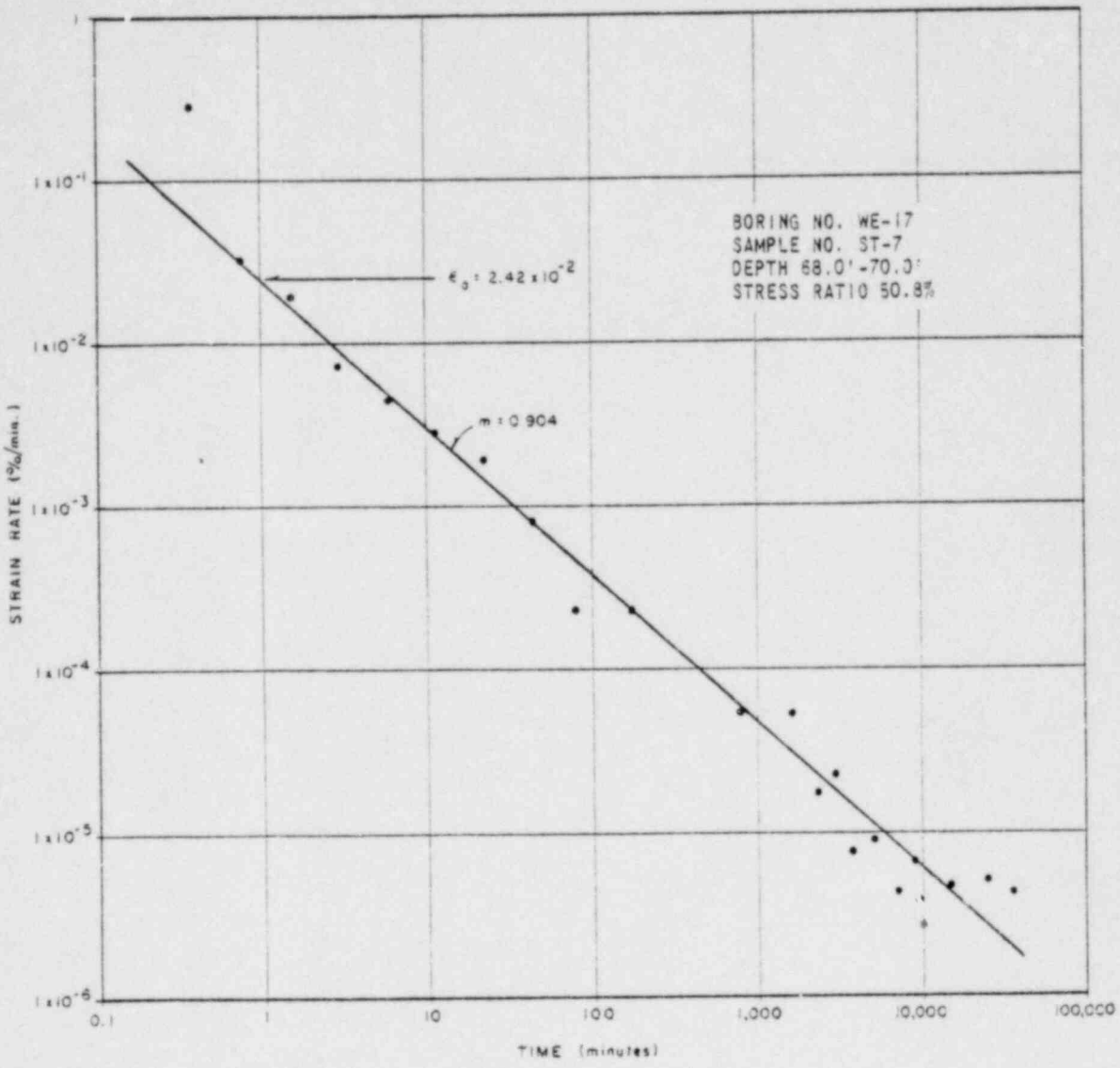

UNDRAINED CREEP TEST
SAPROLITE
VIRGIL C. SUMMER NUCLEAR STATION

FIGURE 8

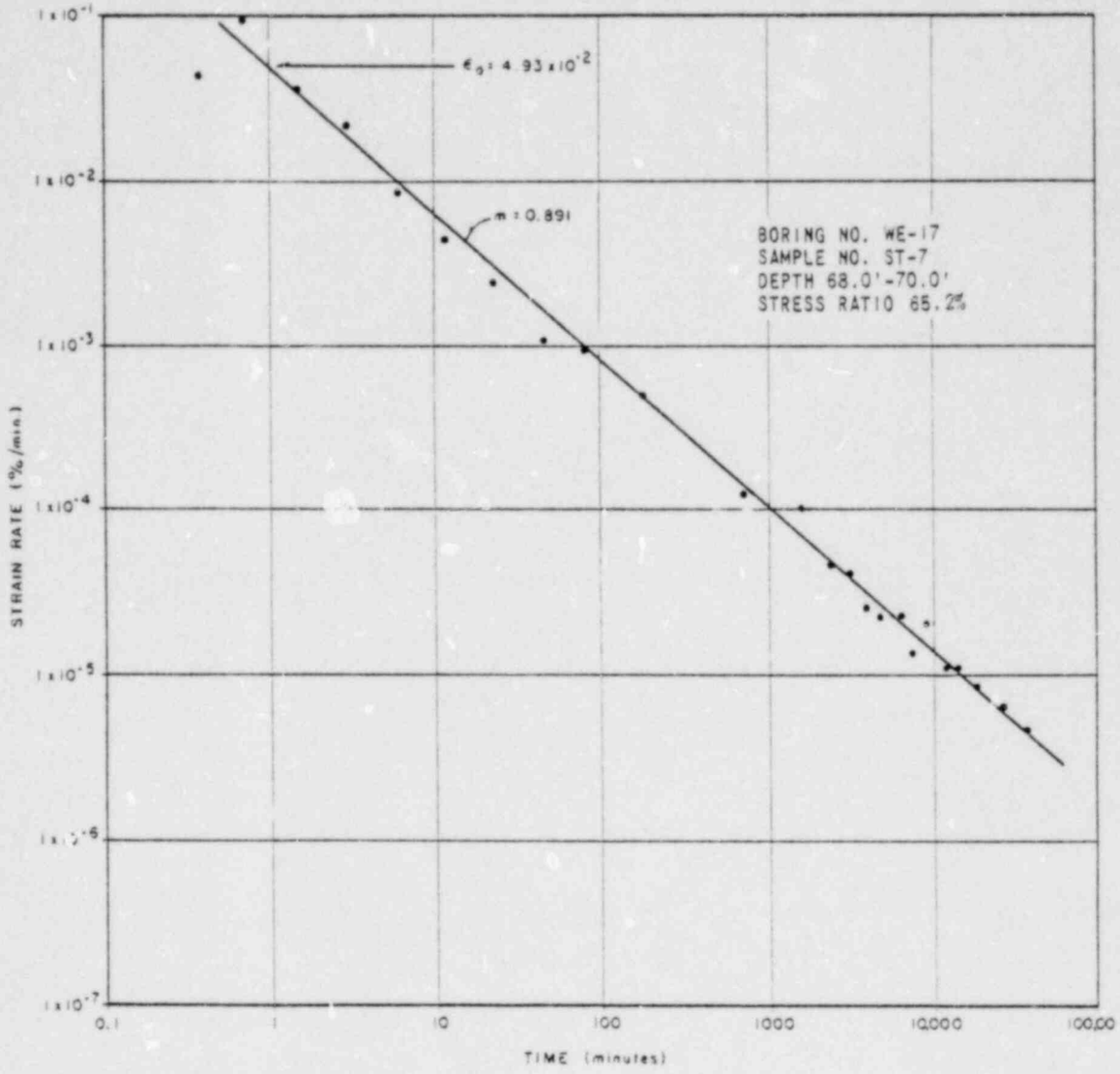

UNDRAINED CREEP TEST
SAPROLITE
VIRGIL C. SUMMER NUCLEAR STATION

FIGURE 9

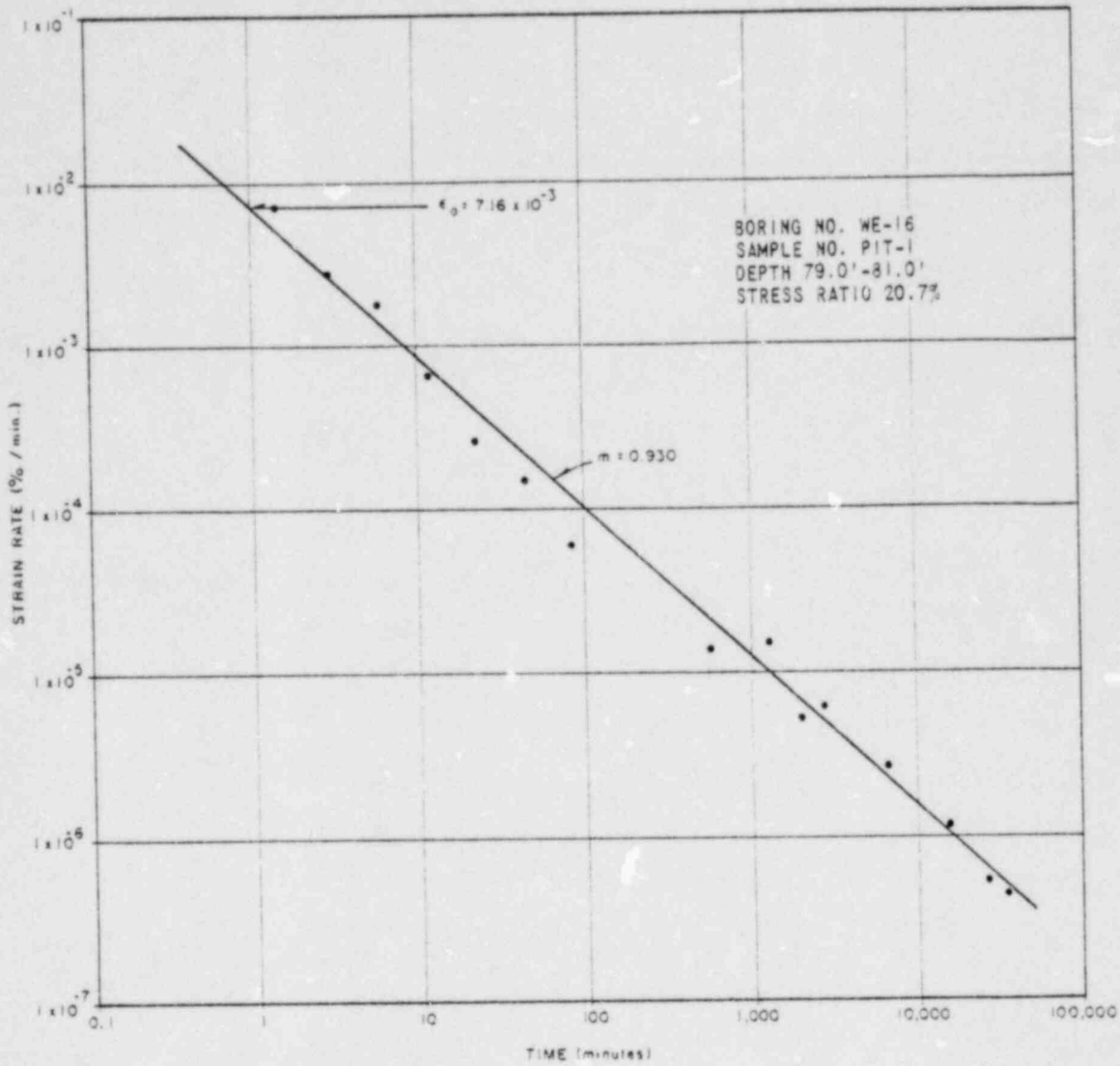

UNDRAINED CREEP TEST
SAPROLITE
VIRGIL C. SUMMER NUCLEAR STATION

FIGURE 10

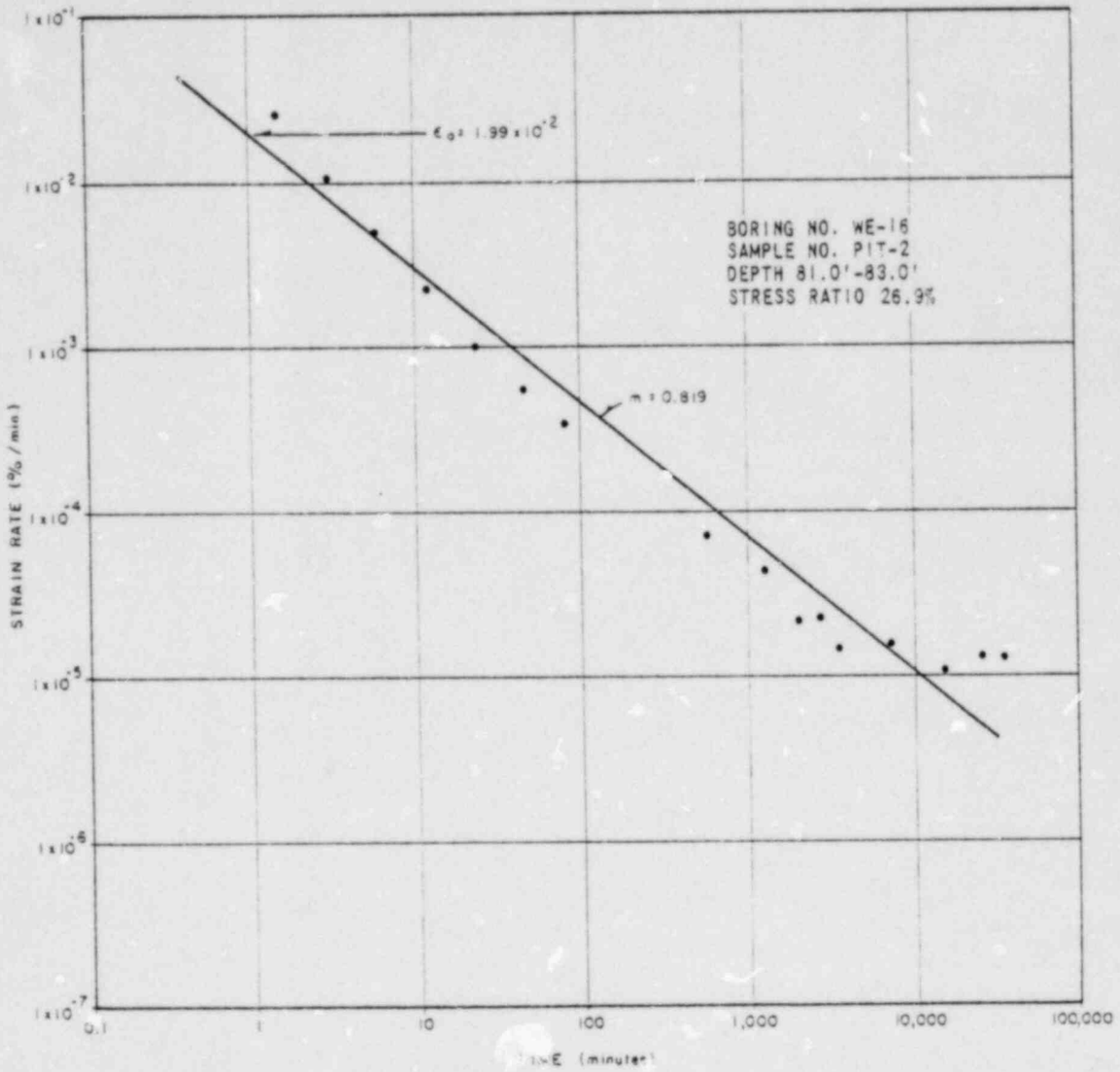

UNDRAINED CREEP TEST
SAPROLITE
VIRGIL C. SUMMER NUCLEAR STATION

FIGURE 11

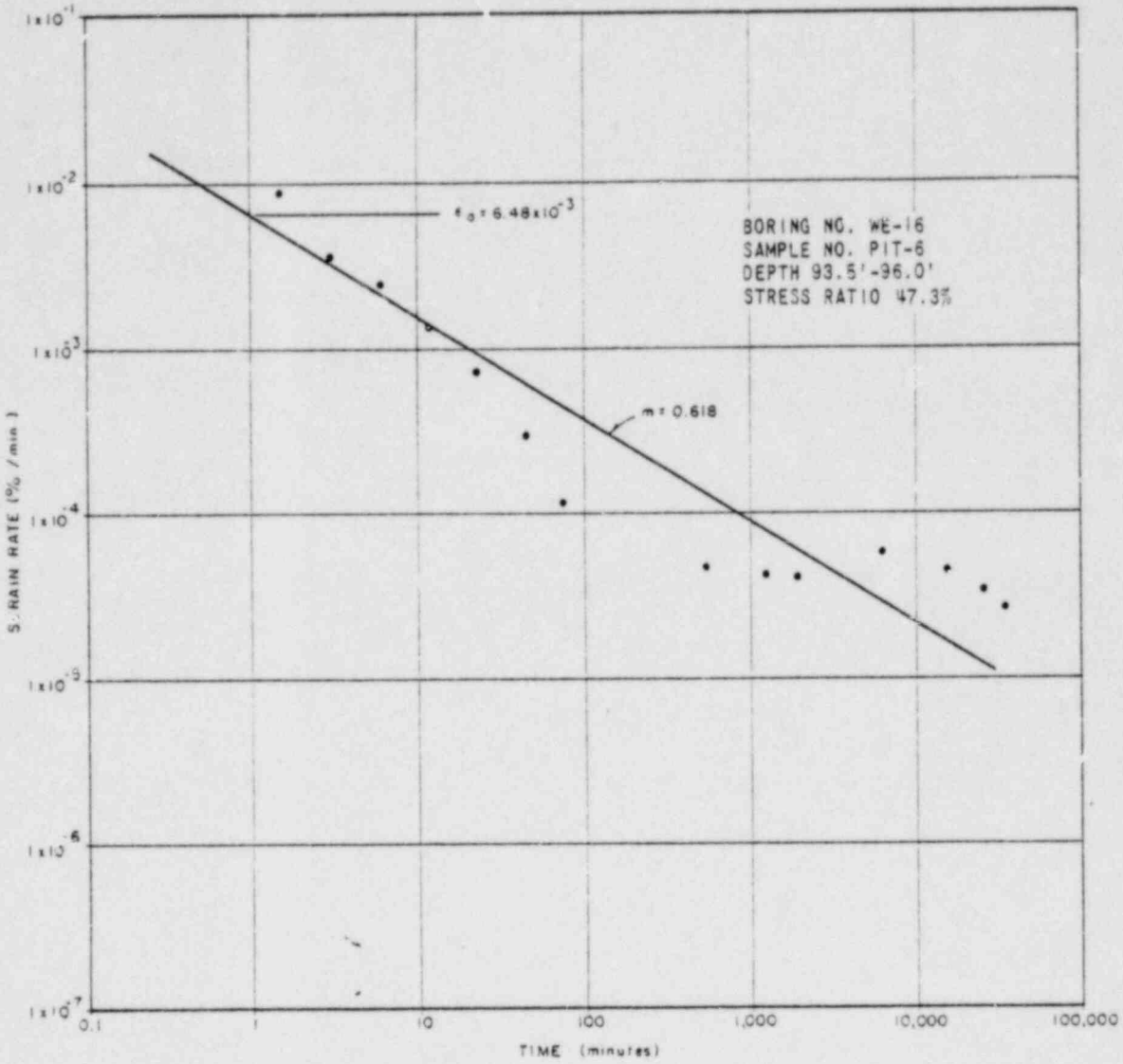

UNDRAINED CREEP TEST
SAPROLITE
VIRGIL C. SUMMER NUCLEAR STATION

FIGURE 12

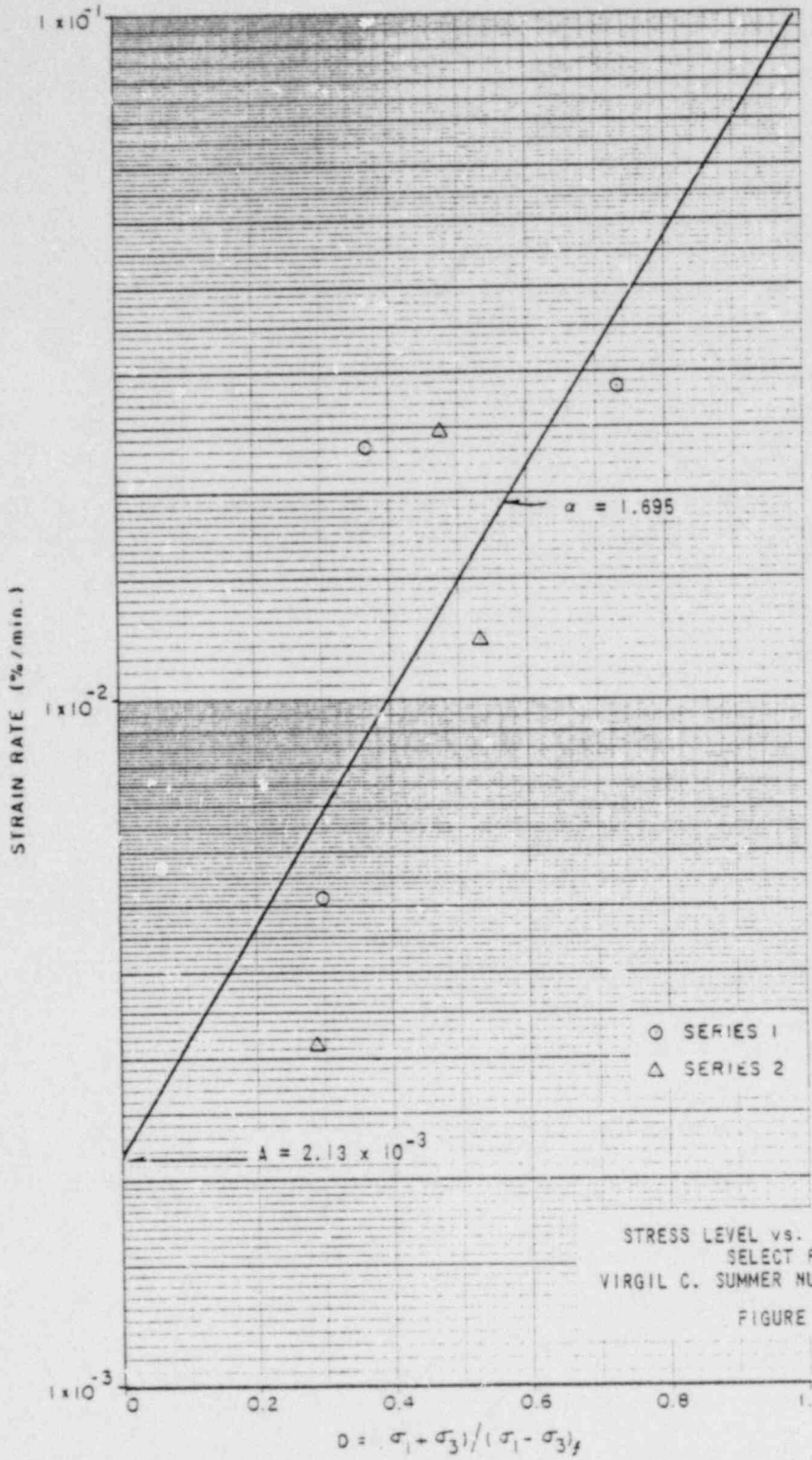

STRESS LEVEL vs. STRAIN RATE
SELECT FILL
VIRGIL C. SUMMER NUCLEAR STATION

FIGURE 13

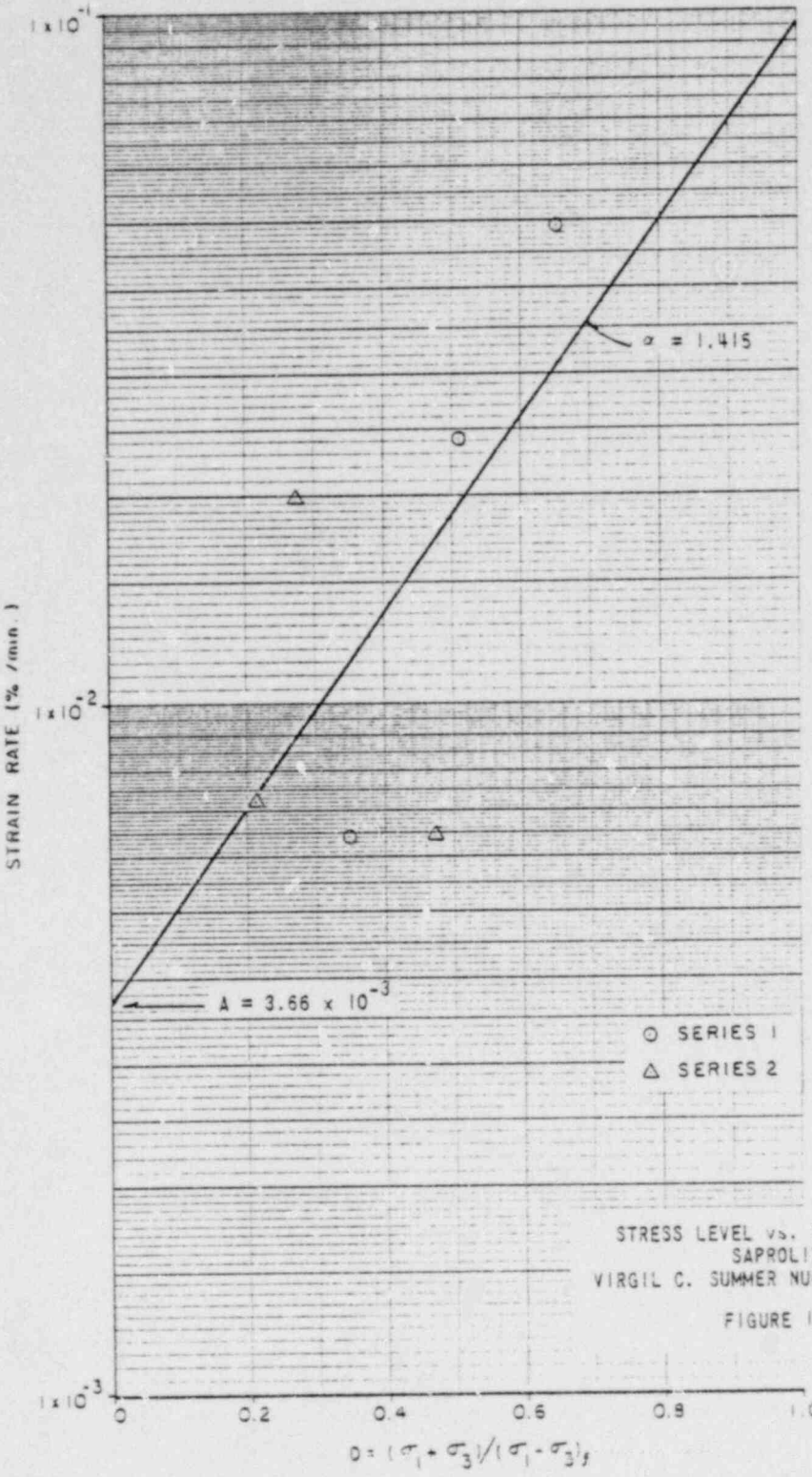

STRESS LEVEL vs. STRAIN RATE
SAPROLITE
VIRGIL C. SUMMER NUCLEAR STATION

FIGURE 14

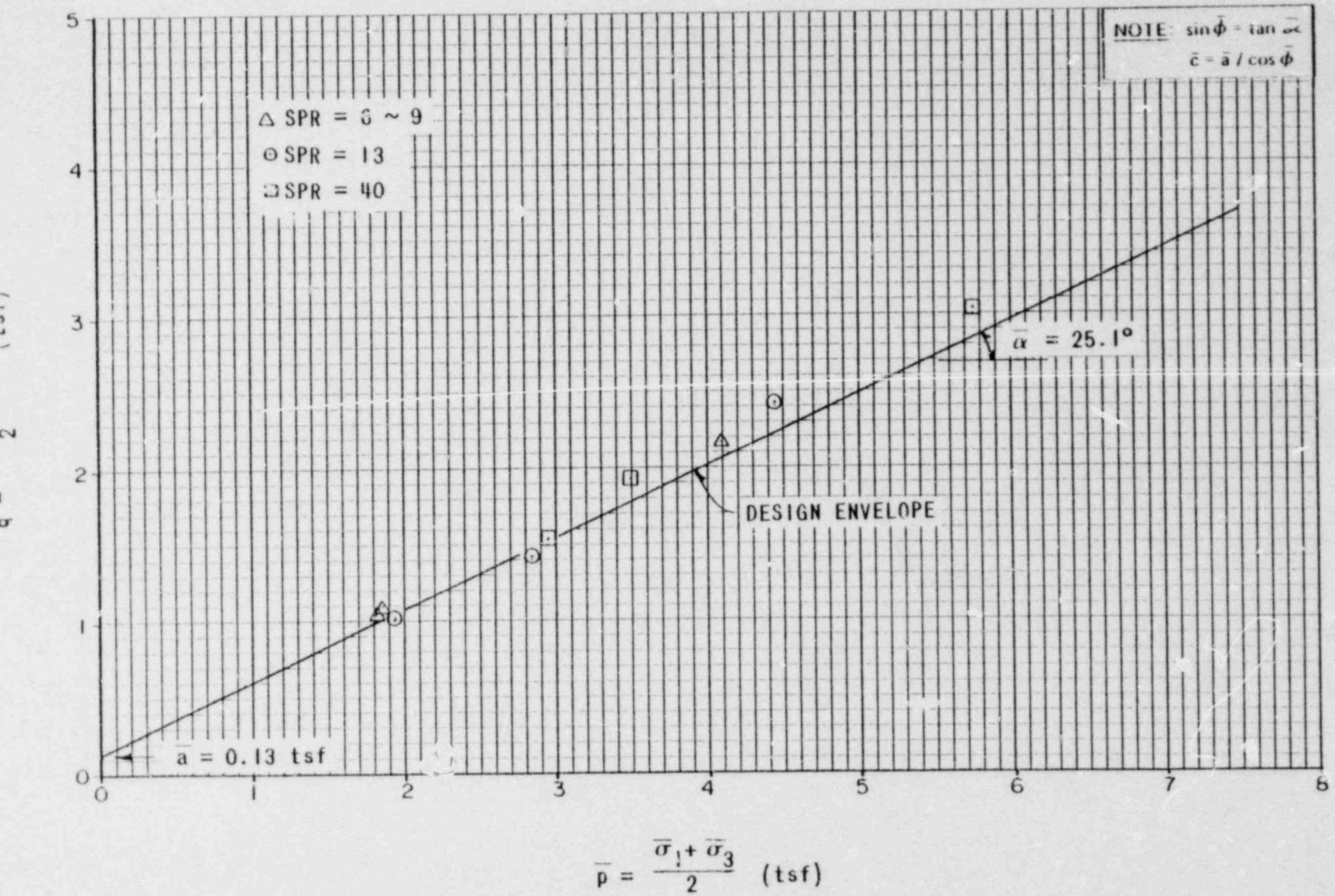

SUMMARY OF TRIAXIAL TESTS
ON SELECT FILL

FIGURE 15

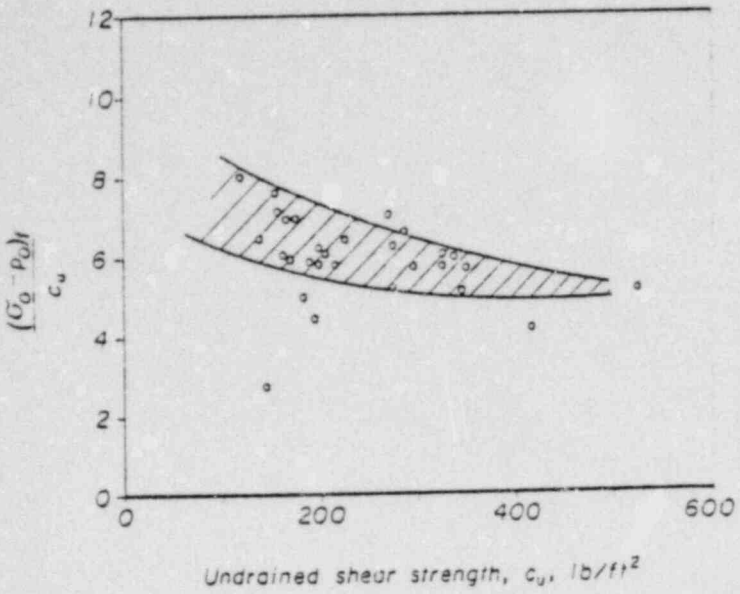

(a) UNDISTURBED SAMPLES

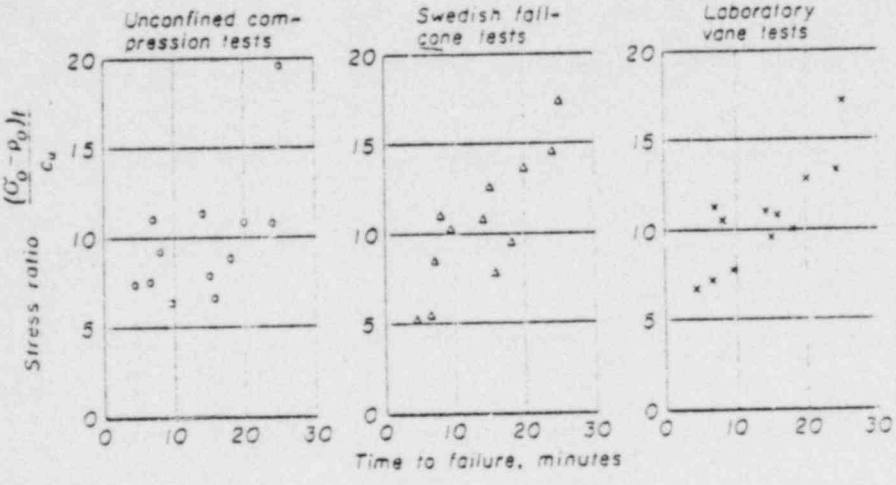

(b) REMOLDED SAMPLES

(after Broms and Bennermark, 1967)

STRESS RATIO FOR SOIL
INTRUSION FROM LABORATORY TESTS

FIGURE 16

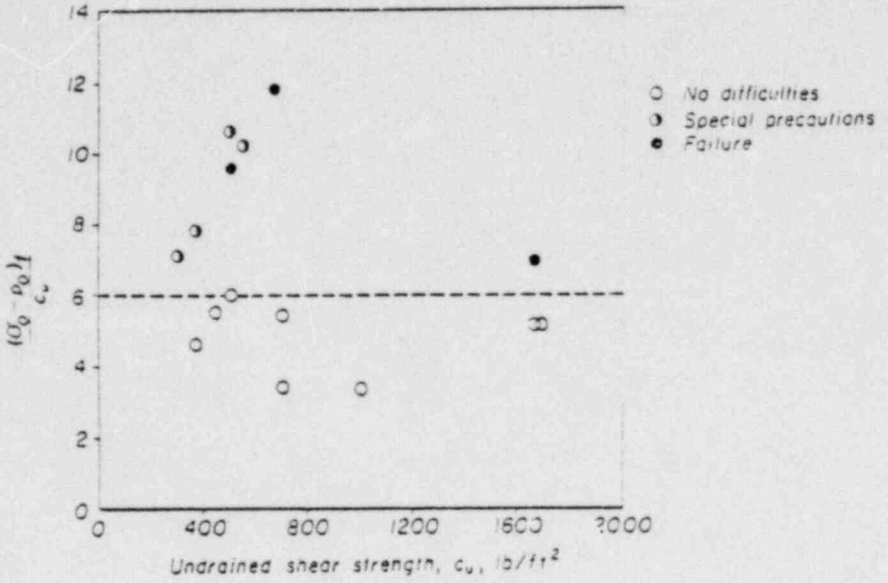

(after Broms and Bennermark, 1967)

STRESS RATIO FOR SOIL INTRUSION
FROM FIELD OBSERVATIONS

FIGURE 17

Table I Field Data on Stability of Tunnels in Saturated Plastic Clays

No.	Case	Reference	Soil	Depth z to Tunnel Axis, ft	Tunnel Diameter 2R, ft	Depth / diameter z/2R	Av. Undrained Shear Strength, s_u, ksf	Overburden Pressure, p_z, at Axis, ksf	Air Pressure p_a, ksf	$\frac{p_z - p_a}{s_u}$ (Stress Ratio)	Remarks
1	London, Ashford	Tattersall et al, 1955	London Clay, fissured, plastic	90	9.3	9.7	21	11.0	0	0.5	(1)
2	London, post office	Ward and Thomas, 1965	do.	55	7.7	7.1	7.2	7.0	0	1.0	(1)
3	London, Victoria	Ward and Thomas, 1965	do.	85	14.0	6.1	7.8	10.8	0	1.4	(1)
4	Ottawa, Sewer	Eden and Bozozuk, 1968	Leda Clay, sensitive	60	10.0	6.0	3.7	6.2	0.6	1.5	(1)
5	Antwerp, Gas Storage	deBeer and Buttiens, 1966	Boom Clay, fissured, plastic	253	17.7	14.3	7.8	31.5	0	4.1	(1)
6	Detroit, Water	Housel, 1942	Plastic glacial clay	68	15.0	4.5	0.8	8.0	3.9	5.1	(2)
7	Toronto, subway	Pers. comm.	Plastic glacial clay	43	17.0	2.5	0.7	5.5	1.4	5.7	(2)
8	Chicago, subway	Terzaghi, 1943	Plastic glacial clay	36	20.0	1.8	0.44	4.3	1.7	5.9	(2)
9	Koto, Tokyo, subway	Shiraishi pers. comm.	Normally loaded sensitive clay	74	23.0	3.2	0.76	5.6	1.2	7.4	(3)
10	Osaka, Municipal Railway	Shiraishi pers. comm.	Normally loaded sensitive clay	51	23.0	2.2	0.60	5.0	1.0	6.6	(3)

(after Peck, 1969)

REMARKS:

(1) Stable, no squeeze
(2) Stable, with some squeeze
(3) Unstable, with excessive squeeze

STRESS RATIO FOR SOIL INTRUSION FROM FIELD OBSERVATIONS

FIGURE 18

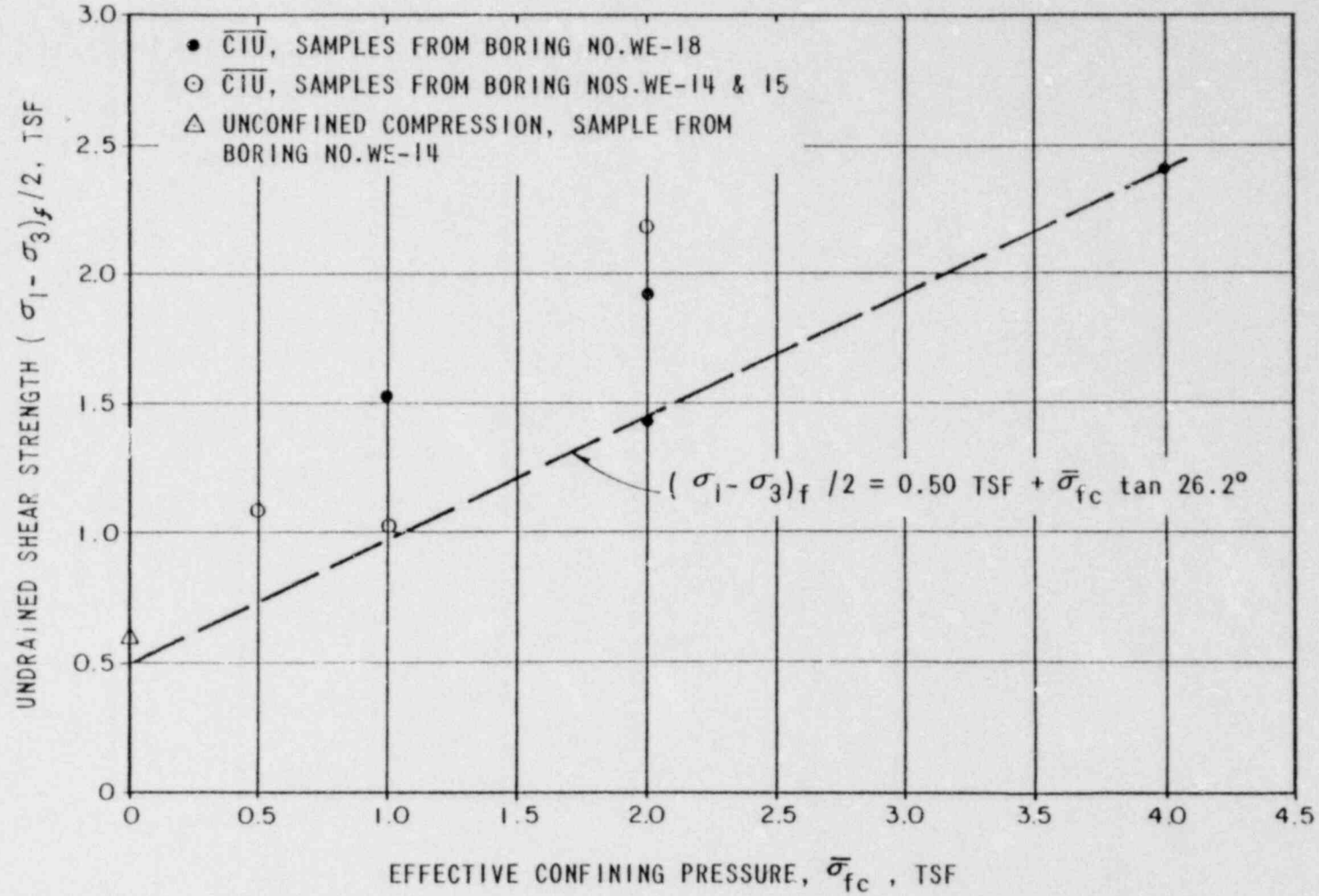

UNDRAINED SHEAR STRENGTH
OF
EMBANKMENT MATERIALS

FIGURE 19

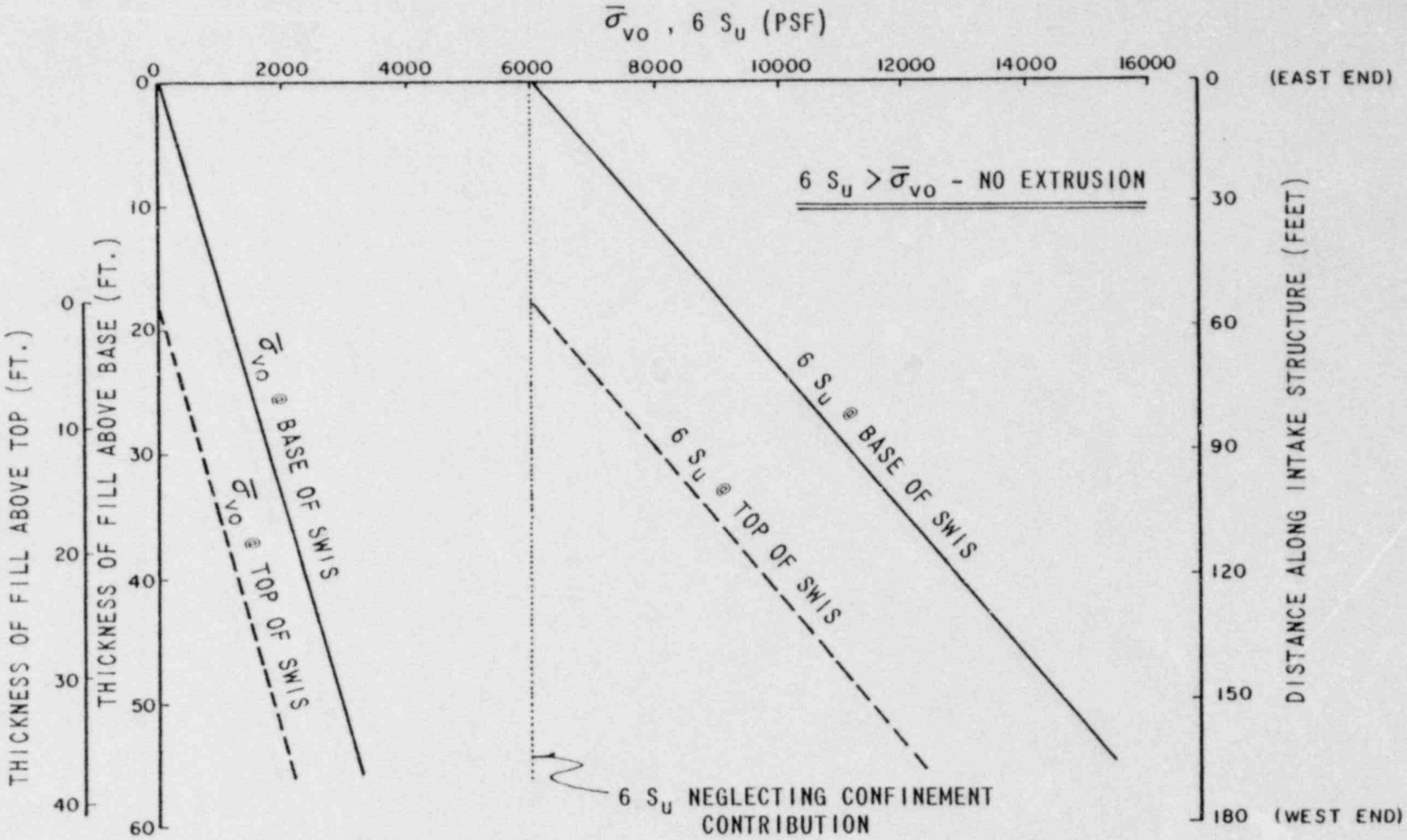

EXTRUSION POTENTIAL
SERVICE WATER INTAKE STRUCTURE

FIGURE 20

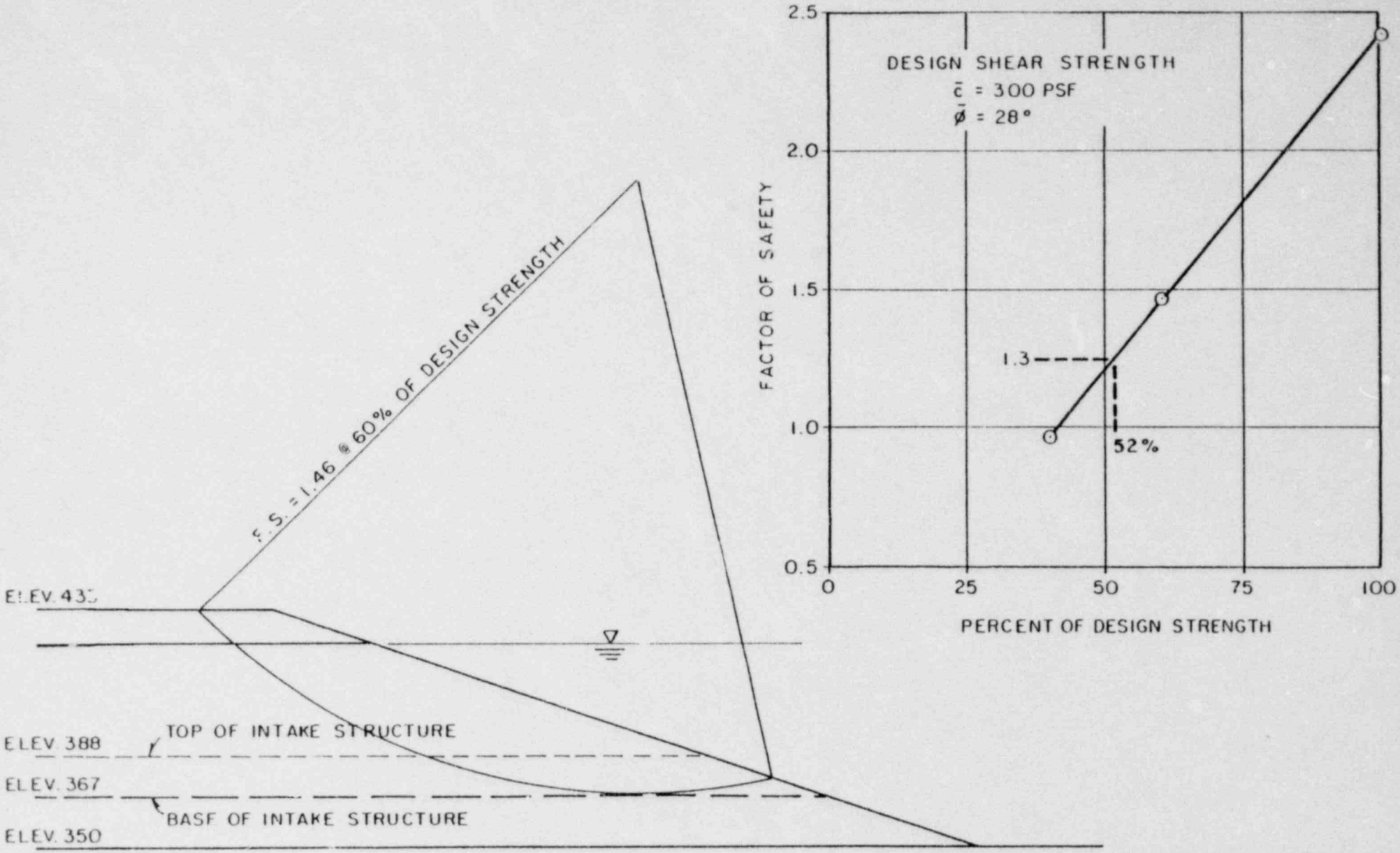

STATIC STABILITY ANALYSIS
WEST EMBANKMENT

FIGURE 21

APPENDIX

A

SUMMARY OF LABORATORY TEST RESULTS

BORING and SAMPLE No	DEPTH - feet	CLASSIFICATION	SPECIAL TESTS	NATURAL WATER CONTENT (%)	ATTERBERG LIMITS		UNCON. COMPRESS.		UNIT DRY WGT (pcf)	SPECIFIC GRAVITY	GRAIN SIZE		OPT. MOIST.	CONSOLID.	TRIAXIAL			
					LIQUID LIMIT	PLASTIC LIMIT	STRESS (tsf)	STRAIN (%)			SIEVE	HYDR.			U.U.	$\overline{CIU}$	CELL PRESSURE (psi)	BACK PRESSURE (psi)
WE-14 S-1	18.0-19.5	Select Fill		26.5														
S-3	24.5-26.0	Select Fill		26.4														
S-4	28.5-29.0	Select Fill		34.9														
S-6	34.5-36.0	Select Fill		28.5														
S-7	38.0-39.5	Select Fill		30.3														
S-8	43.0-44.5	Select Fill		35.4 29.0	70 67	42 42	1.20	6.06	85.7 93.6	2.72 2.73	* *	* *				* 		
S-9	44.5-46.0	Select Fill		29.0														
S-10	48.0-49.5	Select Fill		28.9														
S-12	54.5-56.0	Select Fill		29.9														
WE-15 S-1	34.9-36.4	Select Fill		33.9	60	43												
ST-1	38.6-40.6	Select Fill		34.6	60	44			87.5	2.65	*	*				*		
S-2	40.6-42.1	Select Fill		31.6	64	51												
S-3	45.8-47.3	Select Fill		27.0	NP	NP												
ST-2	48.8-50.3	Select Fill		30.8	NP	NP			89.8	2.69	*	*				*		
S-4	50.3-52.3	Select Fill		36.8	64	40												

* See Test Curves

SUMMARY OF LABORATORY TEST RESULTS

BORING and SAMPLE No	DEPTH - feet	CLASSIFICATION	SPECIAL TESTS	NATURAL WATER CONTENT (%)	ATTERBERG LIMITS		UNCON. COMPRESS		UNIT DRY WGT (pcf)	SPECIFIC GRAVITY	GRAIN SIZE		OPT. MOIST.	CONSOLID.	TRIAXIAL			
					LIQUID LIMIT	PLASTIC LIMIT	STRESS (tsf)	STRAIN (%)			SIEVE	HYDR.			U.U.	$\overline{CIU}$	CELL PRESSURE (psi)	BACK PRESSURE (psi)
WE-15 S-5	55.8-57.3	Select Fill		32.9														
S-6	59.8-61.3	Select Fill		27.0														
S-7	65.8-67.3	Select Fill		28.6														
S-8	69.7-71.2	Select Fill		26.7														
S-9	75.8-77.3	Select Fill		37.6														
WE-16 PIT-1	79.0-81.0	Saprolite	(1)	19.3	NP	NP			113.2	2.89	*	*						
PIT-2	81.0-83.0	Saprolite	(1)	13.3	NP	NP			122.7	2.81	*	*						
PIT-6	93.5-96.0	Saprolite	(1)	11.4	NP	NP			125.9	2.98	*	*						
WE-17 ST-7	68.0-70.0	Saprolite	(1)	28.7	NP	NP			87.7	2.63	*	*						
ST-7	68.0-70.0	Saprolite	(1)	23.6	NP	NP			96.3	2.78	*	*						
ST-7	68.0-70.0	Saprolite	(1)	20.2	NP	NP			101.0	2.74	*	*						
WE-19 ST-2	18.0-20.0	Select Fill	(1)	25.9	NP	NP			95.7	2.71	*	*						
ST-2	18.0-20.0	Select Fill	(1)	23.1	NP	NP			101.0	2.70	*	*						
ST-3	28.0-30.0	Select Fill	(1)	35.7	NP	NP			83.5	2.74	*	*						
ST-5	48.0-50.0	Select Fill	(1)	26.8	NP	NP			95.7	2.58	*	*						

* See Test Curves (1) Undrained Creep Test

SUMMARY OF LABORATORY TEST RESULTS

BORING and SAMPLE No	DEPTH feet	CLASSIFICATION	SPECIAL TESTS	NATURAL WATER CONTENT (%)	ATTERBERG LIMITS		UNCON COMPRESS		UNIT DRY WGT. (pcf)	SPECIFIC GRAVITY	GRAIN SIZE		OPT. MOIST.	CONSOLID.	TRIAXIAL			
					LIQUID LIMIT	PLASTIC LIMIT	STRESS (tsf)	STRAIN (%)			SIEVE	HYDR.			U.U.	$\overline{CIU}$	CELL PRESSURE (psi)	BACK PRESSURE (psi)
WE-19 ST-5	48.0-50.0	Select Fill	(1)	23.6	NP	NP			103.2	2.69	*	*						
ST-5	48.0-50.0	Select Fill	(1)	20.8	NP	NP			105.5	2.59	*	*						

* See Test Curves

(1) Undrained Creep Test

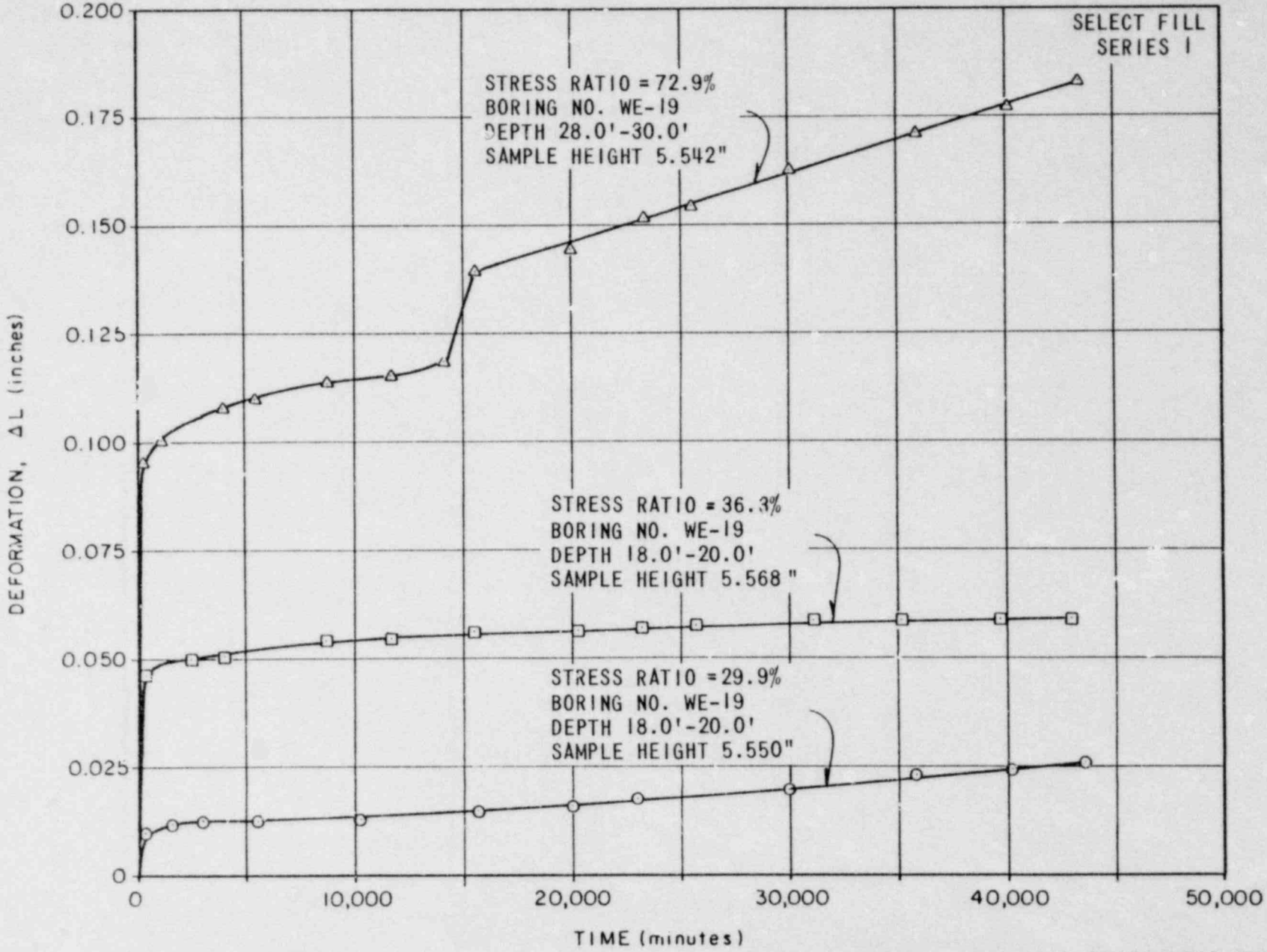

UNDRAINED CREEP TESTS
SELECT FILL
VIRGIL C. SUMMER NUCLEAR STATION

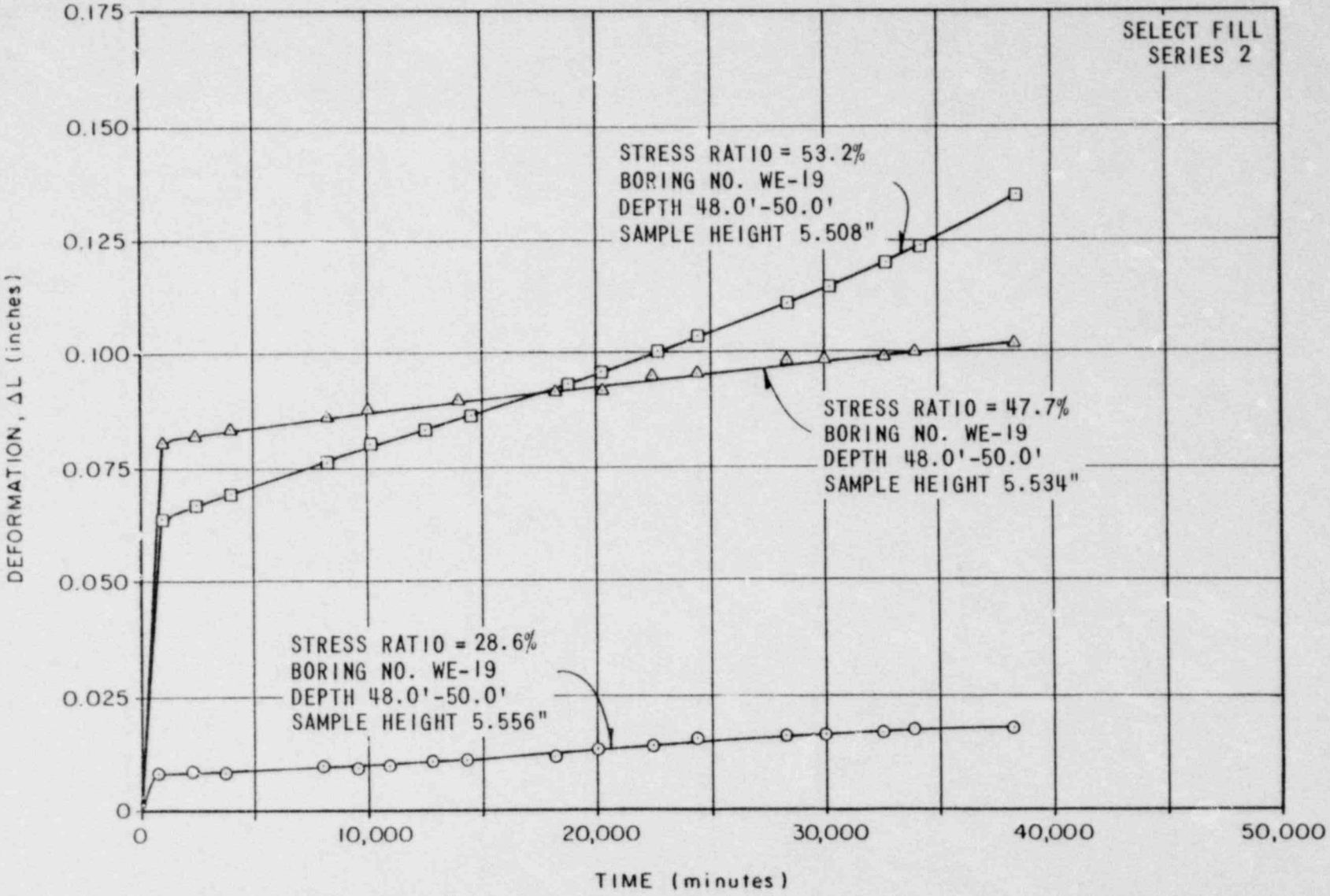

UNDRAINED CREEP TESTS
SELECT FILL
VIRGIL C. SUMMER NUCLEAR STATION

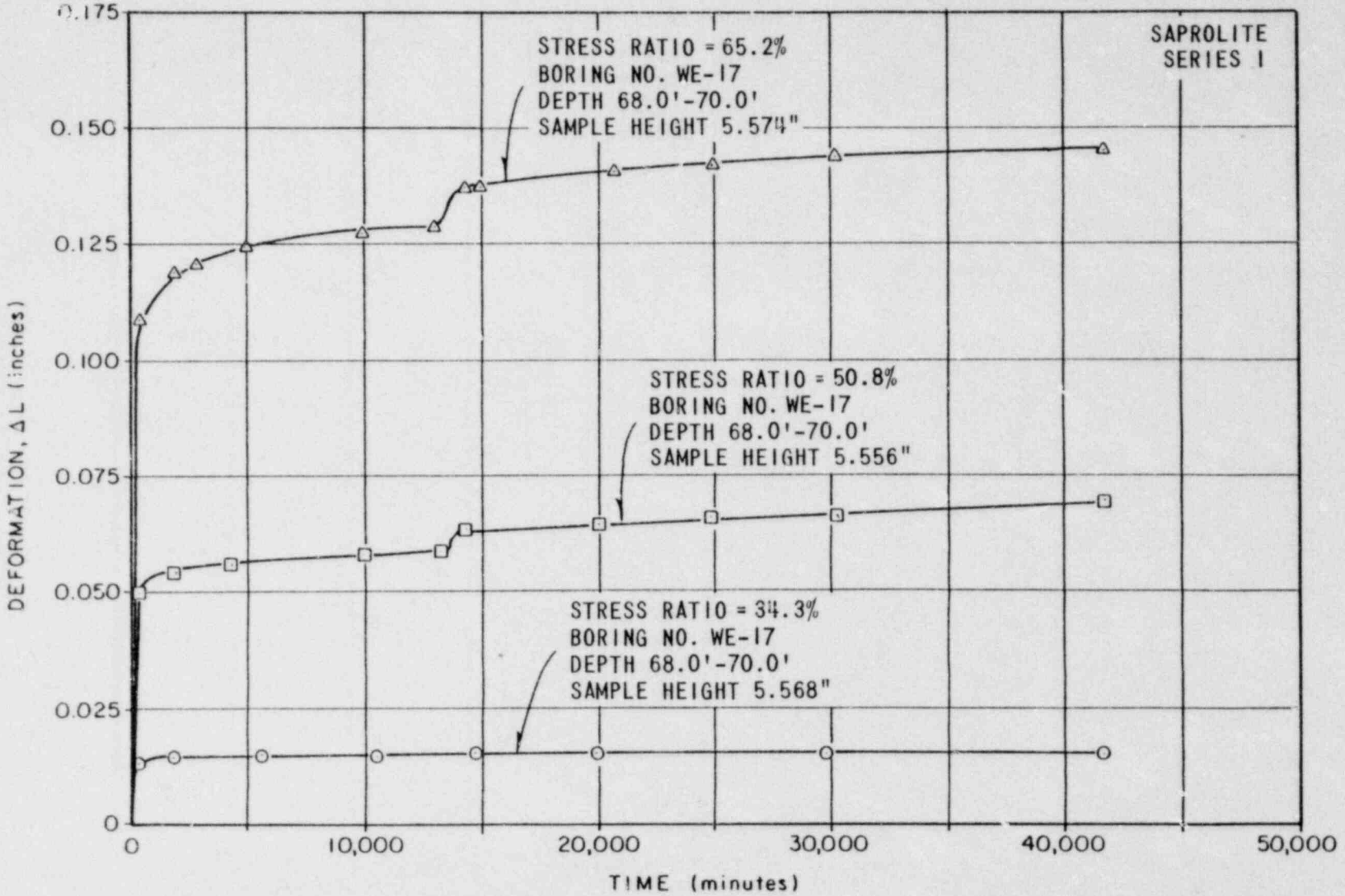

UNDRAINED CREEP TESTS
SAPROLITE
VIRGIL C. SUMMER NUCLEAR STATION

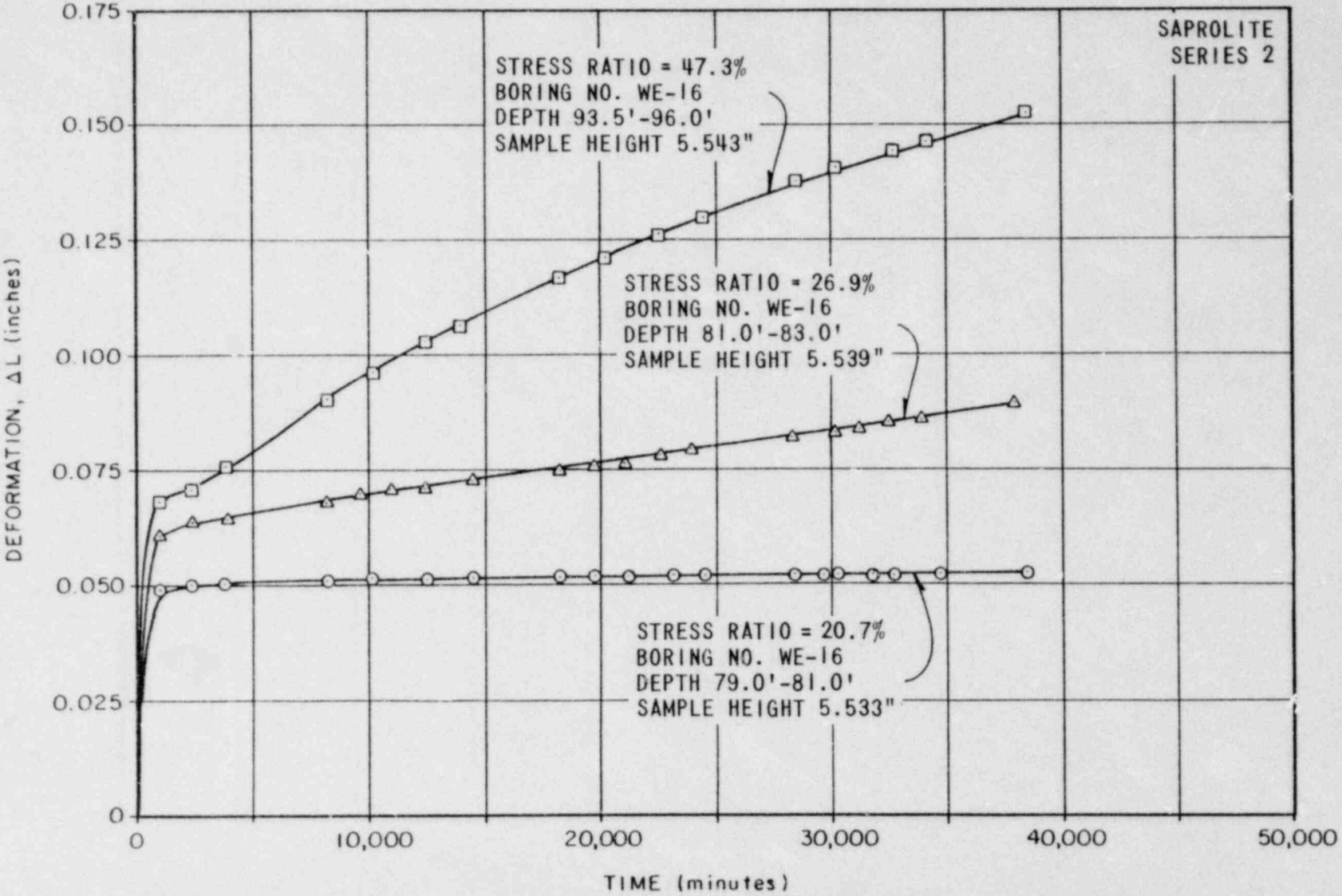

UNDRAINED CREEP TESTS
SAPROLITE
VIRGIL C. SUMMER NUCLEAR STATION

Sample No.	Test No.	Sample Depth Ft.	W_n (%)	γ_d pcf	$\bar{\sigma}_c$ tsf	$\frac{(\bar{\sigma}_1 - \bar{\sigma}_3)}{2}_{max}$ tsf	$\bar{c}$ tsf	$\bar{\phi}$
WE-15 ST-1	1	37.3	34.6	87.5	0.5	1.08		
WE-15 ST-2	2	49.2	30.8	89.8	1	1.03		
WE-14 S-8	3	43.8	29.0	93.6	2	2.18		

NOTE: $\sin\bar{\phi} = \tan\bar{\alpha}$
$\bar{c} = \bar{a} / \cos\bar{\phi}$

PROJECT NO. 71C72-WE
TEST DATE 4-13-81
BORING NO. WE-14 & WE-15

DESIGN ENVELOPE

$\bar{\alpha} = 25.1°$

$\bar{a} = 0.13$ TSF

STRESS DIFFERENTIAL/2 IN TSF

0 0.5 1 1.5 2 2.5

AVERAGE EFFECTIVE STRESS IN TSF

0 0.5 1 1.5 2 2.5 3 3.5 4

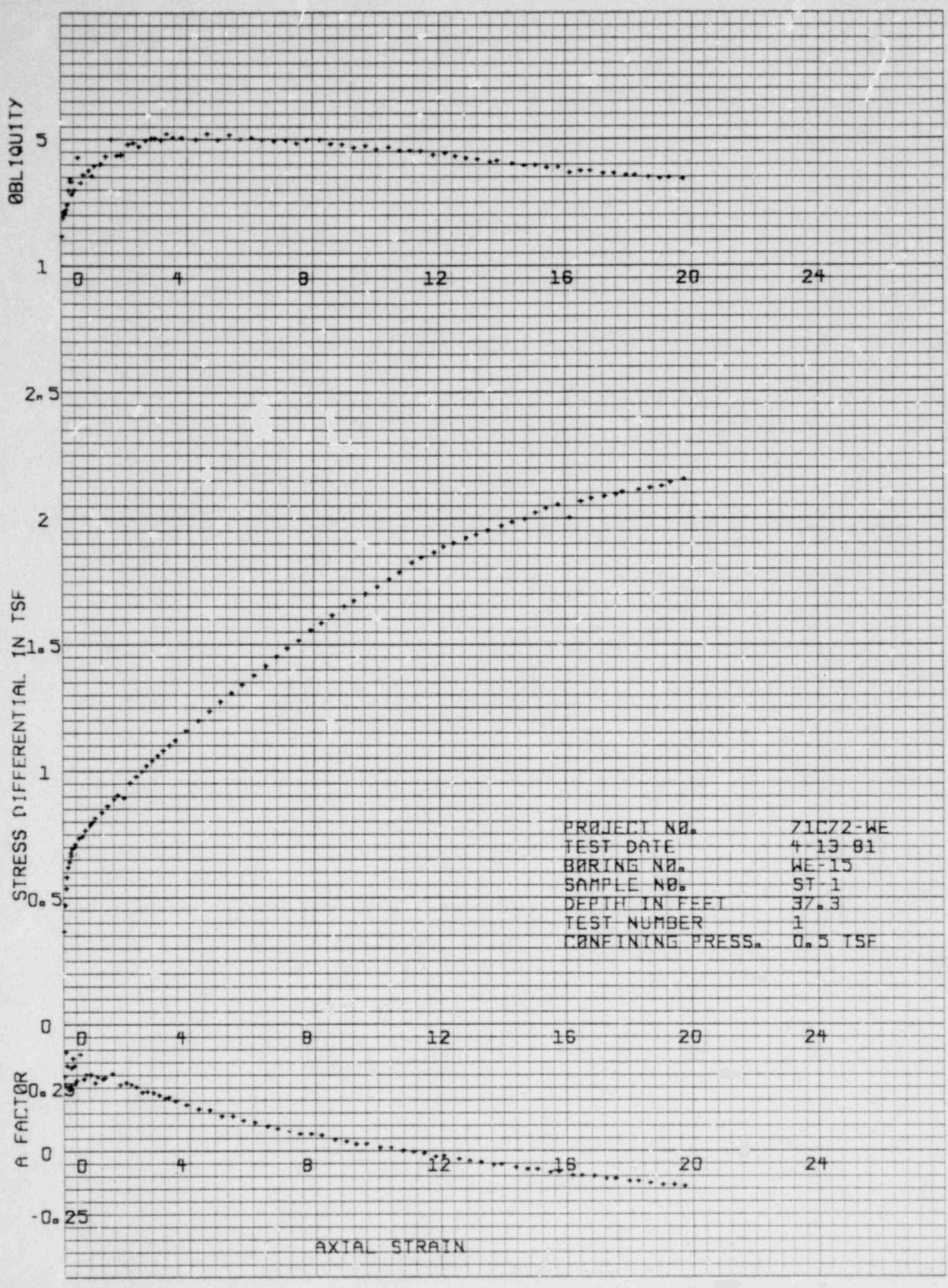

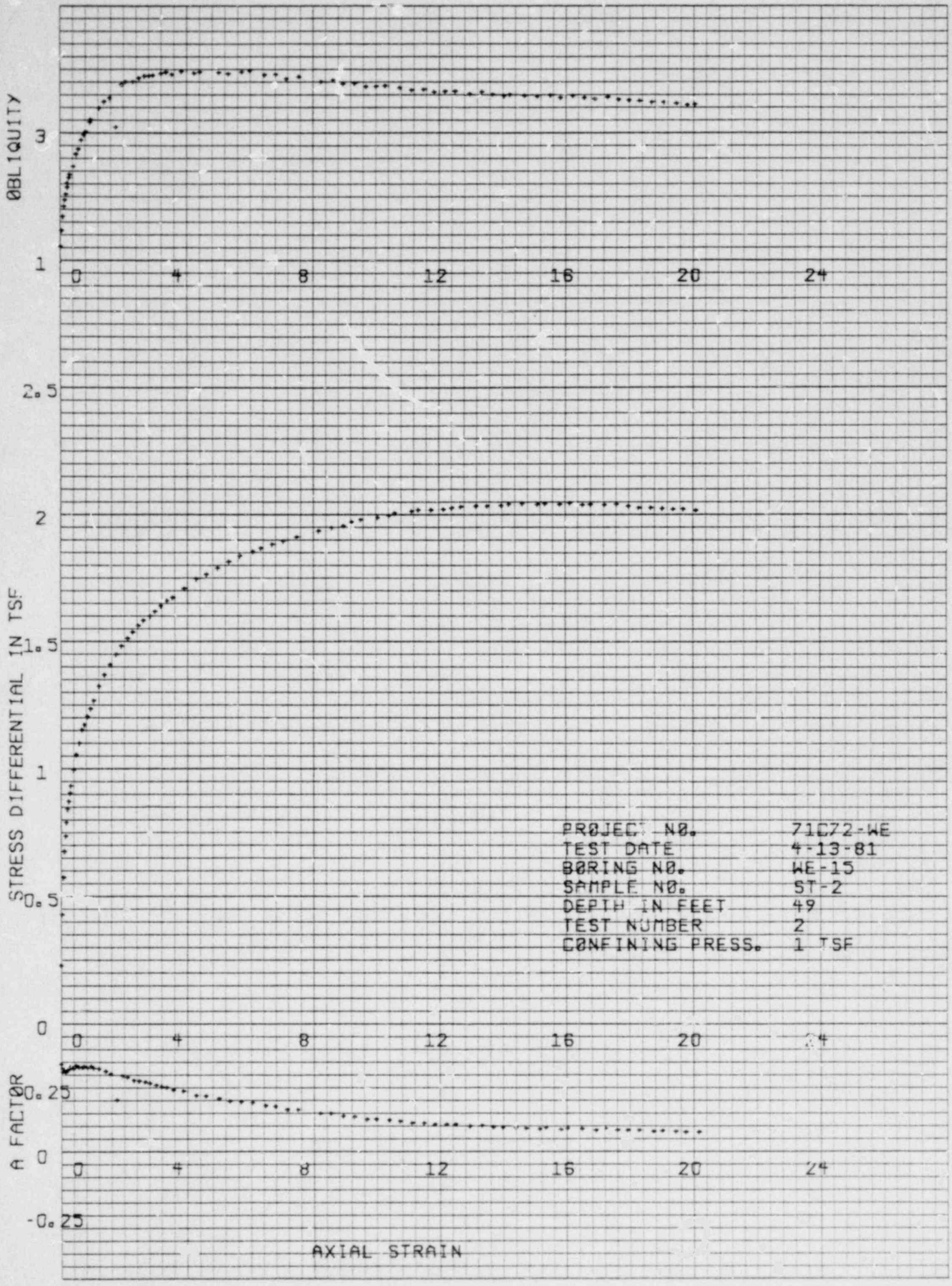

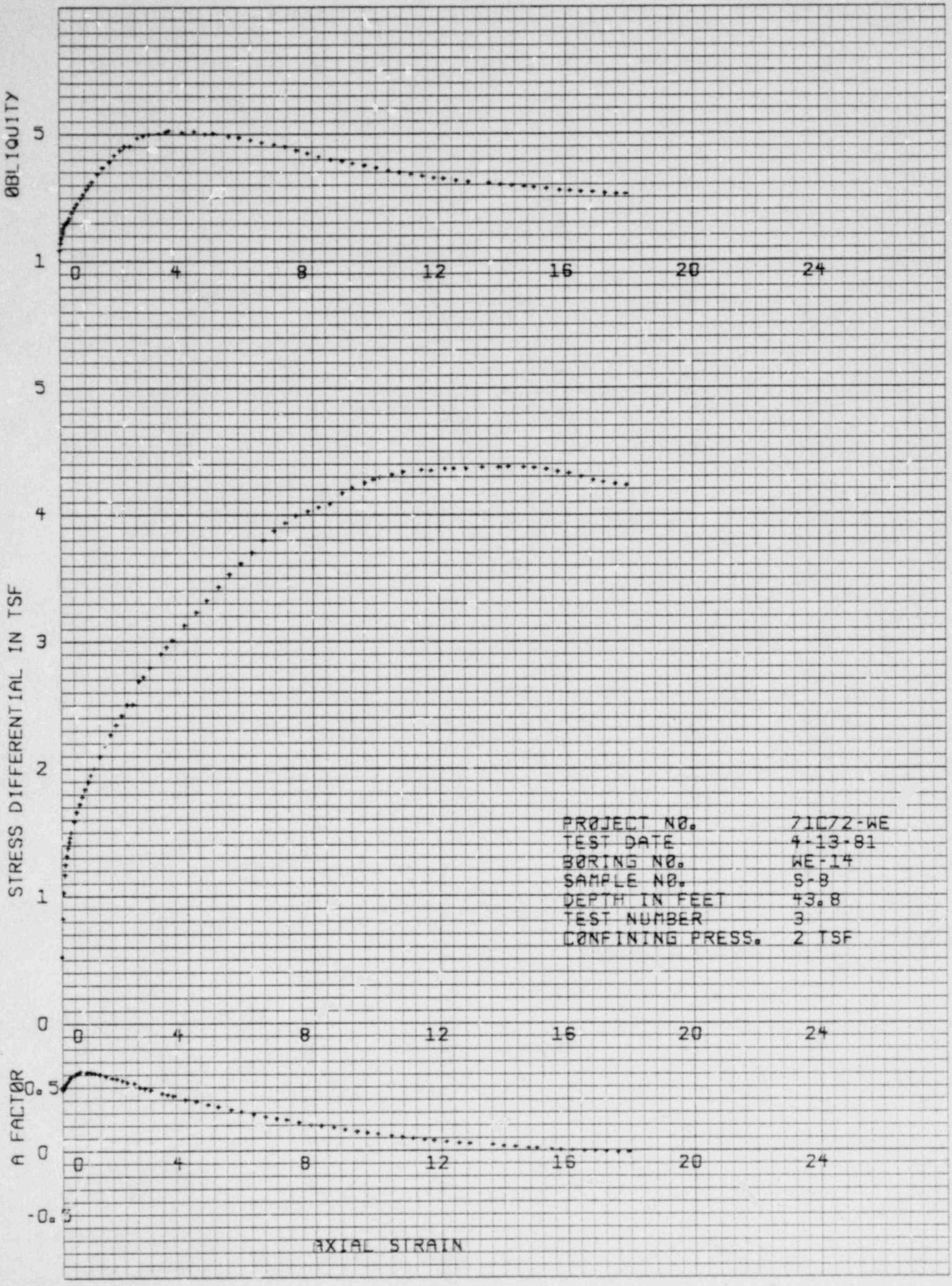

UNCONFINED COMPRESSION TEST

Project	V. C. Summer			
Boring No.	WE-14	Sample No. S-8	Depth 43.0-43.5	Ft.
Description	Red-Brown Micaceous Sandy Clayey Silt (Select Fill)			
Moisture Content	35.4 %		Dry Density 85.7	pcf
Liquid Limit	70 %	Plastic Limit 42 %		
Maximum Axial Stress	1.20 tsf @ 6.06% Strain			

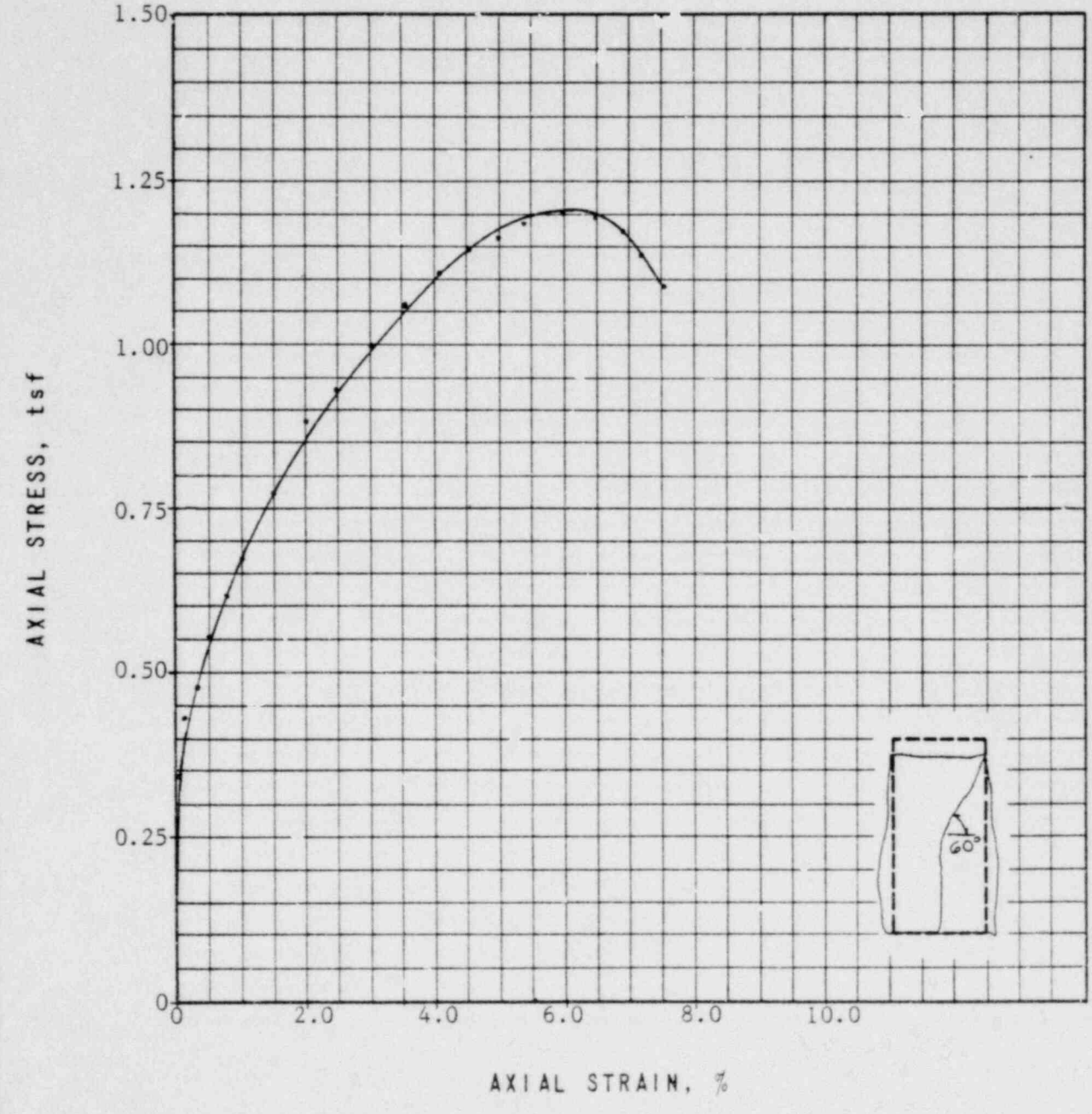

JOB No 71 C 72-WE

UNCONSOLIDATED UNDRAINED TRIAXIAL COMPRESSION TEST*

Project	V. C. Summer				
Boring No.	WE-16	Sample No.	PIT-1	Depth	79.3-79.8 Ft
Description	Green, Brown and Gray Micaceous Sandy Silt (Saprolite)				
Moisture Content	19.3 %			Dry Density	113.2 pcf
Liquid Limit	N.P. %	Plastic Limit	N.P. %	Relative Density	-- %
$(\sigma_1 - \sigma_3)$ max.=	5.28 tsf at	11.1 % Strain		Chamber Pressure, σ_c =	2.81 tsf

*After Undrained Creep

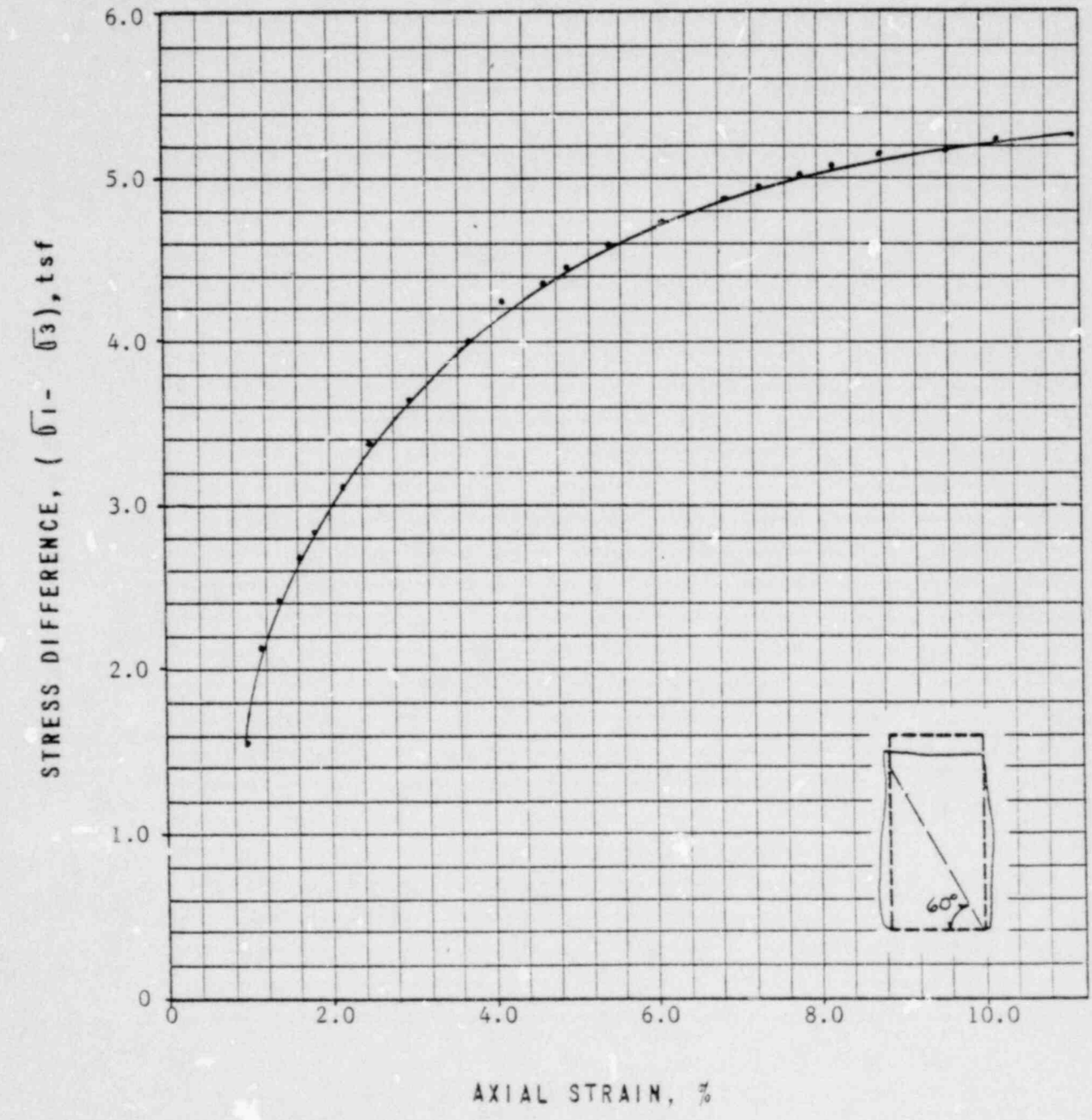

JOB No 71 C 72-WE

UNCONSOLIDATED UNDRAINED TRIAXIAL COMPRESSION TEST*

Project V. C. Summer

Boring No. WE-16 Sample No. PIT-2 Depth 81.3-81.8 Ft

Description Green, Brown and Gray Micaceous Sandy Silt (Saprolite)

Moisture Content 13.3% Dry Density 122.7 pcf

Liquid Limit N.P. % Plastic Limit N.P. % Relative Density -- %

$(\sigma_1 - \sigma_3)$ max.= 9.59 tsf at 11.7 % Strain Chamber Pressure, σ_c = 2.87 tsf

*After Undrained Creep

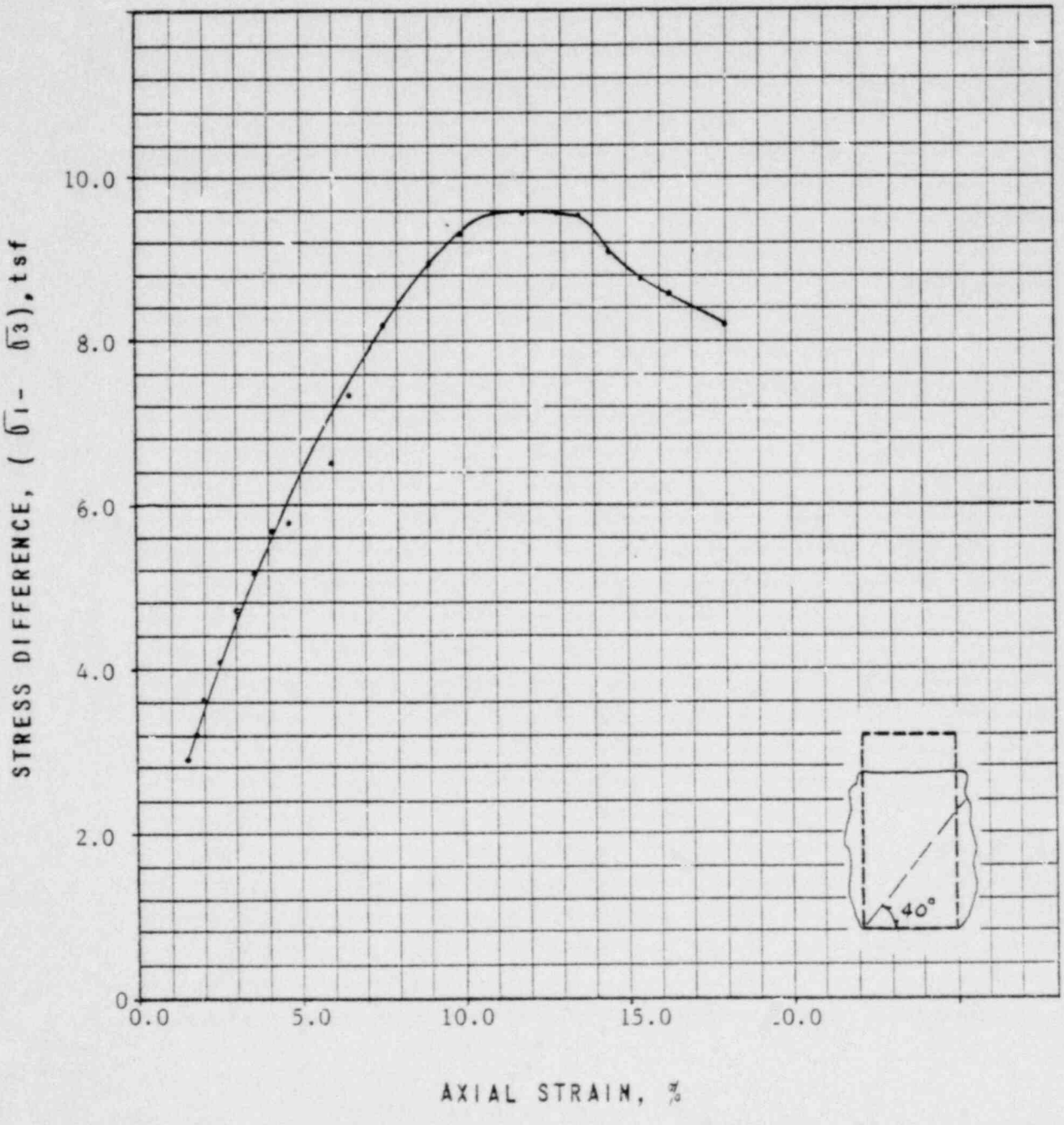

JOB No 71 C 72-WE

UNCONSOLIDATED UNDRAINED TRIAXIAL COMPRESSION TEST*

Project V. C. Summer

Boring No. WE-16 Sample No. PIT-6 Depth 93.7-94.1 Ft

Description Green, Brown and Gray Micaceous Sandy Silt (Saprolite)

Moisture Content 11.4 % Dry Density 125.9 pcf

Liquid Limit N.P. % Plastic Limit N.P. % Relative Density -- %

$(\sigma_1 - \sigma_3)$ max.= 4.16 tsf at 10.7 % Strain Chamber Pressure, σ_c = 3.24 tsf

*After Undrained Creep

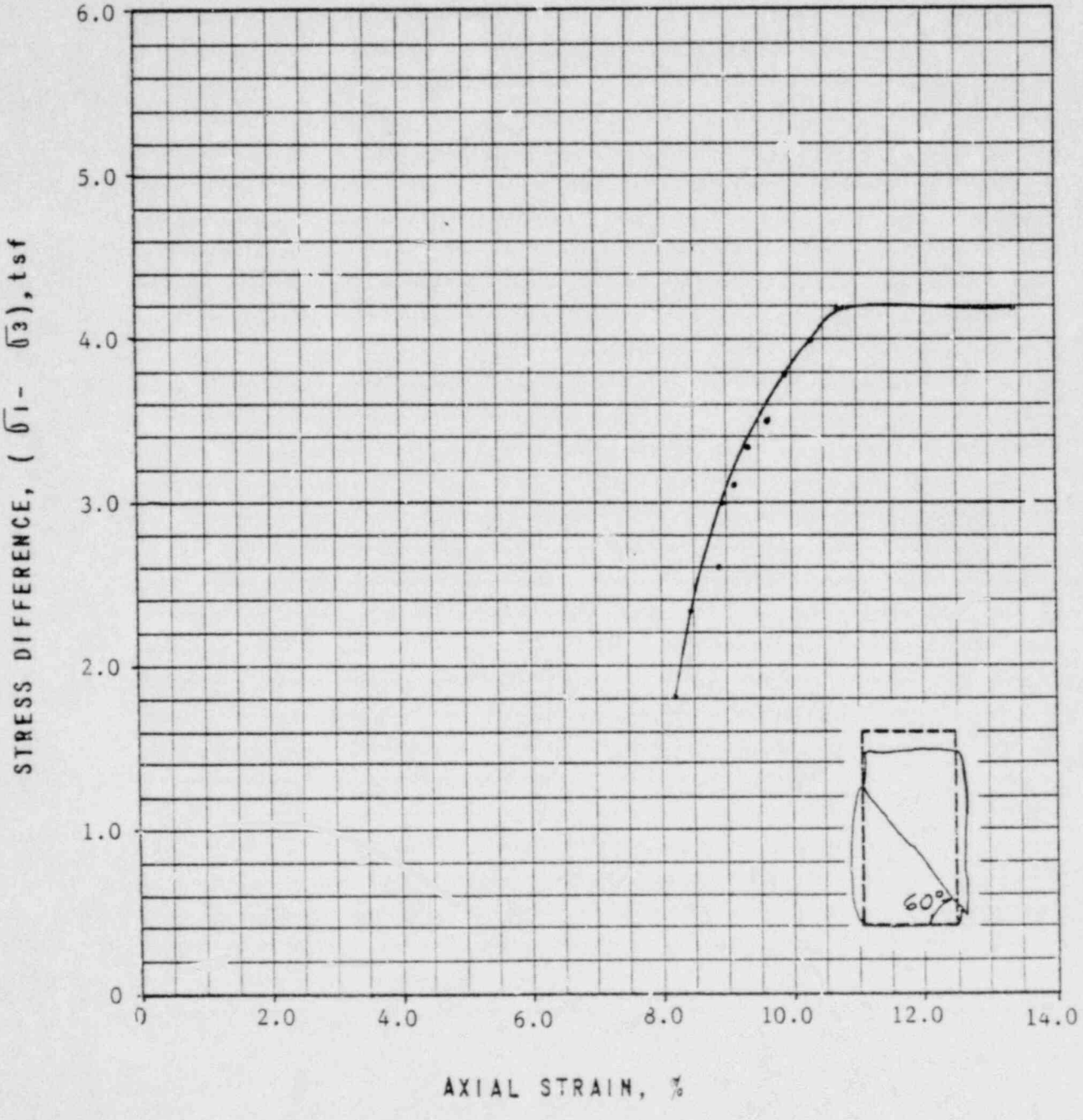

JOB No 71 C 72-WE

UNCONSOLIDATED UNDRAINED TRIAXIAL COMPRESSION TEST *

Project	V. C. Summer				
Boring No.	WE-17	Sample No.	ST-7	Depth	68.0-68.5 Ft
Description	Light brown micaceous fine sandy silt (Saprolite)				
Moisture Content	28.7 %			Dry Density	87.7 pcf
Liquid Limit	NP %	Plastic Limit	NP %	Relative Density	--- %
$(\sigma_1 - \sigma_3)$ max.=	2.89 tsf at	2.81 % Strain		Chamber Pressure, σ_c =	2.3 t.f

* After undrained creep test

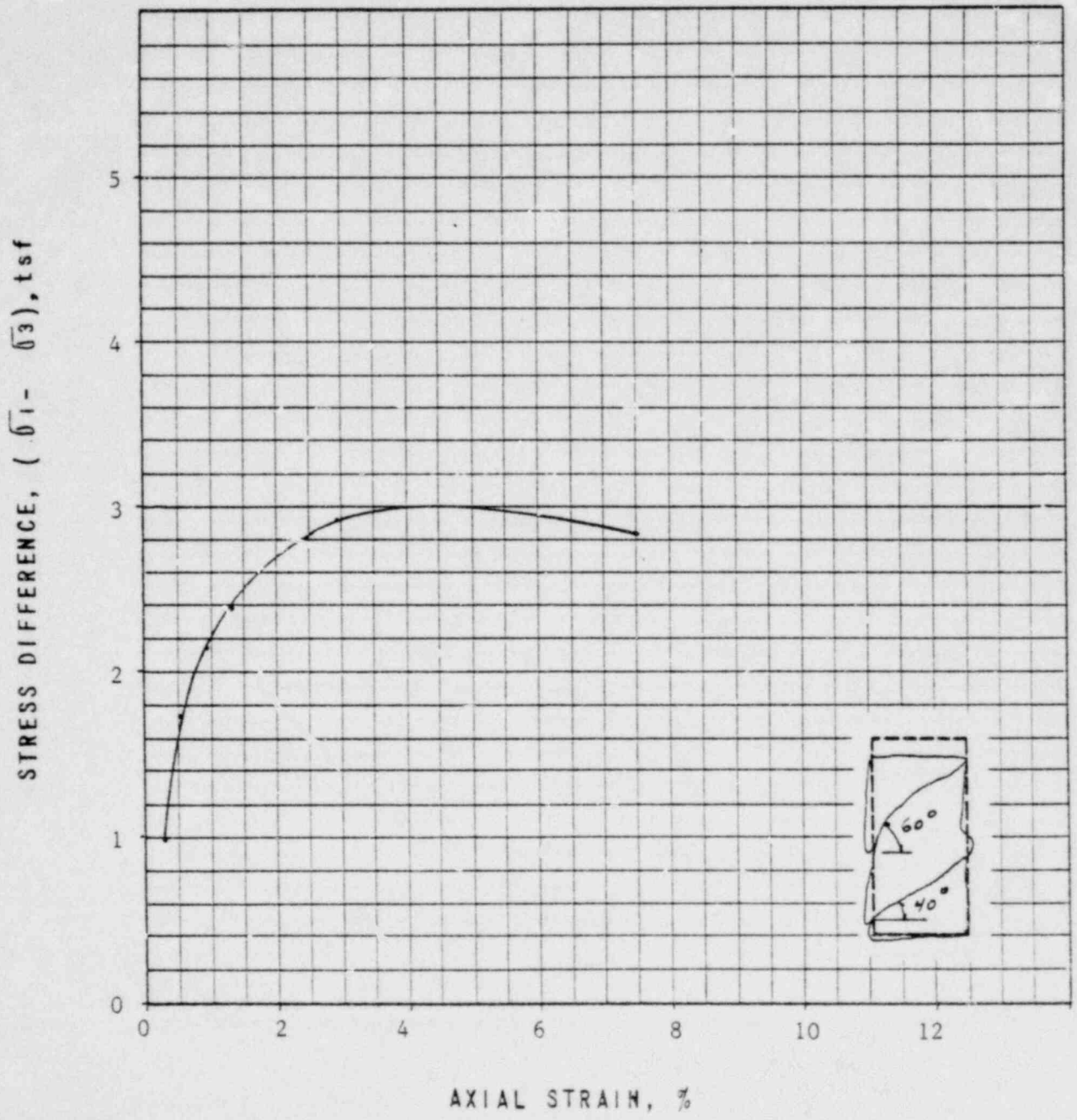

JOB No 71 C 72-WE

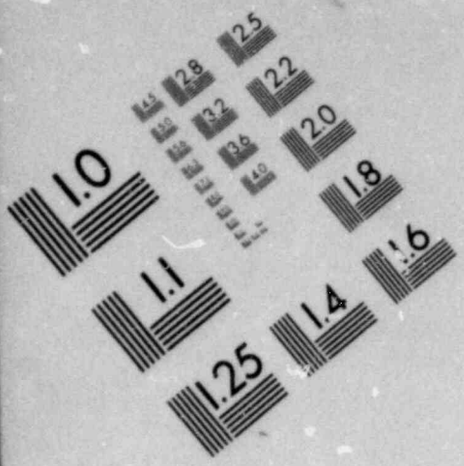

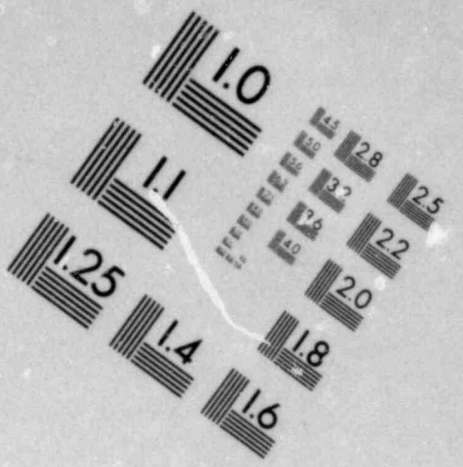

IMAGE EVALUA ION
TEST TARGET (MT-3)

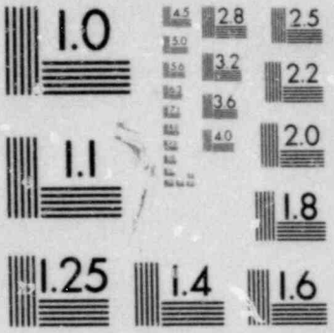

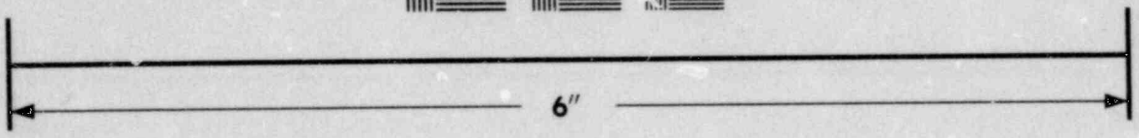

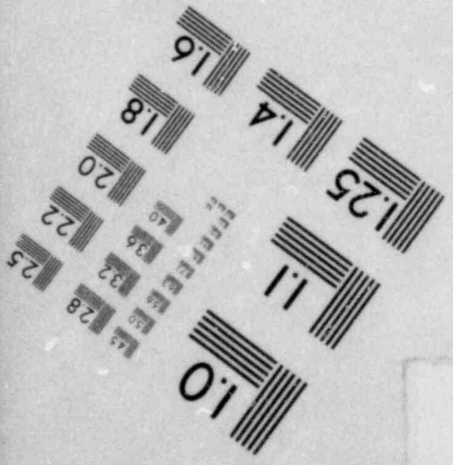

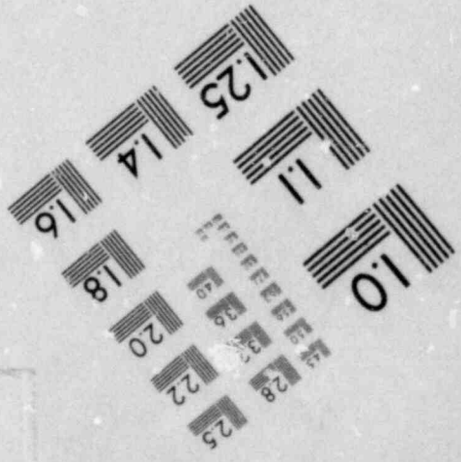

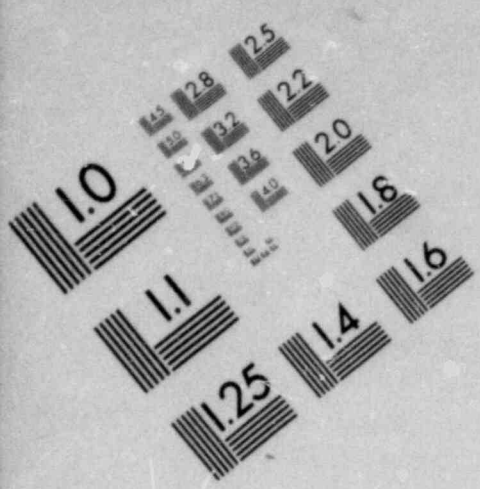

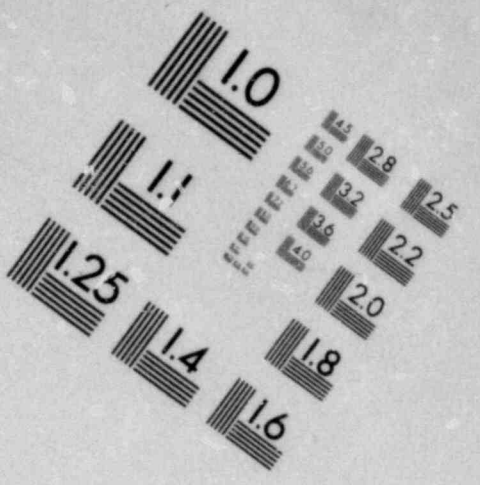

IMAGE EVALUATION TEST TARGET (MT-3)

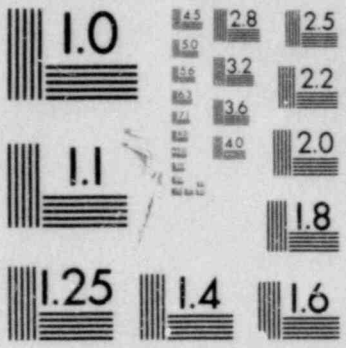

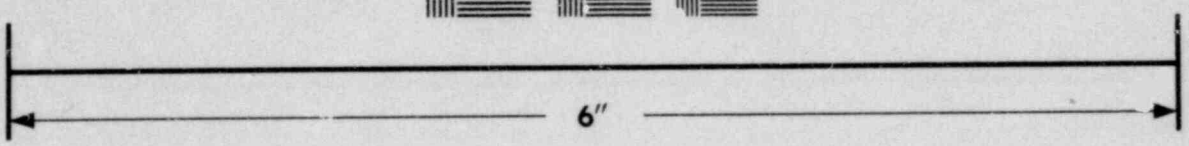

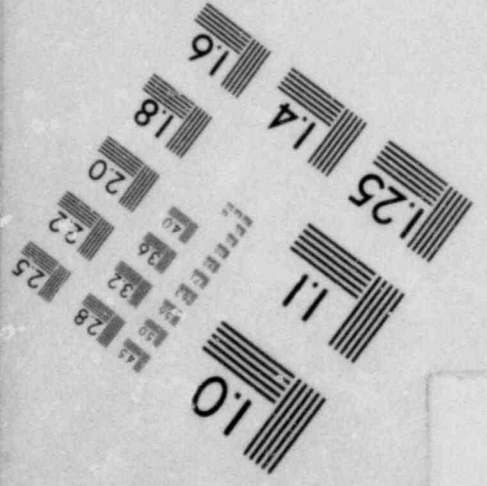

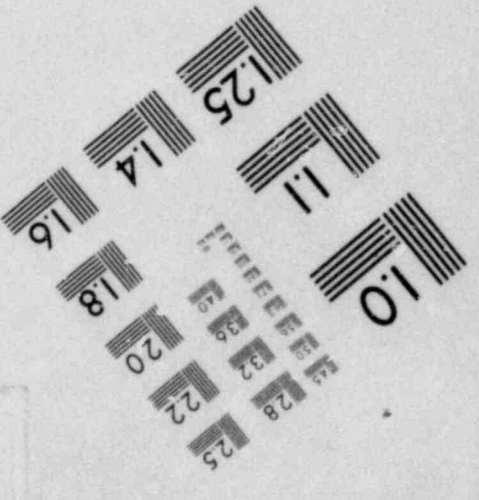

UNCONSOLIDATED UNDRAINED TRIAXIAL COMPRESSION TEST *

Project V. C. Summer

Boring No. WE-17 Sample No. ST-7 Depth 68.5-69.1 Ft

Description Light brown micaceous fine sandy silt (Saprolite)

Moisture Content 23.6 % Dry Density 96.3 pcf

Liquid Limit NP % Plastic Limit NP % Relative Density --- %

$(\sigma_1 - \sigma_3)$ max.= 3.27 tsf at 6.74 % Strain Chamber Pressure, σ_c = 2.3 tsf

*After undrained creep test

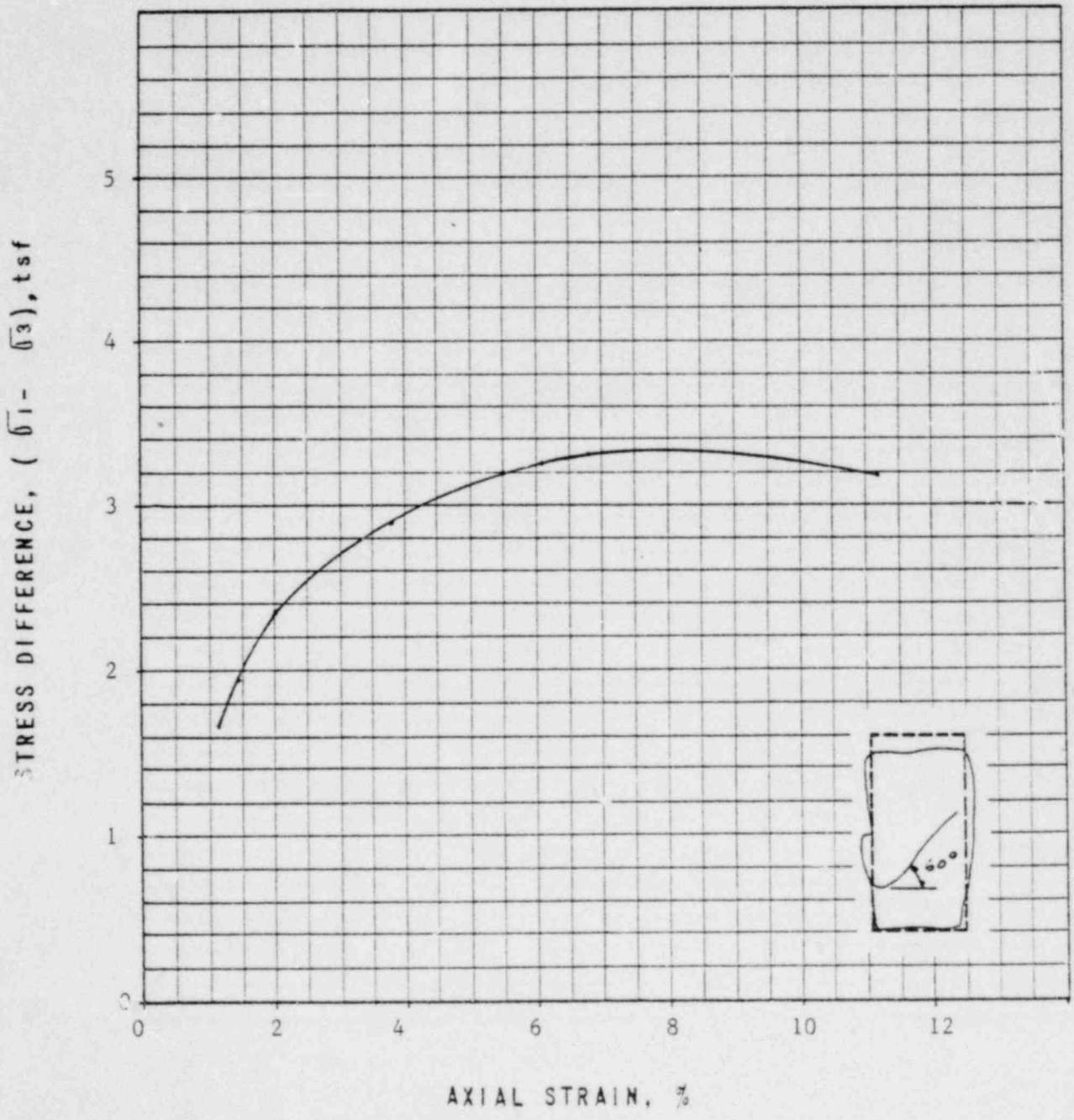

JOB No 71 C 72-WE

UNCONSOLIDATED UNDRAINED TRIAXIAL COMPRESSION TEST *

Project	V. C. Summer				
Boring No.	WE-17	Sample No.	ST-7	Depth	69.1-69.6 Ft
Description	Light brown micaceous fine sandy silt (Saprolite)				
Moisture Content	20.2 %			Dry Density	101.0 pcf
Liquid Limit	NP %	Plastic Limit	NP %	Relative Density	--- %
$(\sigma_1 - \sigma_3)$ max.=	3.56 tsf at	6.06 % Strain		Chamber Pressure, σ_c =	2.3 tsf

*After undrained creep test

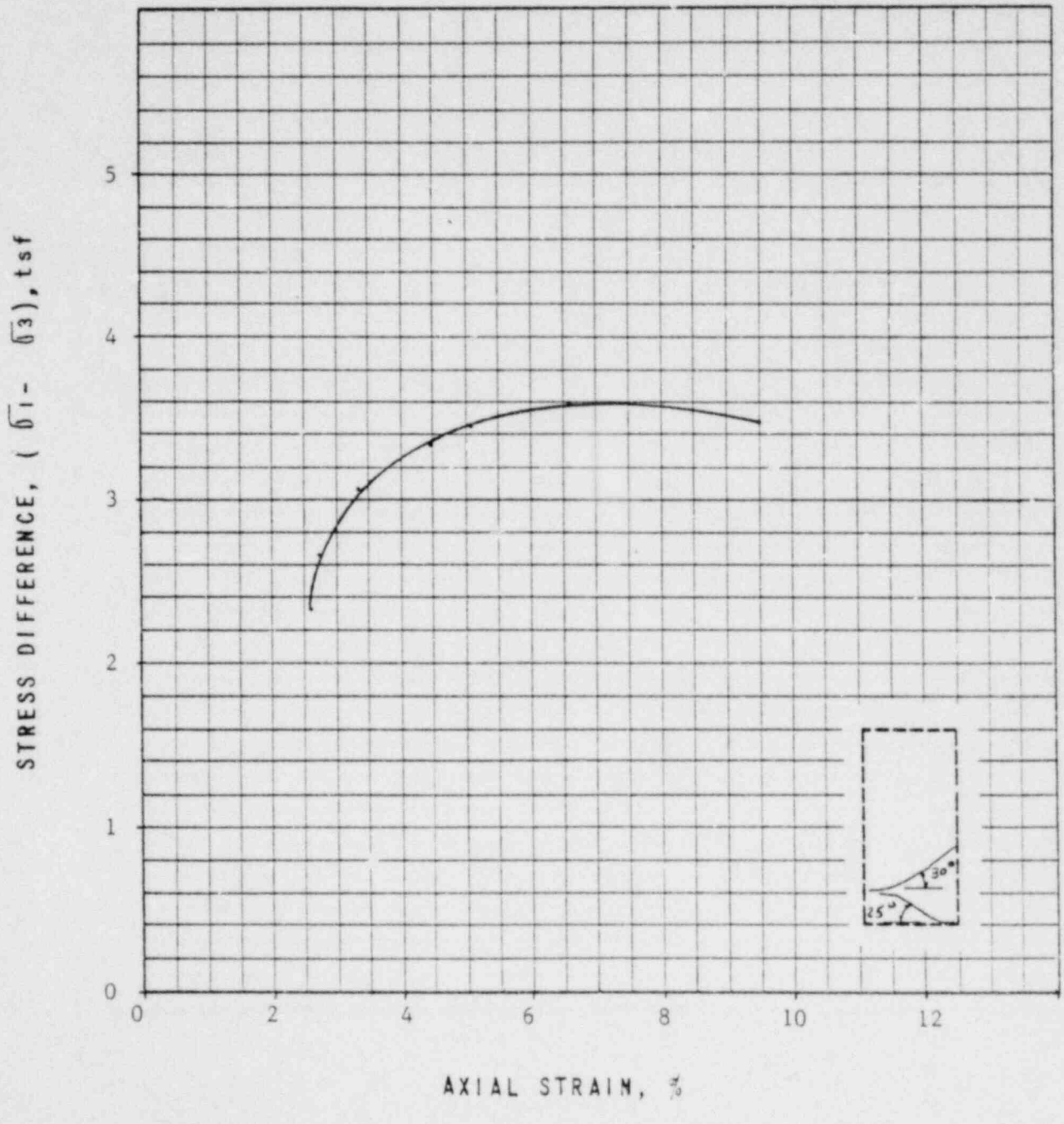

JOB No 71 C 72-WE

UNCONSOLIDATED UNDRAINED TRIAXIAL COMPRESSION TEST *

Project V. C. Summer

Boring No. WE-19 Sample No. ST-2 Depth 18.0-18.7 Ft

Description Red-brown micaceous medium to fine sandy silt (Select Fill)

Moisture Content 25.9 % Dry Density 95.7 pcf

Liquid Limit NP % Plastic Limit NP % Relative Density --- %

$(\sigma_1 - \sigma_3)$ max. = 2.41 tsf at 16.1 % Strain Chamber Pressure, σ_c = 0.90 tsf

* After undrained creep test

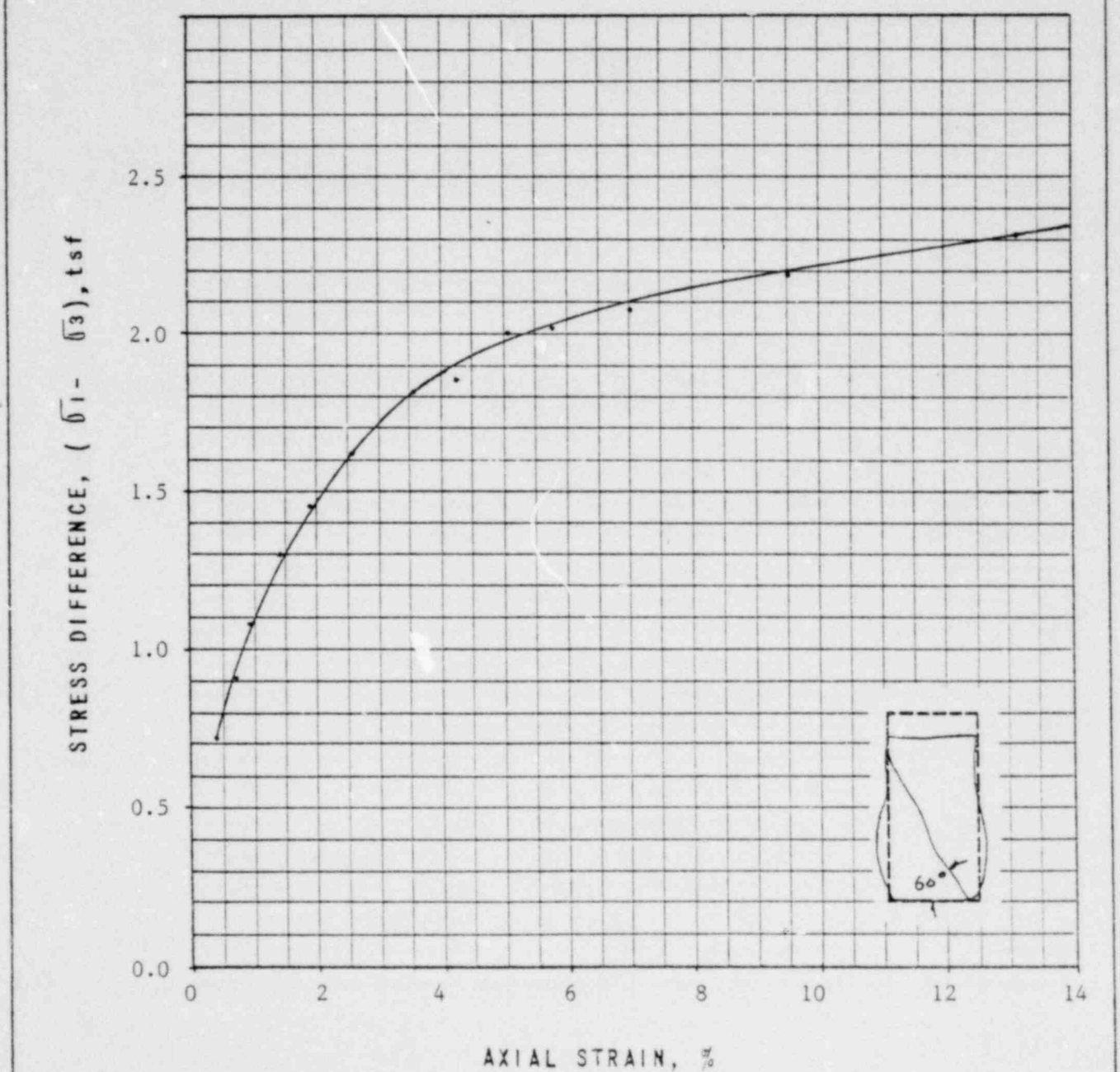

JOB No 71C72-WE

UNCONSOLIDATED UNDRAINED TRIAXIAL COMPRESSION TEST *

Project	V. C. Summer				
Boring No.	WE-19	Sample No.	ST-2	Depth	18.7-19.4 Ft
Description	Red-brown micaceous medium to fine sandy silt (Select Fill)				
Moisture Content	23.1 %			Dry Density	101.0 pcf
Liquid Limit	NP %	Plastic Limit	NP %	Relative Density	--- %
$(\sigma_1 - \sigma_3)$ max.=	3.28 tsf at	9.39 % Strain		Chamber Pressure, σ_c =	0.90 tsf

* After undrained creep test

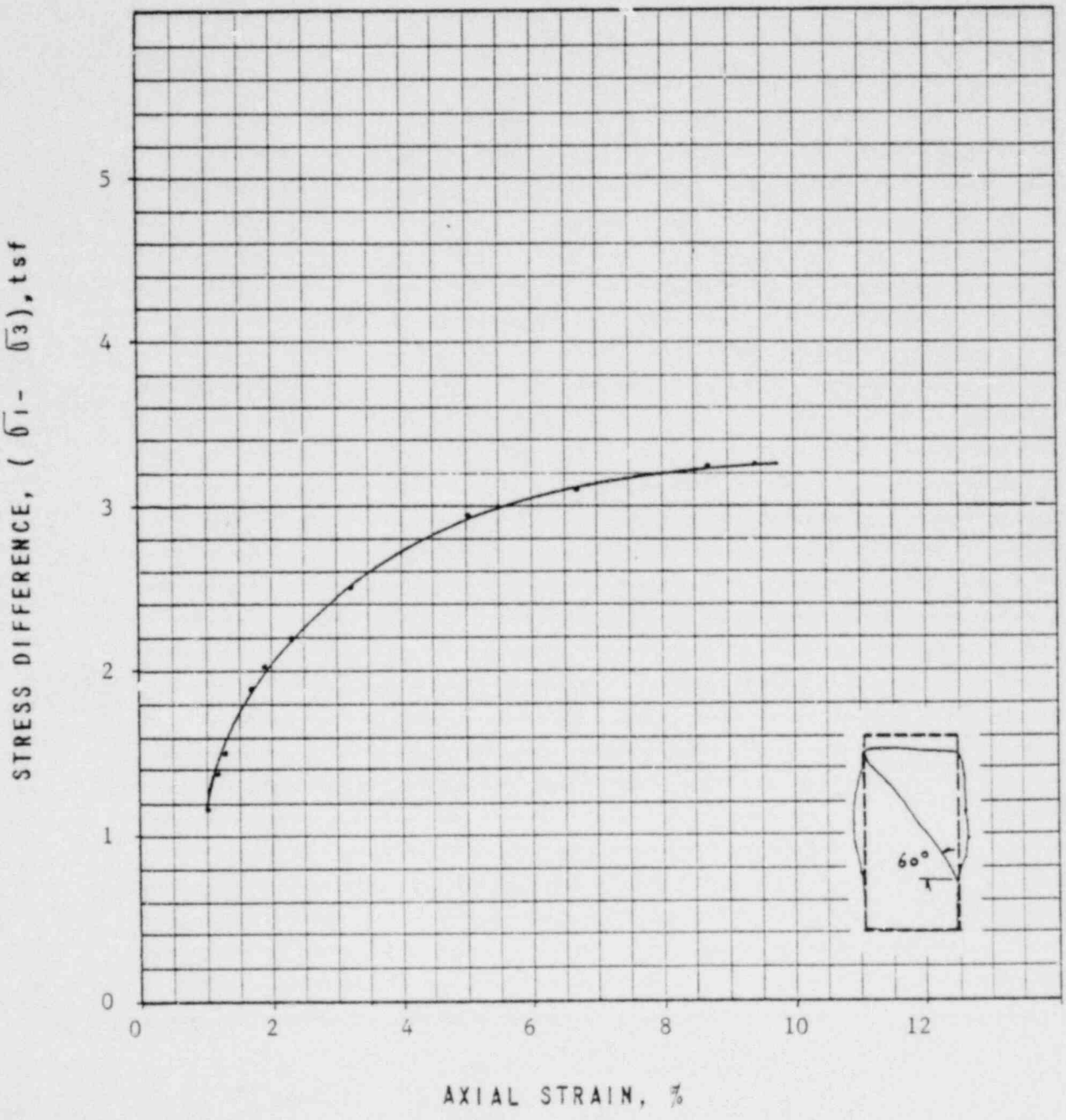

JOB No 71C72-WE

UNCONSOLIDATED UNDRAINED TRIAXIAL COMPRESSION TEST *

Project V. C. Summer

Boring No. WE-19 Sample No. ST-3 Depth 28.0-28.7 Ft

Description Red-brown micaceous medium to fine sandy silt (Select Fill)

Moisture Content 35.7 % Dry Density 83.5 pcf

Liquid Limit NP % Plastic Limit NP % Relative Density %

$(\sigma_1 - \sigma_3)$ max.= 2.55 tsf at 17.8 % Strain Chamber Pressure, σ_c = 1.17 tsf

* After undrained creep test

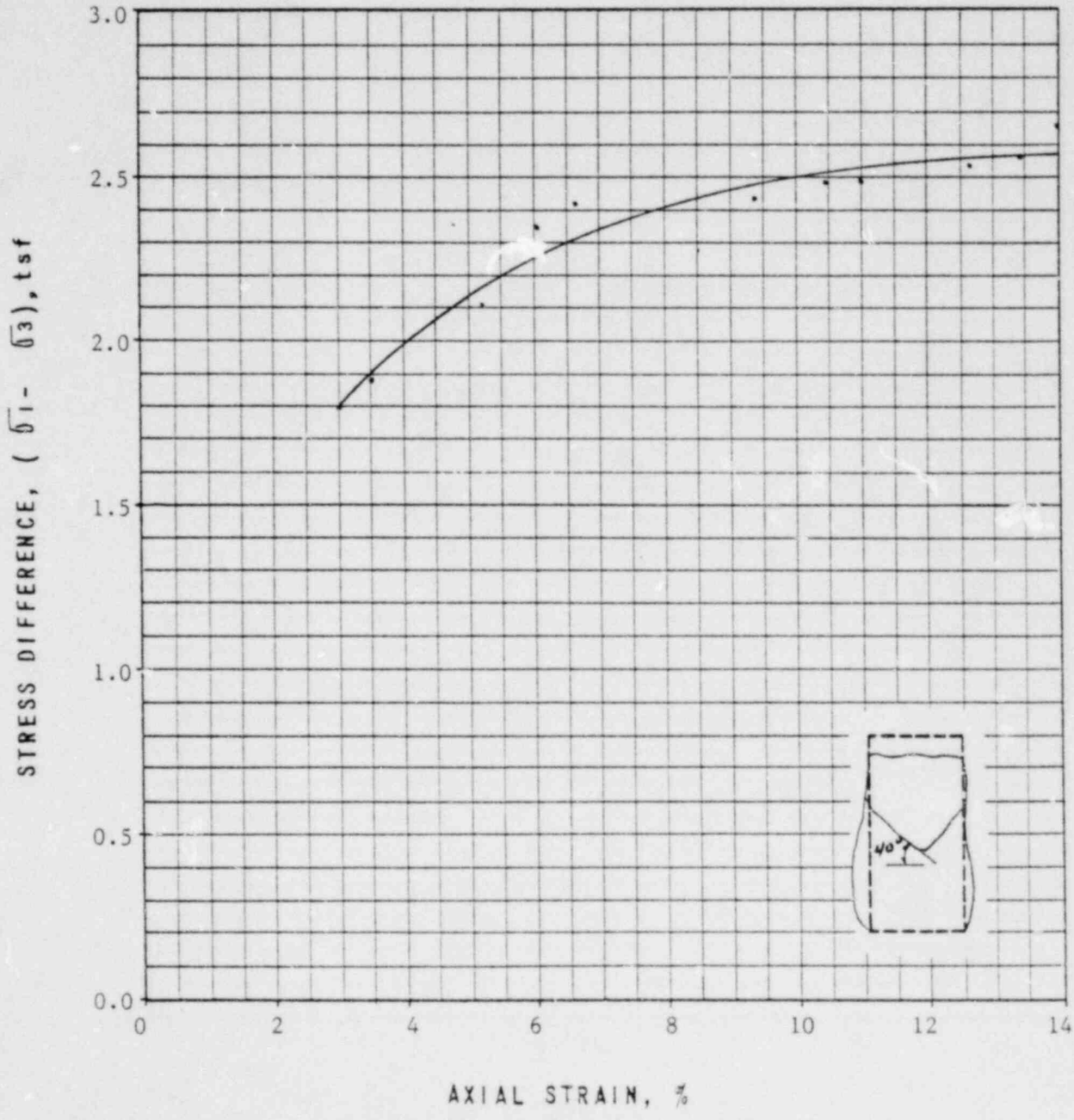

JOB No 71 C 72-WE

UNCONSOLIDATED UNDRAINED TRIAXIAL COMPRESSION TEST *

Project V. C. Summer

Boring No. WE-19 Sample No. ST-5 Depth 48.0-48.5 Ft

Description Red Brown Micaceous Sandy Silt (Select Fill)

Moisture Content 26.8 % Dry Density 95.7 pcf

Liquid Limit 54 % Plastic Limit 39 % Relative Density -- %

$(\sigma_1 - \sigma_3)$ max.= 3.50 tsf at 10.5 % Strain Chamber Pressure, σ_c = 1.87 tsf

*After Undrained Creep

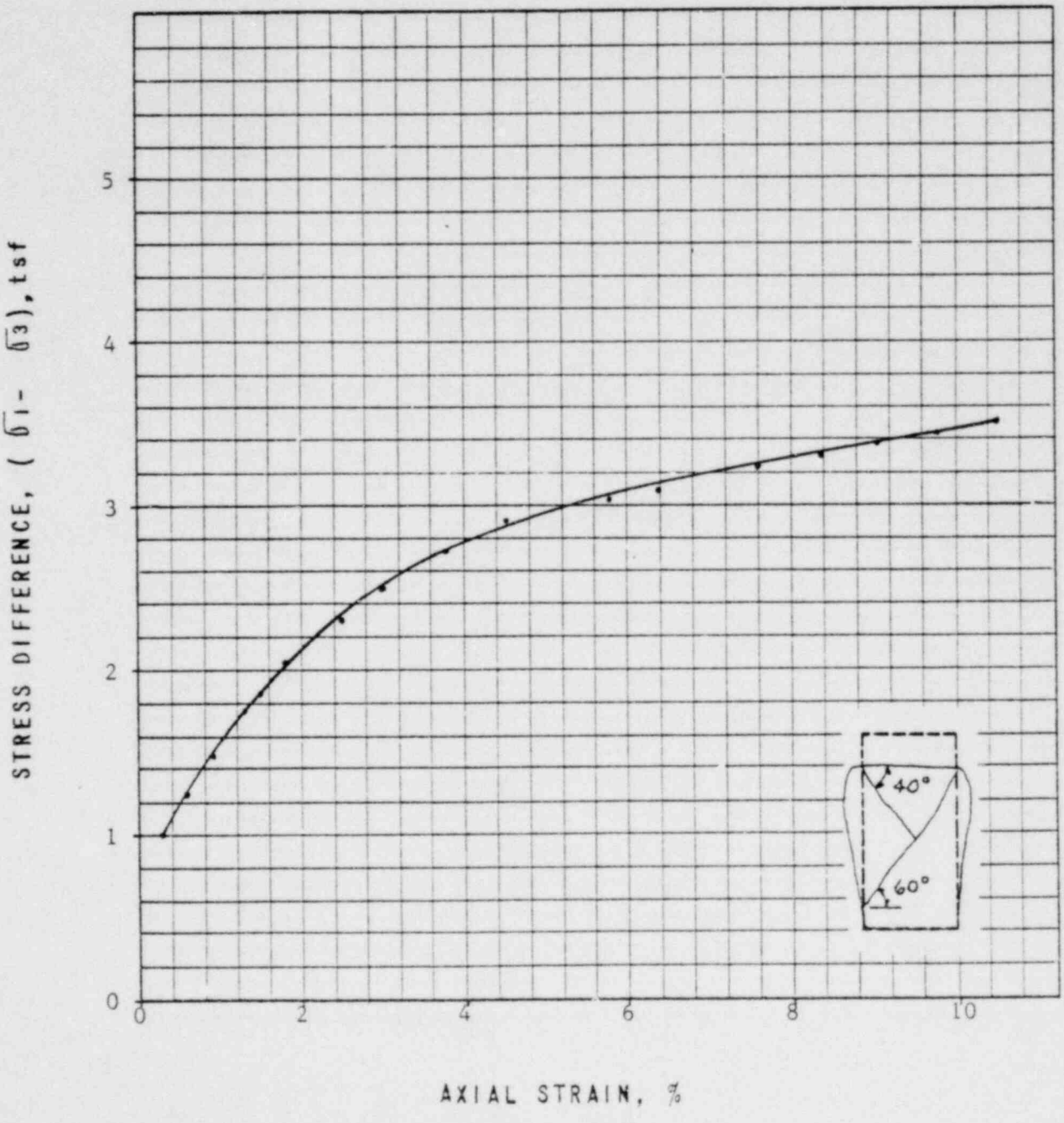

JOB No 71 C 72-WE

UNCONSOLIDATED UNDRAINED TRIAXIAL COMPRESSION TEST*

Project V. C. Summer

Boring No. WE-19 Sample No. ST-5 Depth 48.5-49.0 Ft

Description Red-Brown Micaceous Sandy Silt (Select Fill)

Moisture Content 23.6 % Dry Density 103.2 pcf

Liquid Limit 50 % Plastic Limit 34 % Relative Density -- %

$(\bar{\sigma}_1 - \bar{\sigma}_3)$ max.= 3.14 tsf at 13.07 % Strain Chamber Pressure, $\bar{\sigma}_c$ = 1.87 tsf

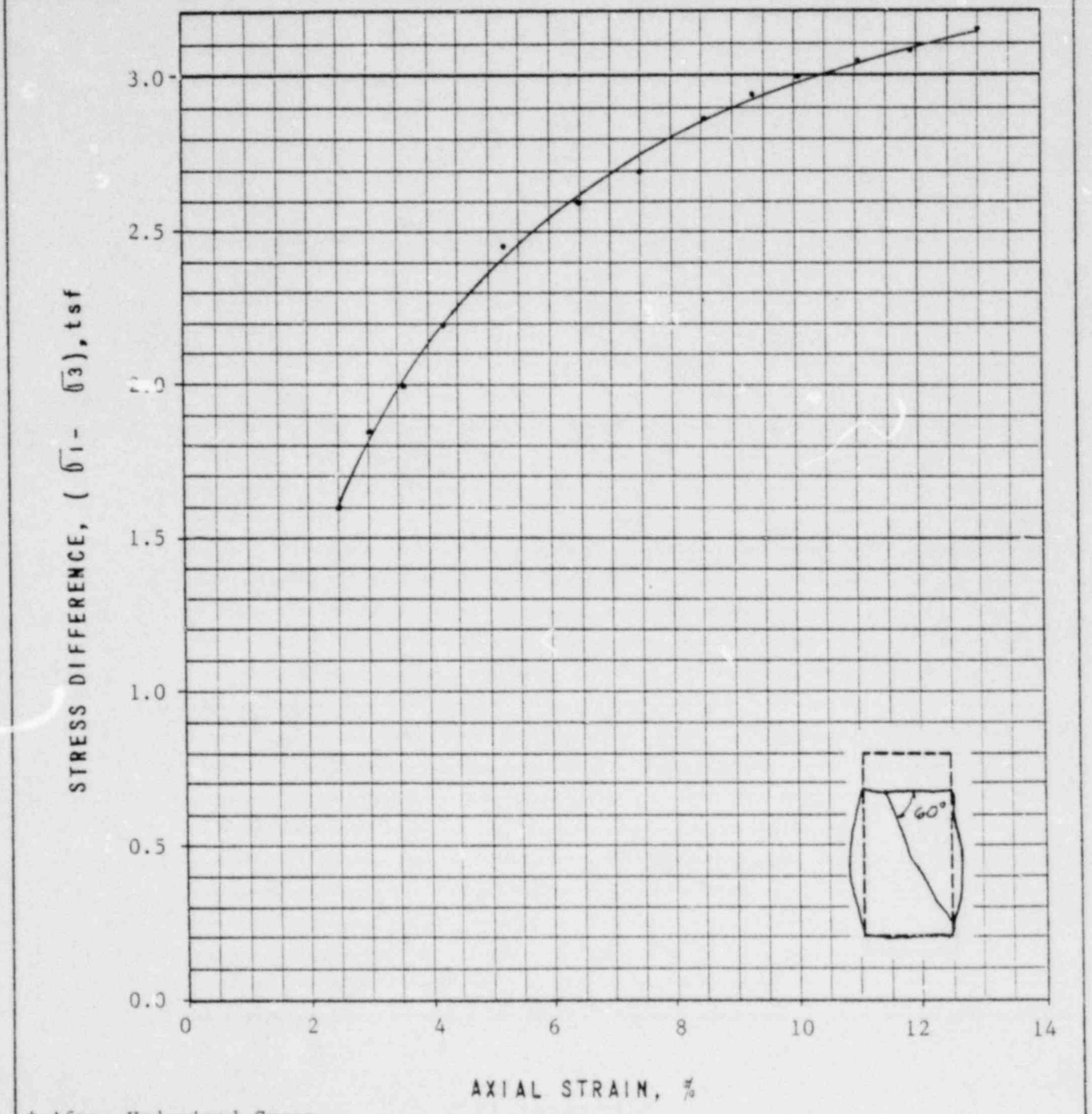

* After Undrained Creep

UNCONSOLIDATED UNDRAINED TRIAXIAL COMPRESSION TEST *

Project V. C. Summer

Boring No. WE-19 Sample No. ST-5 Depth 49.0-49.5 Ft

Description Red-Brown Micaceous Sandy Silt (Select Fill)

Moisture Content 20.8 % Dry Density 105.5 pcf

Liquid Limit N.P. % Plastic Limit N.P. % Relative Density -- %

$(\sigma_1 - \sigma_3)$ max.= 4.90 tsf at 13.66 % Strain Chamber Pressure, σ_c = 1.87 tsf

*After Undrained Creep

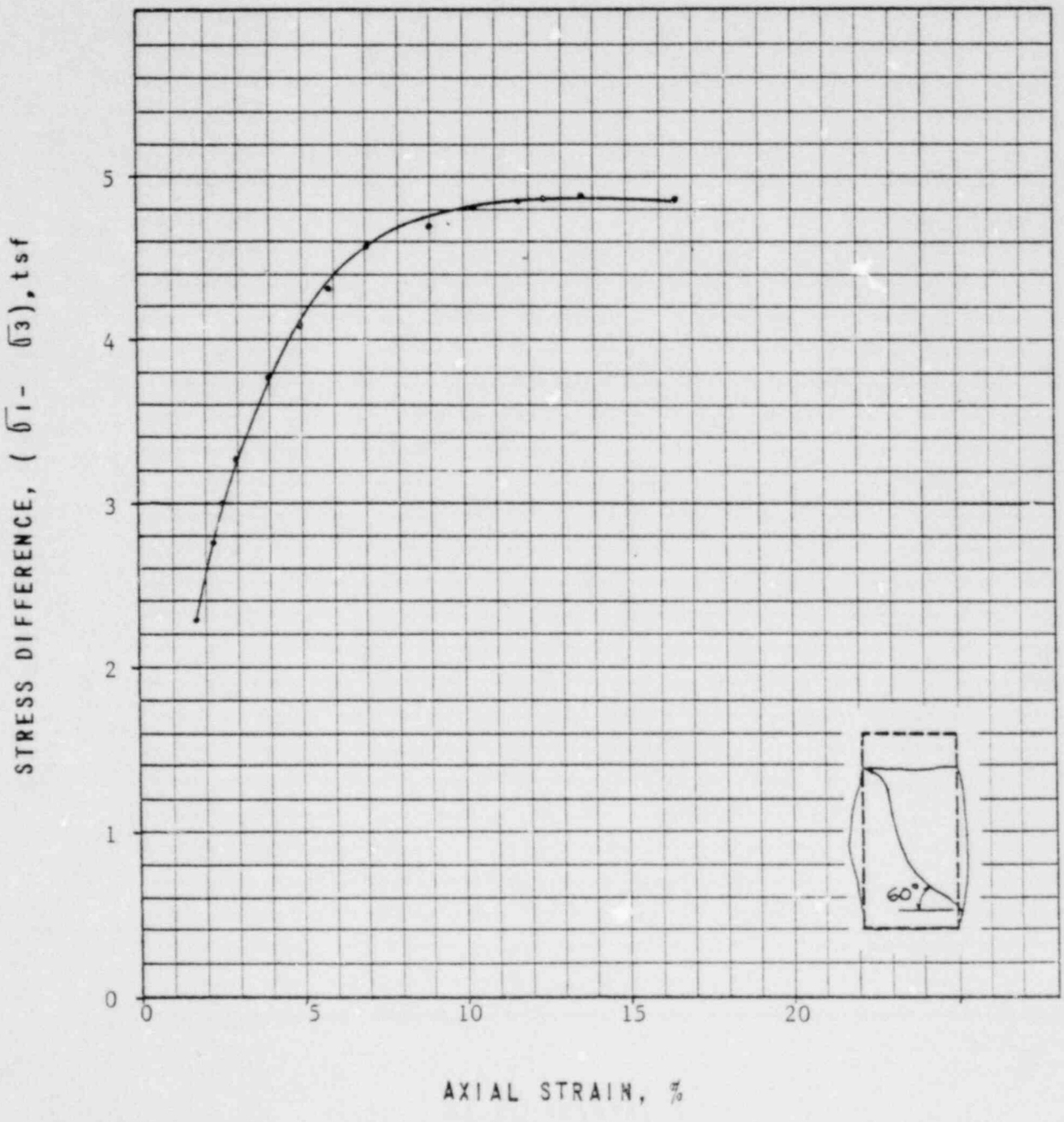

JOB No 71 C 72-WE

MECHANICAL ANALYSIS

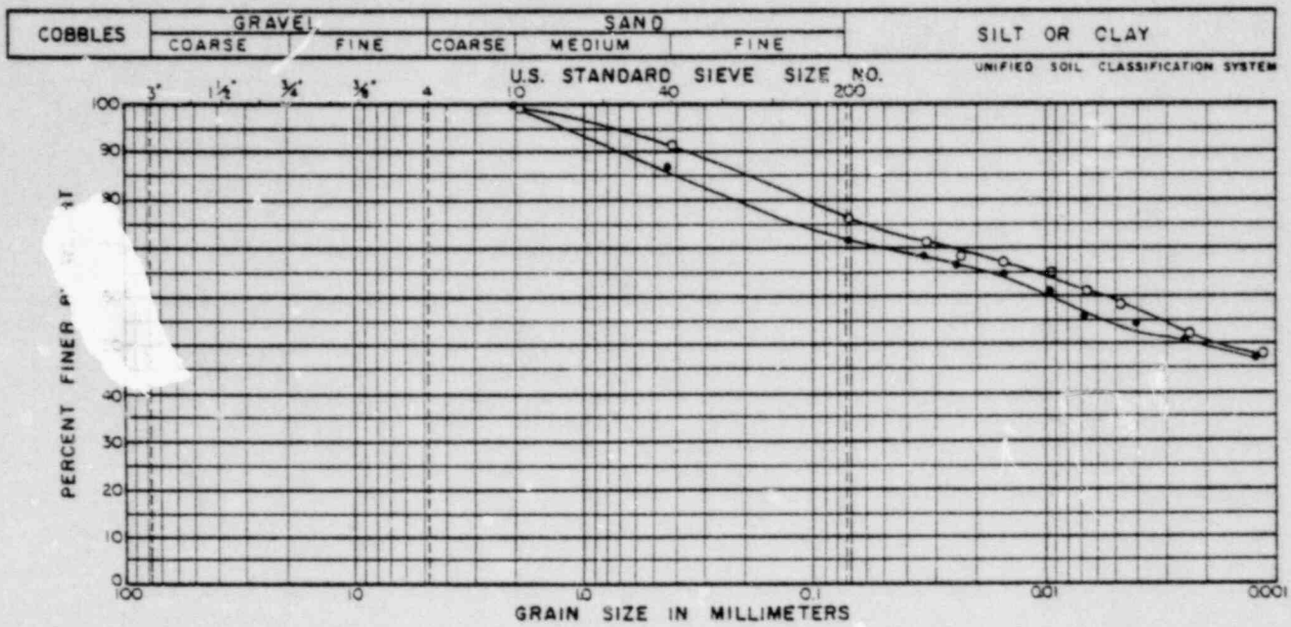

BORING	SAMPLE	DEPTH	SYMBOL	CLASSIFICATION	MC	LL	PL
WE-14	S-8	43'-43.5'	○	Red-brown micaceous medium to fine sandy clayey silt (Select fill)	34.5	70	42
WE-14	S-8	43.5-44.0	●	Red-brown micaceous clayey silty medium to fine sand (Select fill)	29.0	67	42

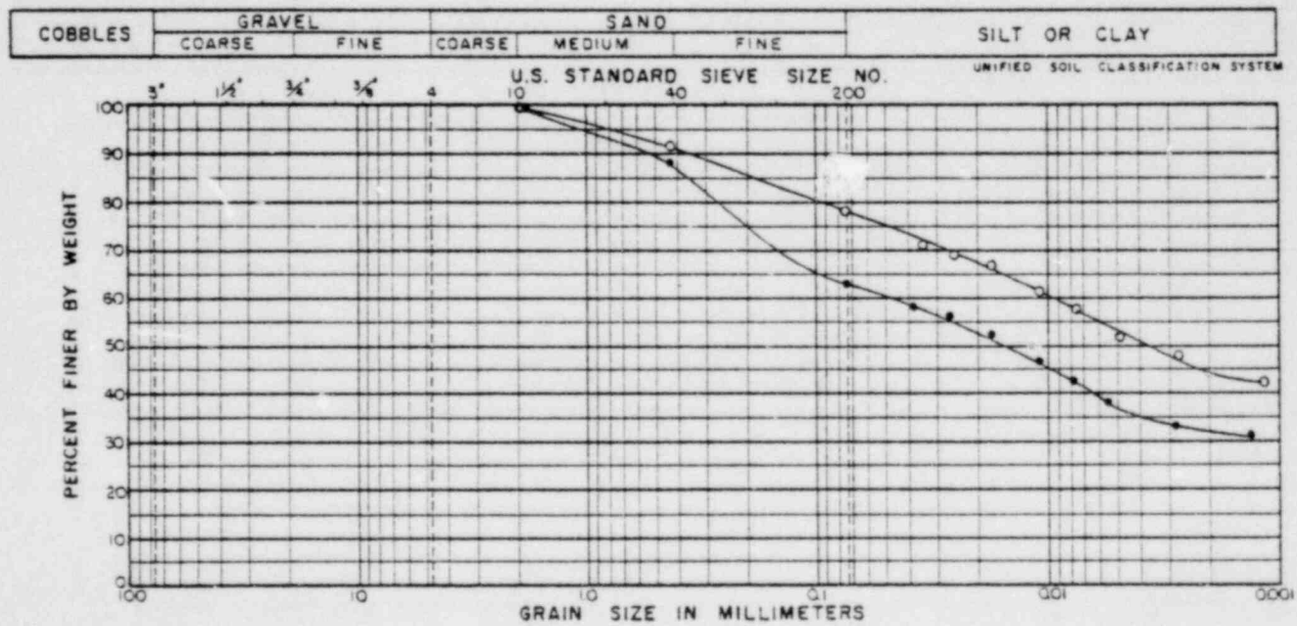

BORING	SAMPLE	DEPTH	SYMBOL	CLASSIFICATION	MC	LL	PL
WE-15	ST-1	37.0-37.5	○	Red-brown micaceous medium to fine sandy clayey silt (Select fill)	34.6	60	44
WE-15	ST-2	48.9-49.5	●	Red-brown micaceous medium to fine sandy silt (Select fill)	30.8	NP	NP

MECHANICAL ANALYSIS

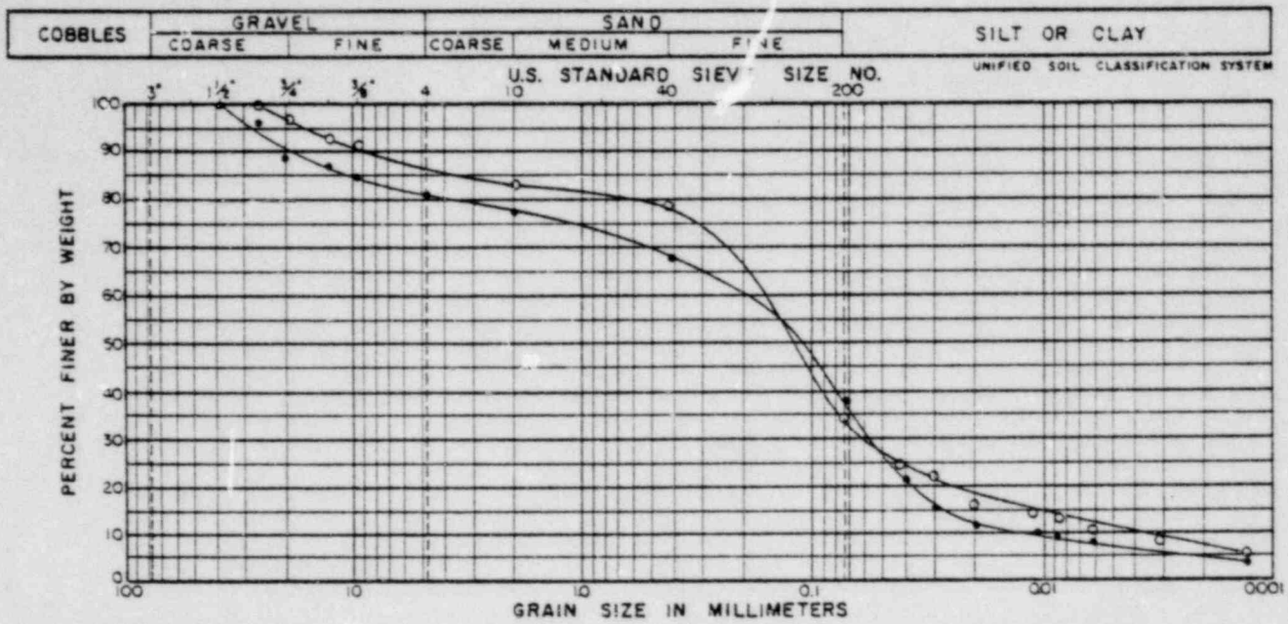

BORING	SAMPLE	DEPTH	SYMBOL	CLASSIFICATION	MC	LL	PL
WE-16	PT-1	79.3-79.8	○	Green, brown and gray micaceous fine gravelly silty fine sand (Saprolite)	19.3	NP	NP
WE-16	PT-2	81.3-81.5	•	Green, brown and gray micaceous gravelly silty coarse to fine sand (Saprolite)	13.3	NP	NP

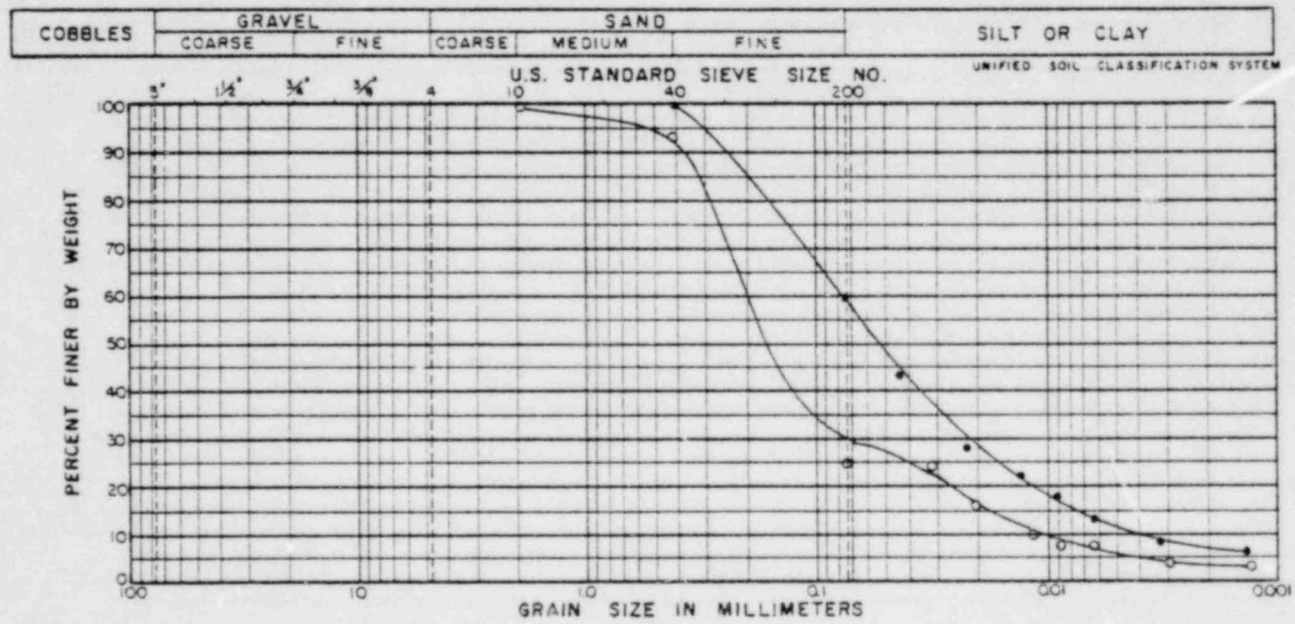

BORING	SAMPLE	DEPTH	SYMBOL	CLASSIFICATION	MC	LL	PL
WE-16	PT-6	93.7-94.1	○	Green, brown and gray micaceous silty fine sand (Saprolite)	11.4	NP	NP
WE-17	ST-7	68.0-68.5	•	Light brown micaceous fine sandy silt (Saprolite)	28.7	NP	NP

MECHANICAL ANALYSIS

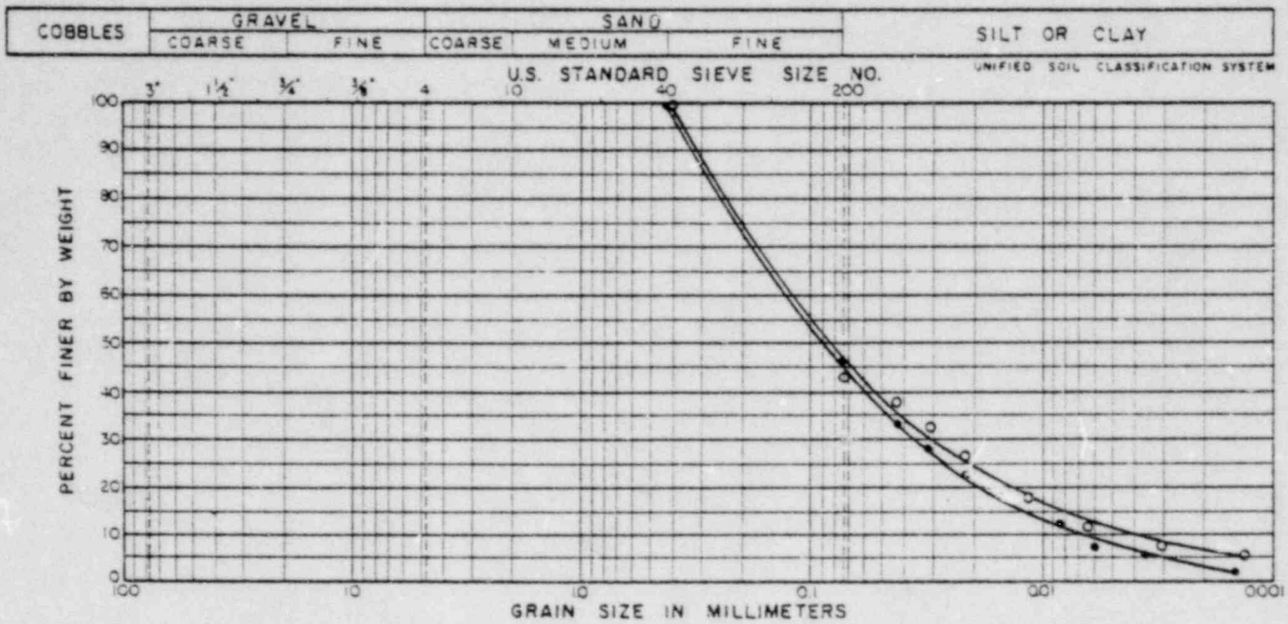

BORING	SAMPLE	DEPTH	SYMBOL	CLASSIFICATION	MC	LL	PL
WE-17	ST-7	68.5-69.1	○	Light brown micaceous fine sandy silt (Saprolite)	23.6	NP	NP
WE-17	ST-7	69.1-69.6	●	Light brown micaceous fine sandy silt (Saprolite)	20.2	NP	NP

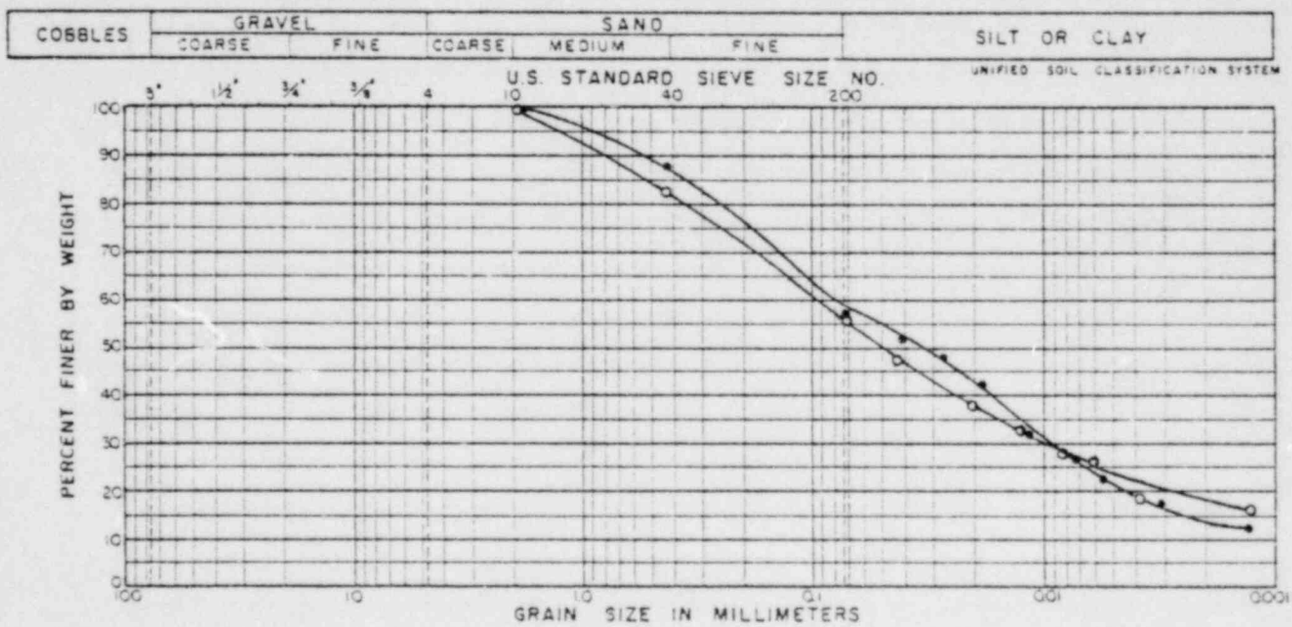

BORING	SAMPLE	DEPTH	SYMBOL	CLASSIFICATION	MC	LL	PL
WE-19	ST-2	18.0-18.7	○	Red-brown micaceous medium to fine sandy silt (Select fill)	25.9	NP	NP
WE-19	ST-2	18.7-19.4	●	Red-brown micaceous medium to fine sandy silt (Select fill)	23.1	NP	NP

MECHANICAL ANALYSIS

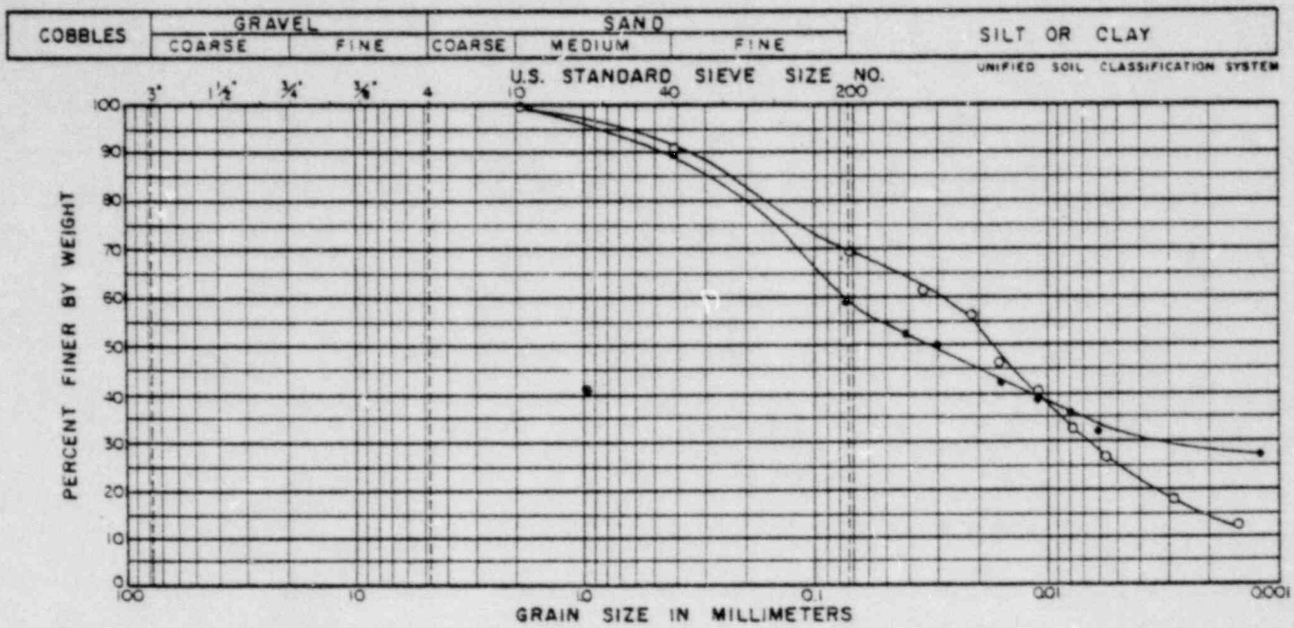

BORING	SAMPLE	DEPTH	SYMBOL	CLASSIFICATION	MC	LL	PL
WE-19	ST-3	28.0-28.7	○	Red-brown micaceous medium to fine sandy silt (Select fill)	35.7	NP	NP
WE-19	ST-5	48.0-48.5	•	Red-brown micaceous medium to fine sandy silt (Select fill)	26.8	NP	NP

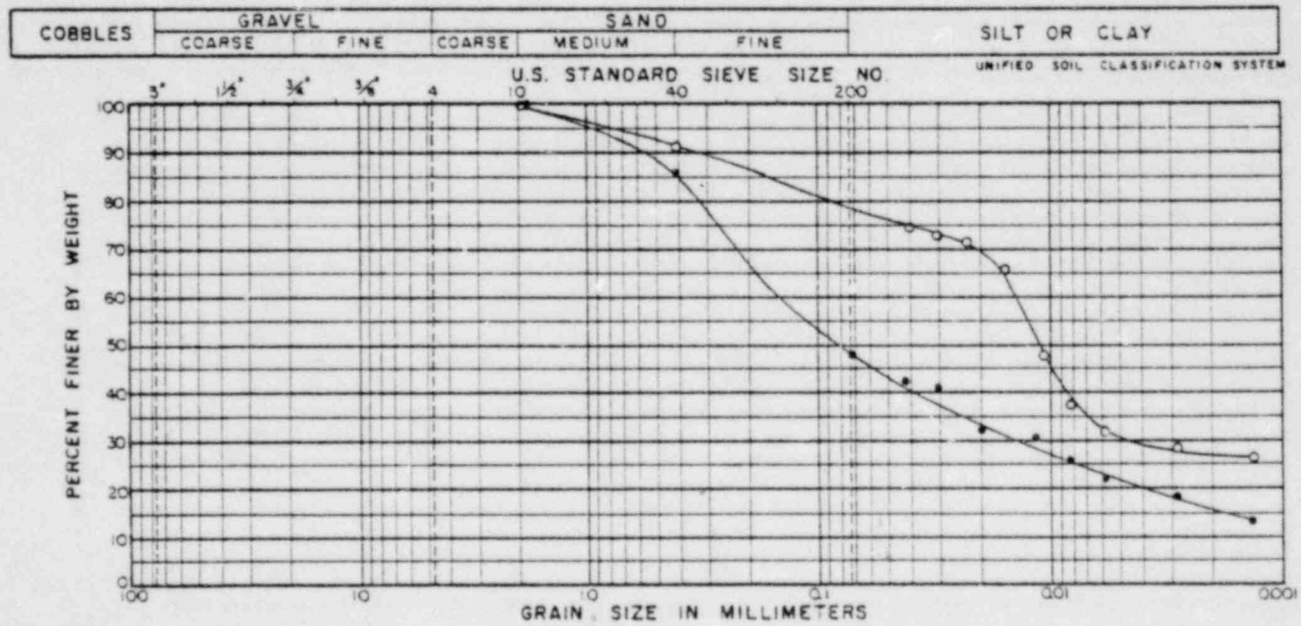

BORING	SAMPLE	DEPTH	SYMBOL	CLASSIFICATION	MC	LL	PL
WE-19	ST-5	48.5-49.0	○	Red-brown micaceous medium to fine sandy silt (Select fill)	23.6	NP	NP
WE-19	ST-5	49.0-49.5	•	Red-brown micaceous medium to fine sandy silt (Select fill)	20.8	NP	NP